

PHARMACOKINETIC EVALUATION OF INVESTIGATIONAL AGENTS OBTAINED
FROM BIOACTIVE MARINE NATURAL PRODUCTS, CHEMICAL SYNTHESIS AND
REFORMULATION

by

BO ZHENG

(Under the Direction of Catherine A. White)

ABSTRACT

Pharmacokinetics is the science dedicated to the study of rate processes such as absorption, distribution, metabolism, and excretion (ADME) of a drug and the multiple interrelationships affecting them, such as incomplete absorption, saturability in transport, biotransformation, or binding. It is becoming increasingly clear that utilizing pharmacokinetic tools to evaluate large numbers of compounds for ADME properties early in the drug discovery process will ultimately save considerable time and money for pharmaceutical and biotechnology companies, but also to improve the likelihood of success. In this dissertation, pharmacokinetic evaluations were performed for investigational agents obtained from bioactive marine natural products, chemical synthesis and reformulation.

INDEX WORDS: Pharmacokinetics, Natural Product, Drug Development, Drug Discovery

PHARMACOKINETIC EVALUATION OF INVESTIGATIONAL AGENTS OBTAINED
FROM BIOACTIVE MARINE NATURAL PRODUCTS, CHEMICAL SYNTHESIS AND
REFORMULATION

by

BO ZHENG

B.S. Shanxi University, China, 1996

M.S. Shanxi University, China, 2002

A Dissertation Submitted to the Graduate Faculty of The University of Georgia in Partial
Fulfillment of the Requirements for the Degree

DOCTOR OF PHILOSOPHY

ATHENS, GEORGIA

2009

© 2009

BO ZHENG

All Rights Reserved

PHARMACOKINETIC EVALUATION OF INVESTIGATIONAL AGENTS OBTAINED
FROM BIOACTIVE MARINE NATURAL PRODUCTS, CHEMICAL SYNTHESIS AND
REFORMULATION

by

BO ZHENG

Major Professor: Catherine A. White

Committee: Robert D. Arnold
J. Warren Beach
Randall L. Tackett

Electronic Version Approved:

Maureen Grasso
Dean of the Graduate School
The University of Georgia
December 2009

DEDICATION

This dissertation is dedicated with love and gratitude to my parents, Gentang Zheng and Ruiyin Nie, my wife, Xiaohua Ji.

.

ACKNOWLEDGEMENTS

First and foremost, I would like to thank my parents, Gentang Zheng and Ruiyin Nie for their endless love and support throughout my student career. To Xiaohua Ji, thank you for being the greatest wife. To other relatives and friends, I love you all. Tomorrow will be the new start of my life and it's time for me to take care of you. I would like to thank my major professor Dr. Catherine A. White and Dr. Lyndon M. West from the bottom of my heart for their help, guidance and support during the past four years. They not only taught me PK principles, experimental designs, data analysis and interpreting, scientific writing skills, but also let me know how to manage a lab and balance my life. I'm also very grateful to my very nice and wonderful committee members: Dr. Robert D. Arnold, Dr. J. Warren Beach, and Dr. Randall L. Tackett. They all gave me very useful suggestions and great comments on my projects and dissertation. Other professors and staff I worked with in PBS also helped me a lot and made me feel warm and welcomed.

I would also like to thank many of my friends in PBS, I don't know how I would have made it through all these years without them. Finally, I would like to thank my labmates: Shawn, Liang, Dawei, and Maia, Prasoon for their knowledge, encouragement, and stimulating conversations. I would never forget the happy and wonderful life in Athens.

TABLE OF CONTENTS

	Page
ACKNOWLEDGEMENTS	v
CHAPTER	
1 INTRODUCTION	1
2 LITERATURE REVIEW	3
3 PHARMACOKINETICS AND TISSUE DISTRIBUTION OF PSEUDOPTEROSIN A IN MICE UTILIZING A NEW HPLC-ULTRAVIOLET DETECTION METHOD WITH DERIVATIZATION	51
4 PHARMACOKINETICS OF A MIDAZOLAM GEL FOLLOWING INTRANASAL DELIVERY IN DOGS	78
5 PHARMACOKINETICS OF L- β -5-BROMOVINYL-(2-HYDROXYMETHYL) 1,3-(DIOXOLANYL)URACIL (L-BVoddU) IN RODENTS.....	101
6 ESTIMATING THE LIPOPHILITY OF NATURAL PRODUCTS USING A POLYMERIC REVERSED PHASE HPLC METHOD	129
7 CONCLUSIONS	153
APPENDIX	
1 QUANTITATIVE DETERMINATION OF (-)-FLURO-CARBODINE IN MOUSE PLASMA, LIVER, BRAIN AND KIDNEY TISSUES BY ION-PAIRING LIQUID CHROMATOGRAPHY	156

CHAPTER 1

INTRODUCTION

Pharmacokinetics is the science dedicated to the study of rate processes such as absorption, distribution, metabolism, and excretion (ADME) of a drug and the multiple interrelationships affecting them, such as incomplete absorption, saturability in transport, biotransformation, or binding. Utilizing pharmacokinetic tools to evaluate bioactive compounds for ADME properties early in the drug discovery process will ultimately save considerable time and money for pharmaceutical and biotechnology companies, but also to improve the likelihood of success.

Chapter 2 gives a detailed literature review of pharmacokinetic evaluation in preclinical drug discovery and development, including pharmacokinetic parameters characterizing pharmacokinetic behavior of investigational agents, *in-vitro* and *in-vivo* assay used in pharmacokinetic evaluation, classic pharmacokinetic modeling and PBPK, PD/PK modeling. The major source of drugs is also briefly introduced in Chapter 2.

Pseudopterosin A, a gorgonian-derived diterpene glycoside first isolated from specimens of the gorgonian coral, is known to possess anti-inflammatory, analgesic and antioxidant activity. Chapter 3 describes a simple, rapid and sensitive method for determination of pseudopterosin A (PsA) in mouse plasma, liver, brain, kidney using pre-column derivatization and HPLC-ultraviolet detection. The pharmacokinetic study of pseudopterosin A following administration of a 50 mg/kg i.v. dose with this validated method was performed in Chapter 3.

Status epilepticus is a medical emergency requiring immediate therapy. Midazolam has a marked anticonvulsive effect in humans and animals. Rapid absorption and attainment of

therapeutic level have been demonstrated for intranasal midazolam in dogs; however, the parenteral formulations are impractical to use in animals. Chapter 4 describes development of a methylcellulose gel formulation of midazolam. A pharmacokinetic study, in chapter 4, compared the pharmacokinetics of a novel midazolam gel formulation given intranasally to the pharmacokinetics of parenteral midazolam given intranasally, intravenously and rectally in dogs.

L- β -5-Bromovinyl-(2-hydroxymethyl)-1,3-(dioxolanyl)uracil (L-BVOddU) has both *in vitro* and *in vivo* activity against herpes simplex virus type 1 (HSV-1) and varicella zoster virus (VZV). Recent research has shown anti-cancer activity of L-BVOddU. The pharmacokinetic and tissue distribution at steady state of L-BVOddU was studied in rats and mice, respectively, in Chapter 5. An HPLC method for the quantification of L-BVOddU in mouse plasma, brain, liver, heart, lung, spleen, kidney, skins and rat plasma was developed and utilized in this study.

The integration of physicochemical profiling screens such as Log *P* into natural products drug discovery programs is emerging as an approach to front-load drug-like properties of natural product libraries for high-throughput screening. In chapter 6, a fast-gradient HPLC method using a polystyrene-divinylbenzene PRP-1 column was developed to estimate the lipophilicity of marine natural products. An excellent correlation was found between the results of the experimentally determined and the literature log *P* values for a diverse set of commercially available drugs using the PRP-1 column.

Chapter 7 summarizes the final conclusions.

In the Appendix, a HPLC method developed for the analysis of (-)-Fluro-Carbodine in mouse plasma and tissue and stability studies are included.

CHAPTER 2

LITERATURE REVIEW

1. Introduction

In the fields of medicine, biotechnology and pharmacology, drug discovery is the process by which drugs are discovered and/or designed. The process of drug discovery involves the identification of candidates, synthesis, characterization, screening, and assays for therapeutic efficacy. Usually, drug discovery is divided into 4 stages: target identification, target prioritization/validation, lead identification (hit to lead), and lead optimization (lead to drug candidate).

In the mid 1990s, to shorten the cycle time between target validation and lead discovery, the majority of pharmaceutical companies established highly specialized facilities responsible for high throughput screening. This technique has compressed the lead identification process from months to days, and dramatically changed the drug discovery process in the pharmaceutical industry during the last decade [1-5]. In recent years, combinatorial chemistry and computer-assisted drug design have significantly increased the number of compounds entering the drug discovery process as hits. However, significant amplification in the number of hits does not automatically translate into an increase in new chemical entities progressing into pre-clinical studies [6-9], nor ultimately to successful compounds in clinical development. As a result, the cost of discovery, development, and marketing of new drugs has increased dramatically [9].

Poor pharmacokinetics and toxicity were causes of costly late-stage failure in drug discovery and development accounting for approximately 20 – 40% of drug failure in investigational drug discovery. A rational approach to increase the efficiency and reduce the cost of pharmaceutical research and development is moving pharmacokinetic evaluations into early discovery stages, such as lead identification or optimization, to be conducted in parallel with activity and selectivity assays [10-15]. This enables all properties to be optimized simultaneously, thus resulting in cost and time savings. According to a survey by the Food and Drug Administration (FDA) in 1991, approximately 40% of clinical failure was attributable to poor pharmacokinetic properties [16]. By 2000, the pharmacokinetic attrition rate was down to 10% [17]. This significant improvement was due to a change in drug discovery strategies, as pharmaceutical companies began assessing pharmacokinetic properties of new chemical entities at the very early stages of drug discovery [18, 19].

2 Pharmacokinetic evaluations in preclinical drug discovery and development

Pharmacokinetics is cited as a science dedicated to the study of rate processes such as absorption, distribution, metabolism, and excretion of a drug and the multiple interrelationships affecting same, such as incomplete absorption, saturability in transport, biotransformation, or binding. It is becoming increasingly clear that utilizing pharmacokinetic tools to evaluate large numbers of compounds for ADME properties early in the drug discovery process will ultimately save considerable resources in time and money for pharmaceutical and biotechnology companies [20-25], and to improve the likelihood of success [26-29].

2.1 Parameters that define the PK behavior of a drug

Pharmacokinetic parameters (i.e., clearance (CL), volume of distribution (Vd), etc.) are constants quantifying the relationship of drug input (dose, dosing interval, dosing time, sampling

times) to output (drug concentrations). Knowledge about these parameters is important in terms of providing prior estimates for designing clinical trials [30], predicting concentration–time profiles in future studies and clinical practice [31], and Bayesian population analysis [32].

A. C_{\max} and t_{\max}

Following intravenous (i.v.) or extravascular drug administration, the maximum observed concentration in the concentration-time profile (C_{\max}) and the time to reach that concentration (t_{\max} , which equals 0 for i.v. bolus dosing) are important descriptors of the extent and nature of drug exposure. C_{\max} , an indicator of maximum drug exposure, may sometimes relate better to pharmacological or toxicological effects than other measures of exposure [19].

B. Area under the curve (AUC)

When blood, plasma (most commonly obtained), or serum drug concentrations are plotted versus time, the AUC is the primary measure of overall exposure following i.v. or extravascular administration of a drug. AUC is most commonly determined using the linear trapezoidal method [25]. $AUC_{0 \rightarrow \infty}$ represents the total amount of drug absorbed by the body, irrespective of the rate of absorption. Therefore, this term is useful when trying to determine whether two formulations of the same drug (for example a capsule and a tablet) release the same dose of drug to the body. Another use is in the therapeutic monitoring of toxic drugs.

In some case, AUC is useful for determining the average concentration over a time interval, AUC/t . Also, AUC is referenced when talking about elimination. The amount eliminated by the body = clearance (volume/time) * AUC (mass*time/volume). AUC is used to calculate bioavailability which, along with volume of distribution and clearance, constitutes the most important primary PK parameters.

C. Clearance (CL)

Clearance is the term that describes the efficiency of irreversible elimination of a drug from the body [20]. Elimination in this context refers either to the excretion of the unchanged drug into urine, gut contents, expired air, etc., or to the metabolic conversion of the drug into a different chemical compound, usually in the liver but also in other organs. In the latter case, even though the metabolite is still in the body, the parent drug has been cleared or eliminated. Uptake of the drug into tissues is not clearance if the unchanged drug eventually comes back out of the tissue, however slowly this occurs.

Clearance is defined as ‘the volume of blood cleared of drug per unit time’ and the units are thus volume per time, usually liters per hour or milliliter per minute [28]. We can refer to clearance by a particular organ, such as liver or kidney, by a particular metabolic pathway, or by the whole body. Total body clearance is the sum of all the different clearance processes occurring for a given drug.

D. Bioavailability (F)

Bioavailability describes the rate and extent to which the active drug ingredient is absorbed from a drug product and becomes available at systemic circulation [30]. The bioavailability of a drug product often determines the therapeutic efficacy of that product since it affects the onset, intensity and duration of therapeutic response of the drug. In most cases, one is concerned with the extent of absorption of drug, (that is the fraction of the dose that actually reaches the bloodstream), since this represents the "effective dose" of a drug. This is generally less than the amount of drug actually administered in the dosage form.

"Absolute" bioavailability, F , is the fraction of an administered dose which actually reaches the systemic circulation, and ranges from $F = 0$ (no drug absorption) to $F = 1$ (complete drug absorption) [31]. Since the total amount of drug reaching the systemic circulation is directly

proportional to the area under curve (AUC) when clearance keeps consistent, F is determined by comparing the respective AUCs of the test product and the same or different dose of drug administered intravenously. The intravenous route is the reference standard since the dose is, by definition, completely available. $F_{\text{oral}} = (\text{AUC}_{\text{oral}} * \text{Dose}_{\text{iv}}) / (\text{AUC}_{\text{iv}} * \text{Dose}_{\text{oral}})$.

"Relative" or "Comparative" bioavailability refers to the availability of a drug product as compared to another dosage form or product of the same drug given in the same or different dose [31]. These measurements determine the effects of formulation differences on drug absorption.

$$F_A = (\text{AUC}_A * \text{Dose}_B) / (\text{AUC}_B * \text{Dose}_A)$$

E. Volume of Distribution (V_d)

The apparent *volume of distribution* is the theoretical volume of fluid into which the total drug administered would have to be diluted to produce the concentration in plasma [20]. Volume of distribution is an indicator of how extensively a molecule distributes in the body. The volume of distribution is a proportionality constant relating the amount of drug in the body to blood or plasma concentrations. The volume of distribution is given by the following equation: $V_d = (\text{total amount of drug in the body}) / (\text{drug blood concentration})$

F. Volume of Distribution at Steady-State (V_{ss})

Although the V_d usefully relates the amount of drug in body to plasma concentration during the terminal phase, its value is influenced by elimination [22]. A need exist to define a volume term to reflect purely distribution. Therefore, a useful volume of distribution term, V_{ss} , is defined as a ratio of the total quantity of drug in the body (A_{ss}) to the total concentration of drug in plasma ($C_{p,ss}$) at steady state condition(pseudo-equilibrium) [23]. In other words, V_{ss} corresponds to the equivalent volume in which a drug is distributed into the body. V_{ss} can also be calculated from intravascular pharmacokinetic data (with only central or plasma drug

elimination) using the following equation: $V_{ss} = CL * MRT_{iv}$, where MRT is the mean residence time (defined below). Therefore, this steady-state parameter can be calculated without steady-state data. V_{ss} is most useful for predicting the plasma concentrations following multiple dosing to a steady-state or pseudo-equilibrium. For a general linear pharmacokinetic system, it is proven that $V_{\beta} \geq V_{ss}$.

G. Half-life ($t_{1/2}$)

Half life is the time needed to clear 50% of the drug from plasma. It also determines the length of time necessary to reach steady state. The general rule is that the time to reach steady state of a drug is 5 times of this drug's half life [24]. The knowledge of the half-life is useful for the determination of the frequency of administration of a drug (the number of intakes per day) to obtain the desired plasma concentration. Generally, the half-life of a particular drug is independent of the dose administered. In certain cases, it varies with the dose: it can increase or decrease according to, for example, the saturation of a mechanism (elimination, catabolism, binding to plasma proteins etc).

H. Mean Residence Time (MRT)

MRT is the arithmetic mean of the duration that each drug molecule resides in the body [25]. For a one compartment model, $MRT \text{ in hours} = 1.44 * (\text{half-life in hour}) = (\text{volume of distribution in L}) / (\text{clearance in L per hr})$. Following intravascular administration, it is equivalent to the ratio of AUMC/AUC, where AUMC is the area under the first moment curve. MRT is related to the overall apparent $t_{1/2}$ of a drug.

2.2 Assays of preclinical pharmacokinetic evaluation

During the drug discovery process, all compounds must be screened for their absorption, distribution, metabolism and excretion (ADME) properties using both in vitro and in vivo

resources. Accurate predictions of human pharmacokinetics would reduce failures in clinic related to poor ADME properties by enabling the early selection of the best candidates for development and the rejection of those with a low chance of success. To predict human pharmacokinetics as early as possible, there has been a growing demand to optimize the use of pharmacokinetic evaluation or screening. Such pharmacokinetic predictions could be also used to help choose the first dose for a clinical trial, to test the suitability of the compound for the particular dosage regimen, and even to predict the expected variability in the intended population.

2.2.1 *In vitro* pharmacokinetic evaluation assay

The goal of *in vitro* ADME characterization or pharmacokinetic evaluation assay is to provide, with reasonable accuracy, a preliminary prediction of the *in vivo* behavior of a compound to assess its potential to become a drug. A variety of experimental assays have been developed to characterize each aspect of the drug discovery process

A. Physicochemical properties assay

A basic knowledge of the physicochemical properties of compounds is important for understanding interactions between chemical moieties and biological systems.

The charge state of a molecule has traditionally been assessed by determining the ionization constant, pKa. Capillary electrophoresis (CE) has been widely used for determination of pKa. It has the advantage of low sample consumption and insensitivity to impurities [33].

The determination of log P or log D by direct measurement in a two phase system (water-octanol) is slow and troublesome. Reversed-phase chromatography is much more convenient, allowing estimates of log P and log D based on column retention time. Aqueous solubility is

usually determined in a 96-well plate format, with the dissolved concentration determined by LC-UV or LC-MS.

B. Membrane permeability assay

Oral absorption, penetration of the blood-brain barrier and access to intracellular sites of action all depend, in most cases, on the ability of compounds to cross cell membranes. Permeability *in vivo* is a complex phenomenon, involving several possible mechanisms: passive diffusion, paracellular diffusion, active transport and efflux. Several assays exist for *in vitro* permeability testing.

Early methods used liposomes or immobilized artificial membrane chromatography [33]. Immobilized artificial membrane packings are prepared by covalently immobilizing monolayers of cell membrane phospholipids to silica particles. These immobilized artificial membrane surfaces mimic fluid cell membranes. The chromatographic retention (capacity) factors (k') of an analyte has been shown to correlate e.g. with the equilibrium partition coefficients in fluid liposome systems [34] or with the permeability through Caco-2 monolayers and intestinal absorption [35].

Over the last 10 years, assays that measure compound permeability across layers of cell such as Caco-2 and MDCK (Madin-Darby canine kidney) cells, have become routine in the pharmaceutical industry [36-38]. Cell culture models for drug absorption are based on the assumption that passage of drugs across the intestinal epithelium (a monolayer of cells) is the main barrier for drugs to reach the portal circulation. The validity of *in vitro* models depends on the degree of representation of the *in vivo* situation. Caco-2 cells, which are derived from a human colonic adenocarcinoma, exhibit morphological as well as functional similarities to intestinal (absorptive) enterocytes [36]. The cells form tight junctions and express many brush

border enzymes, some cytochrome isoenzymes, and phase II enzymes such as glutathione S-transferase and sulphotransferase [37]. Many active transport systems found in small intestinal enterocytes are also expressed on Caco-2 cells [37]. These even include transport systems for amino acids, dipeptides, vitamins, and cytostatics. The unusually high degree of differentiation, together with the fact that these cells differentiate spontaneously under normal cell culture conditions, has resulted in Caco-2 becoming one of the most popular cell culture models to study intestinal epithelial integrity and drug transport. Cells are grown for at least 20 days to form differentiated monolayers on a porous permeable filter. The filter (consisting of an inert material such as polycarbonate) should have pores with a diameter of 0.4 μm in order to avoid cell migration from the apical to the basolateral side. The 20-day culture time is required to obtain tight junctions, cell polarity and a high expression of drug efflux mechanisms such as P-glycoprotein (PgP). For transport experiments, test compounds are typically added to the apical (A) side of the monolayer, and appearance in the basolateral compartment is measured. The rate of compound appearance on the basolateral (B) side is measured using HPLC or LC-MS to calculate permeation rate [38]. Test compounds are compared to standard marker compounds, such as those listed in the Biological Classification System published by the FDA[39]. The Caco-2 cell model usually incorporate several mechanisms of permeability. Diagnosis of each mechanism for structural optimization requires studies under multiple sets of conditions [e.g. A \rightarrow B, B \rightarrow A, with P-glycoprotein (Pgp) inhibitors]. Expression of transporters on Caco-2 cells varies with laboratory or passage and must be monitored. Lipinski [39] noted that Caco-2 experiments are most appropriate at 100 μm for predicting GI absorption of a 1 mg kg^{-1} dosed drug, where transporter saturation is more likely. Also 1 μm is most appropriate for predicting CNS penetration. However, Caco-2 is commonly performed at 10 μm . Inaccurate results are also

generated for compounds that are not fully soluble at the intended assay concentration. Higher throughput 96-well versions of Caco-2 have been reported [40].

The parallel artificial membrane permeability assay is receiving considerable attention [41, 42]. Instead of a cellular monolayer, an artificial membrane is created using lipid in organic diluent. An UV plate reader is used for rapid and inexpensive quantitation. PAMPA is higher throughput than Caco-2 and requires $\sim 5\%$ of the resources [41]. Permeability measurements with PAMPA can be used to prioritize molecules for further study and to reject some molecules altogether. Besides information on permeability properties, PAMPA can also provide information on the solubility, lipophilicity and ionization status of a drug.

C. Metabolic stability assay

Metabolic stability refers to the susceptibility of compounds to biotransformation in the context of selecting and/or designing drugs with favourable pharmacokinetic properties. Metabolic stability results are usually reported as measures of intrinsic clearance, from which secondary pharmacokinetic parameters such as bioavailability and half-life can be calculated when other data on volume of distribution and fraction absorbed are available. Many discovery compounds exhibit low bioavailability because of high rates of metabolism. Metabolic stability assays are conducted with liver microsomes [43], S9 fraction [44, 45], hepatocytes [46] and plasma [47].

Liver microsomes are the simplest and most useful tools for determining metabolic stability during the early stages of drug discovery. Microsomes contain the cytochrome P450 oxidizing enzymes (CYP) and some phase II conjugating enzymes (e.g. UDP-glucuronosyltransferases). Microsomes are commercially available, and are stable for up to 5 years at -80°C . S9 fraction is a cruder preparation than microsomes. S9 fraction contains the

microsomal and cytosolic fractions and includes a wide range of Phase I and Phase II enzymes, a broader range than microsomes, albeit at lower activity. Hepatocytes contain all the liver metabolizing enzymes that are found *in vivo*. Microsomes are easiest and cheapest to use, but increased detail can be obtained with the S9 fraction and hepatocytes. Human liver tissues are the best material for prediction of human *in vivo* metabolism. However, availability of human liver tissue is often a problem, which is likely to improve with the development of cryopreservation methods. Plasma contains other types of enzymes found in blood, such as esterases and amidases, so stability in plasma needs to be evaluated sometimes. Metabolic stability assays are generally automated on laboratory robotic workstations. The metabolic stability assay requires high sensitivity ($<1 \mu\text{M}$) and selectivity (from incubation matrix interferences) that can only be achieved using LC–MS–MS. Metabolic stability results are greatly affected by DMSO concentration, sample concentration and microsomal preparation. The data can be misleading with improper methodology.

The intrinsic hepatic metabolic clearance (CL_{int}) of human and preclinical species can be predicted by measuring enzyme kinetics parameters, K_m (Michaelis-Menton constant) and V_{max} (maximum velocity) ($CL_{\text{int}} = V_{\text{max}} / K_m$). However, it is time consuming to measure K_m and V_{max} . In drug discovery, one can use a single substrate concentration ($\ll K_m$) to determine the parent drug disappearance half-life ($T_{1/2}$). The intrinsic hepatic metabolic clearance (CL'_{int}) can be calculated based on scaling factors from microsomes as well as hepatocytes [48]. Then, the hepatic metabolic clearance (CL_h) and hepatic extraction ratio (E_h) can be calculated.

It is important to remember that metabolism rates and mechanisms vary among animal species. Thus, rodent metabolism studies are most useful in early discovery to assist interpretation of rodent pharmacology studies, provide alerts of liabilities and assist structural

modification. Human metabolism studies become more important as the project moves toward development and require increased safety precautions.

D. Major metabolite screening assay

If metabolic stability testing reveals high Cl_{int} values, the metabolites need to be identified in order to discover the weak points in the parent molecule. Also, metabolites can be synthesized and tested for activity and toxicity. Thus, metabolite studies should be performed during lead optimization synthesis. Liver microsomes are well suited for this purpose in many cases. Incubating a few compounds with hepatocytes can help to validate the use of liver microsomes as the primary screen (if microsomal metabolism is predominant) or indicate the need to modify the assay (e.g. by the inclusion of specific cofactors). LC–MS–MS provides rapid structure elucidation by using the fragmentation of the parent compound as a template to rapidly interpret the structures of metabolites, and requires minimal sample (10–100 ng) [49 and 50]. When MS does not provide sufficient structural detail, LC–NMR [51] is used, but this requires 1–100 μ g of sample.

E. Active transporters assay

Screening compounds for their interactions with certain transporters that are known to modulate drug disposition is becoming widely practiced in the pharmaceutical industry. Several families of cloned transporters are known to play a role in drug disposition, including the APT-binding cassette (ABC) family, the organic anion transporting polypeptide family, the organic cation and organic anion transporter families. The cloning of these transporters has allowed assay systems based on microinjected oocytes or transfected cells to be developed, in which transport is measured by the intracellular accumulation of compound. In vitro systems include isolated cells or cell lines that represent the tissue of origin, or natural or transfected cell lines that

express a certain transporter protein. Commonly used efflux monolayer systems include the human cells Caco-2, HT-29 and T-84, as well cDNA-transfected MDCK and LLC-PK1 pig kidney cells. Caco-2 cell monolayers are currently the most commonly used in vitro technique. For nine of 10 efflux proteins from the ABC transporter family investigated, Caco-2 cells have been reported to resemble human jejunum in transcript levels. An area of increasing interest is that of drug-drug interactions mediated by transporters. In recent years, efflux transporters such as P-gp have been shown to be responsible for many such interactions [52]. P-gp is one of the most studied efflux transporters and is active in the intestine, BBB and drug-resistant cancer cells [52]. Many groups use the Caco-2 cell line for studying P-gp. P-gp screening helps to avoid some compounds for which P-gp greatly limits permeability. Some P-gp substrates are also CYP3A4 substrates, resulting in extraction through ‘cycling’ [53]. Reduced P-gp affinity might improve bioavailability, brain penetration or activity in cancer cells.

F. CYP450 inhibition assay

CYP inhibition has become a major concern as a cause of drug interaction. Several drug products have been withdrawn because they inhibit the metabolism of a co-administered drug, resulting in toxicity [54]. Early methods for measuring CYP inhibition were based on the co-incubation of test compounds and specific CYP substrates with human liver microsomes, followed by HPLC analysis to measure the reaction rate [54, 55]. Automated, multiwell plate-based assays are now available for all major CYPs. Recombinant CYPs are incubated with standard substrates in the presence of the test compound. The rate of metabolism of a ‘probe’ compound to its fluorescent metabolite by a particular CYP450 isoenzyme is measured in the presence and absence of test compound. If the probe metabolism is inhibited, a reduced amount of the probe metabolite is observed by fluorescence [56] or MS [57] detection. CYP450

inhibition can be monitored at a single concentration (e.g. 3 μM) and then predict IC_{50} values from models [58] or measure a full curve for inhibitory compounds. If CYP inhibition has been identified as a major issue with a particular chemical series, automated CYP inhibition assays are likely to be run before permeability or metabolic screening assays. During lead optimization, data obtained with recombinant CYPs need to be confirmed with human liver microsomes.

G. Cellular exposure assay

Cellular pharmacology can correlate with cell-associated drug concentration. If activity is lower than expected, cellular concentration might be the cause. Low concentration of drug associated with the cell could be the result of efflux, poor passive membrane permeation or intracellular metabolism. When intracellular biochemical conversion is necessary for activity, formation of the active species is monitored. These experiments usually dose cells in culture, followed by washing and LC–MS–MS analysis [59].

H. Plasma protein binding assay

Assessment of the binding properties of drug candidates is important in the overall analysis of the pharmacokinetic profiles of drugs as well as to extrapolate the profiles determined in animals to those in human. Several methods have been used for the measurement of plasma protein binding including equilibrium dialysis, ultra filtration and ultracentrifugation combined with LC-MS/MS. Currently, equilibrium dialysis is the most widely used method for protein binding measurements, which uses a semipermeable membrane that separates the protein and protein-bound drug from the free or unbound drug (f_u). However, those conventional methods are not suitable for high through-put screening because they are tedious and time-consuming. A rapid, microscale and reliable analytical method for binding of drugs to plasma proteins has been developed using capillary electrophoresis (CE) with ionic cyclodextrins (CD) combined with

frontal analysis. The binding values obtained by this method were highly consistent with those determined by the ultrafiltration method [60].

2.2.2 *In vivo* pharmacokinetic study

In vivo pharmacokinetic evaluation consists of an in-life phase (dosing and sampling of animals or subjects), a bioanalytical phase, and analysis of the resulting blood, plasma, or serum concentration versus time data using compartmental or non-compartmental pharmacokinetic methods. In drug discovery, initial *in vivo* pharmacokinetic studies are most commonly conducted in rodents and/or the species used for the assessment of *in vivo* efficacy. Subsequently, experiments in a large animal species such as dog or monkey are performed to better describe the disposition of a compound (in multiple species), support toxicology studies, and generate data useful in predicting human pharmacokinetic parameters.

In vivo evaluation of drug absorption in laboratory animals is a commonly used method to predict the extent of absorption of compounds intended for oral administration in humans. After dosing a compound both orally (PO) or intraduodenally (ID) as well as intravenously (IV) and determining plasma levels at various time points after administration, areas under the plasma level vs. time curves (AUCs) can be calculated. By comparison of these AUCs after oral or intraduodenal administration with those after intravenous administration, the oral bioavailability of a compound can be calculated. Intestinal absorption is typically higher than bioavailability when first-pass elimination of the drug in the liver occurs. However, due to physiological factors such as pH, gastrointestinal motility, transit time and different distribution of transporters, extrapolation of animal data to humans should be performed with caution.

Cassette dosing. *In vivo* studies in laboratory animals are resource intensive, due to experimental animal work and bioanalysis of a large number of samples. Higher throughput can

be attained by screening *in vivo* absorption with a limited number of blood samples (e.g. only 1 and 2 h) after oral administration. This allows more drug candidates to be screened. However, results are less accurate and give only rough estimates of bioavailability. Cassette dosing of multiple compounds in a single animal can be considered to increase throughput of *in vivo* absorption studies, although its potential limitations (e.g., enzyme inhibition leading to exaggerated exposure or “false positives”) must be considered [61-63]. In recent years several pharmaceutical companies have published on this method of simultaneous injection of several up to a large number of compounds in a single animal [62]. In this way, pharmacokinetic parameters of compounds can be determined, but the major drawback is potential drug-drug interaction. For cassette dosing, therefore, parenteral routes of administration (e.g. intravenous administration by short infusion) are advised, since enteral routes (e.g. oral administration) strengthen and increase the frequency of drug-drug interaction. After intravenous administration, values for compound clearance can be ordered, but no information will be gained about permeability of the gut wall.

Microdialysis is a probe-based sampling method, which, if linked to analytical devices, allows for the measurement of drug concentration profiles in selected tissues. [64-67], and has been used frequently in pharmacokinetic studies [68, 69]. In this technique, a small, semi-permeable membrane (MD probe) is placed into the interstitial space fluid (ISF) of the tissue of interest. The probe is perfused with a physiological solution (e.g. Lactated Ringer’s) at a constant flow-rate of 1–5 mL/min and at specified time intervals protein-free compound is collected for analysis. The MD-sampling technique provides numerous advantages, most notable is its ability to provide a concentration–time profile of pharmacologically active drug within the ISF and assess the penetration of drug into the tissue of interest [70, 71]. The advantage of *in vivo* microdialysis over traditional methods relates to its ability to continuously sample the unbound

drug fraction in ISF. This is of particular importance because the ISF may be regarded as the actual target compartment for many drugs, e.g. antimicrobial agents or other drugs mediating their action through surface receptors. In contrast, plasma concentrations are increasingly recognized as inadequately predicting tissue drug concentrations and therapeutic success in many patient populations. Thus, the minimally invasive microdialysis technique has evolved into an important tool for the direct assessment of drug concentrations at the site of drug delivery in virtually all tissues. During the last two decades, microdialysis has become increasingly popular for preclinical and clinical pharmacokinetic studies. The combined use of microdialysis with non-invasive imaging methods such as positron emission tomography and single photon emission tomography opened the window to exactly explore and describe the fate and pharmacokinetics of a drug in the body. Linking pharmacokinetic data from the ISF to pharmacodynamic information appears to be a straightforward approach to predicting drug action and therapeutic success, and may be used for decision making for adequate drug administration and dosing regimens. Hence, microdialysis is nowadays used in preclinical and clinical studies to test new drug candidates that are in the pharmaceutical industry drug development pipeline [72, 73].

In summary, *in vivo* pharmacokinetic evaluation assays with selected compounds provide an overview of series pharmacokinetic performance. If pharmacokinetic properties are poor, root causes can be diagnosed, so that structural modifications can be made to improve pharmacokinetics. Less expensive *in vitro* tests can then be used to monitor future compounds in the series [74]. In some cases, pharmacokinetic samples from animal activity studies are used to correlate plasma concentration with pharmacology. If no *in vivo* activity is observed, exposure data helps discern if this is due to a lack of sufficient drug concentration in plasma or tissue [75],

or because of *in vivo* factors that reduce the expected activity. If *in vivo* activity is observed, exposure data are used for SAR.

2.3 ADME evaluation in drug discovery and development

Pharmacokinetics is the study of absorption, distribution, metabolism, and excretion, which is often written as an acronym, ADME. Although each process (e.g., ADME) has very specific definitions, in general, the pharmacokinetic process describe the movement of drugs into, within, and out of the body as well as the relationship of these processes to the pharmacological, toxicological, or therapeutic effect of a drug. The study of these processes and the factors that influence them is fundamental to choosing an appropriated drug candidate.

2.3.1 Absorption evaluation

For a drug to exert the desired pharmacological effect, therapeutic concentrations of the drug need to be available at the cellular sites of action. Absorption from the site of administration is one of the foremost hurdles that a drug molecule encounters before it can reach the systemic circulation. Depending on the route of drug administration, several anatomical barriers to drug absorption and resultant systemic bioavailability exist. The ability of a drug to cross these barriers depends not only on the physicochemical properties of the drug molecule and the formulation characteristics (drug product design), but also on various physiological process at the site of absorption. In addition, interactions between drug-drug, drug-food, drug-disease, as well as the presence of various drug-metabolizing enzymes, uptake and efflux transport proteins at the membrane barriers, influence drug absorption.

Use of drug absorption models early in the drug development process increase the probability of success by identification of drug candidates with good absorption potential. Systemic bioavailability of drugs is a composite of processes that favor and inhibit absorption

such as active/passive/facilitated uptake processes, removal via efflux transporters such as P-gp, degradation via drug metabolizing enzymes such as CYP450s. Therefore, early assessment of the relative contributions of each of these components to drug absorption is useful to eliminate potential ‘problem’ drugs and identify those molecules that have a good pharmacokinetic profile to go hand in hand with their biological effectiveness. Moreover, this information could be extremely valuable to medicinal chemists in the selection of favorable chemo-types.

Numerous in vitro and in vivo model systems have been used to assess the potential absorption of new chemical entities. Many laboratories rely on cell culture models of intestinal permeability such as, Caco-2, HT-29 and MDCK. To attempt to increase the throughput of permeability measurements, several physicochemical methods such as, immobilized artificial membrane (IAM) columns and parallel artificial membrane permeation assay (PAMPA) have been used. More recently, much attention has been given to the development of computational methods to predict drug absorption. Other in vitro techniques available for studying drug absorption include everted rat intestinal sac model, Ussing-chambers, in situ and in vivo perfusion of rat intestines. However, those techniques have own limitations including the loss of viability of various isolated intestinal preparations, as well as the difficulty of extrapolating results obtained in animal models to humans. Now, it is clear that no single method is sufficient for studying drug absorption, but most likely a combination of systems is needed.

2.3.2 Distribution evaluation

Drug distribution describes the movement of drug molecules from the systemic circulation to extravascular site. Since most drug targets are not in the vasculature, access to target sites commonly relies on drug distribution. The distribution process is controlled by the passive diffusion across lipid membranes, the presence of carrier-mediated active transport

processes involving the xenobiotic, and the protein binding in the blood and tissues. When distribution reaches equilibrium between blood and tissue, drug concentrations in tissues and extracellular fluids are reflected by the plasma concentration (if no drug elimination in tissues). Metabolism and excretion occur simultaneously with distribution, making the process dynamic and complex.

Volume of distribution (V_d): Volume of distribution has nothing to do with the actual volume of the body or its fluid compartments but rather involves the distribution of the drug within the body. It is a useful parameter in considering the relative amount of drug outside the central compartment or in the tissues. Drugs that remain in the circulation tend to have a low volume of distribution. For drugs that are highly tissue-bound, comparatively little of a dose remains in the circulation to be measured; thus, plasma concentration is low and volume of distribution is high. If V_d approximates plasma volume (~ 0.04 L/kg in humans), this suggests that the molecule distributes only in the vasculature. On the other hand, a $V_d \sim 0.6$ L/kg indicates distribution into total body water. A volume greater than ~ 2 L/kg implies extensive distribution into tissues. Each drug is uniquely distributed in the body. Some drugs distribute mostly into fat, others remain in ECF, and others are bound extensively to specific tissues. Volume of distribution provides a reference for the plasma concentration expected for a given dose but provides little information about the specific pattern of distribution.

Binding: A thorough understanding of plasma and tissue (brain, liver, etc.) protein binding is crucial for evaluating the distribution of drug candidates. Binding of drugs to plasma proteins [e.g. human serum albumin, α_1 -acid glycoprotein (α -AGP)] limits drug free motion, and reduces the volume of distribution, renal extraction, liver metabolism and tissue penetration. In some cases, plasma protein binding data is useful for diagnosing complex *in vivo* effects, such as

low brain penetration, once *in vivo* experiments have been performed. Moreover, plasma protein binding data are useful to design optimal dose regimens for efficacy studies and to estimate safety margins during drug development. Drug tissue binding can cause accumulation of drugs in tissues or body compartments, which can prolong drug action because the tissues release the accumulated drug as plasma drug concentration decreases. Some drugs accumulate within cells because they bind with proteins, phospholipids, or nucleic acids [75].

In vitro studies with plasma have proven to be a valuable tool for predicting *in vivo* protein binding. Plasma and tissue protein binding can be measured by equilibrium dialysis and ultrafiltration. Plasma protein binding can also be estimated using Human serum albumin (HAS) HPLC chromatography [76], 96-well equilibrium dialysis [77], Biacore[®], or 96-well Microcon[®] ultrafiltration.

Blood-brain barrier: Drugs reach the central nervous system (CNS) via brain capillaries and cerebrospinal fluid (CSF). Although the brain receives about $\frac{1}{6}$ of cardiac output, distribution of drugs to brain tissue is restricted [78]. In some cases, lipid-soluble drugs (eg, thiopental) enter the brain readily, polar compounds do not. The reason is the blood-brain barrier (BBB), which consists of the endothelium of brain capillaries and the astrocytic sheath. The endothelial cells of brain capillaries, which are more tightly joined to one another than those of most capillaries, slow the diffusion of water-soluble drugs. That make the brain's permeability characteristics differ from those of other tissues The drug penetration rate into CSF, as for other tissue cells, is determined mainly by the extent of protein binding, degree of ionization, lipid-water partition coefficient of the drug and active transporters. Recently, *in vitro* cell models have been developed to assess blood-brain barrier permeability and the transport of novel compounds [78]. Primary culture models of endothelial cells grown in the presence or absence of astrocytes

provide good models of blood-brain barrier properties, but are too slow and costly for routine use. Instead, generic permeability models such as Caco-2 or MDCK cells are commonly used to predict blood-brain barrier permeability, though their limitations need to be recognized [79]. The astrocyte co-culture blood-brain barrier model remains the models of choice for more detailed mechanistic studies [80].

2.3.3 Metabolic evaluation

Metabolism is the conversion of drug in the body to another chemical form or metabolite. The metabolite may be active or inactive, but, once metabolism occurs, drug is considered out of the body even though the metabolite remains. The metabolite would have a different kinetic profile from that of the drug. Metabolism is usually enzymatic, most often occurs in the liver, and may involve either phase 1 reaction (i.e., oxidation, reduction, hydrolysis, and/or dealkylation) or phase 2 reaction (i.e., acetylation, sulfation, and glucuronidation). The most important enzyme system of phase I metabolism is cytochrome P-450 (CYP-450), a microsomal superfamily of isoenzymes that catalyze the oxidation of many drugs. CYP-450 enzymes can be induced or inhibited by many drugs and substances, helping explain many drug interactions in which one drug enhances the toxicity or reduces the therapeutic effect of another drug.

Drug metabolism plays an increasingly important role in drug discovery and development. Understanding the metabolic fate of a drug and routes of elimination early in drug development can provide valuable information for further development. Such information can help identify the potential for drug interactions in human, explain interindividual and ethnic differences, and indicated the need for further pharmacological characterization or structure modification.

Determination of metabolic pathways. It is important to understanding the metabolic pathways in order to accurately predict human clearance. To understand the metabolic pathways,

identification of the metabolites is critical. *In vivo* systems can be used to generate a large quantity of metabolites by selective use of various reagents and cofactors. The structure of metabolites can be elucidated by LC/MS, LC/MS/MS or NMR, which will help to confirm the metabolic pathway [81]. It is important to select animal species that have metabolic profiles similar to humans. The metabolic profile of a drug obtained *in vitro* generally reflects the *in vivo* metabolite pattern, although limited to qualitative aspects. From physiological and biochemical points of view, precision-cut liver slices are especially useful to obtain the complete *in vitro* metabolite profile of a drug, because this system retains the physiological conditions of enzymes and cofactors of both phase I and phase II reactions and, therefore, better simulates the *in vivo* situation [82]. Isolated and cultured hepatocytes are also used often as *in vitro* models for identifying metabolic pathways of drugs. Another important consideration is the choice of drug concentrations for *in vitro* studies. The major metabolic pathway may be shifted, depending on the drug concentration used [83].

Identification of drug-metabolizing enzymes. To identify which cytochrome P-450 isozymes are responsible for metabolizing drugs in humans, several *in vitro* approaches have been developed, including (1) use of selective inhibitors with microsomes, (2) demonstration of catalytic activity in cDNA-based vector systems, (3) metabolic correlation of an activity with markers for known enzymes, (4) immunoinhibition of catalytic activity in microsomes, and (5) catalytic activity of purified enzyme isoforms [84]. Each approach has its advantages and disadvantages, and a combination of approaches is usually required to accurately identify which cytochrome P-450 isozyme is responsible for metabolizing a drug. Metabolism of drugs is usually very complex, involving several pathways and various enzyme systems. In some cases,

all the metabolic reactions of a drug are catalyzed by a single isozyme, whereas, in other cases, a single metabolic reaction may involve multiple isozymes or different enzyme systems.

Drug-drug interactions. Drug-drug interactions are a major source of clinical problems, sometimes with dramatic consequences. Drug-drug interaction studies have become an important aspect of the development process of new drug candidates because of potential adverse effects. Various efficient *in vitro* approaches have been developed during recent years and powerful computer-based data handling is becoming widely available [85]. All these tools allow us to initiate, early in the development of new chemical entities, large-scale studies on the interactions of drugs with selective CYP isozymes, drug receptors, and other cellular entities. Standardization and validation of these methodological approaches significantly improve the quality of the data generated and the reliability of their interpretation. The simplicity and the low costs associated with the use of *in vitro* techniques have made them a method of choice to investigate drug-drug interactions.

Prediction of *in vivo* metabolic clearance. One of the main objectives of *in vitro* metabolism studies is the quantitative prediction of *in vivo* drug metabolism from *in vitro* data. The prediction of metabolic clearance from *in vitro* systems is difficult and highly controversial. Despite the difficulty of extrapolating *in vitro* data, it is believed that quantitative *in vitro* metabolic data can be extrapolated reasonably well to *in vivo* situations with the application of appropriate pharmacokinetic principles [86].

2.3.4 Excretion evaluation

The kidneys, which excrete water-soluble substances, are the principal organs of excretion. The biliary system contributes to excretion to the degree that drug is not reabsorbed

from the GI tract. Generally, the contribution of intestine, saliva, sweat, breast milk, and lungs to excretion is small, except for exhalation of volatile anesthetics [56].

Renal excretion. The kidneys are responsible for the elimination of many endogenous byproducts and, through the same mechanisms, many drugs are cleared from the body. There are three major processes for drug elimination in the kidney: glomerular filtration, tubular secretion and tubular reabsorption. The principles of transmembrane passage govern renal handling of drugs. Drug filtration is a diffusional passive process. Drugs bound to plasma proteins remain in the circulation; only unbound drug is contained in the glomerular filtrate. Tubular secretion and reabsorption involve both passive and active transport processes across the membranes. Un-ionized forms of drugs and their metabolites tend to be reabsorbed readily from tubular fluids. The extent to which changes in urinary pH alter the rate of drug elimination depends on the contribution of the renal route to total elimination, the polarity of the un-ionized form, and the molecule's degree of ionization [67].

Active tubular secretion in the proximal tubule is important in the elimination of many drugs. The tubular secretion of drugs is mediated by many active transporters, which take up compounds from the kidney interstitium and efflux them into the tubular lumen. Organic anion (OATs) and organic cation transporters (OCTs) are the two major classes of uptake transporters, but OCTNs and OATPs can also be found in the kidney. Efflux transporters such as P-glycoprotein and MRPs are also found in the kidney tubule [69].

Active transport in the kidney can be studied by the preparation of vesicles from brush border membranes or tubules, by using uptake in kidney derived cell lines like MDCK and HEK cells, or vesicles prepared from these cells; as well as using isolated perfused rat kidney. *In vitro*

studies can be useful to predict a potential mechanism of clearance or a potential drug-drug interaction, and allow for well-designed, focused clinical trials to address these questions [70].

Biliary excretion. Some drugs and their metabolites are extensively excreted in bile. Because they are transported across the biliary epithelium against a concentration gradient, active secretory transport is required. When plasma drug concentrations are high, secretory transport may approach an upper limit (transport maximum). Drugs with a mol wt > 300 g/mole and with both polar and lipophilic groups are more likely to be excreted in bile; smaller molecules are generally excreted only in negligible amounts. Conjugation, particularly with glucuronic acid, facilitates biliary excretion. In the enterohepatic cycle, a drug secreted in bile is reabsorbed into the circulation from the intestine. Biliary excretion eliminates substances from the body only to the extent that enterohepatic cycling is incomplete—when some of the secreted drug is not reabsorbed from the intestine [74].

Studies designed to measure biliary excretion in rats and dogs should take into account that compounds need first to be taken up or transferred from the plasma to the liver cell, either by passive diffusion or an active transporter; and then be effluxed by one or several transporters in the canalicular side. By measuring bile flow, and drug concentration in plasma and bile, biliary clearance can be calculated as $CL_B = (\text{concentration in bile}) * \text{bile flow} / \text{concentration in plasma}$ [75].

2.3.5. Active transporters evaluation in pharmacokinetics

Specific transport proteins catalyze the movement of many water-soluble ions, nutrients, metabolites and drugs across cell membranes. It has been estimated that there are at least 2000 transporters in the human genome, most of which have yet to be cloned, and it is becoming clear that transporters play a significant role in ADME processes [58]. For absorption, a clear role has

emerged for P-glycoprotein in limiting permeability across the gastrointestinal tract. As a result, a wide variety of drugs suffer from incomplete, variable and non-linear absorption. Similarly, at the blood-brain barrier a range of drugs has limited brain penetration due to P-glycoprotein-mediated efflux, which can limit therapeutic effectiveness of CNS agents [67]. In the liver, transport proteins are present on the sinusoidal membrane that can be the rate-limiting step in hepatic clearance for some drugs. Mechanistic studies clearly suggest a key role and broad substrate specificity for the OATP family of sinusoidal transporters. Mainly ATP-dependent transport proteins such as P-glycoprotein and MRP2 govern active biliary excretion. Moreover, drug-drug interactions have been demonstrated involving inhibition or induction of transport proteins. Clinically significant interactions in the gastrointestinal tract and kidney have been observed with inhibitors such as ketoconazole, erythromycin, verapamil, quinidine, probenecid and cimetidine. Transporter involvement in humans cannot currently be accurately predicted from non-clinical studies. Prediction based on animal data could be flawed because some reports indicate that there are marked species differences in the tissue distribution of transporters and their substrate specificity. Thus, current best practice include performing bidirectional transport studies in Caco-2 cell, using concentrations corresponding to clinical dosage dissolved in 250 ml or less (thereby achieving a concentration similar to that in the GI tract following oral dosing in humans) [67].

2.4 Mathematical models of Pharmacokinetics

Pharmacokinetic models are used to permit the rational prediction, of the events occurring during the processes of drug disposition throughout the body, thus yielding tissue levels.

2.4.1 Compartmental modeling

In drug concentration versus time profiles, drug concentrations are often observed to decline in a mono- or multi-exponential fashion. In compartmental PK analysis, these data are fit to an exponential equation that is derived by assuming that the body consists of one or more compartments through which the administered drug distributes. In general, the number of compartments used in the model is equal to the number of identifiable phases when the $\ln C$ are plotted versus time. Compartmental approaches allow some level of “physiological” interpretation of what the body does to the drug (i.e. should be consistent with physiologically reasonable pathways of drug elimination). At least one of the compartments must be a sampling compartment (typically the central compartment). Rate constants describe drug transfer between compartments and a set of differential equations is written to describe the concentrations in each compartment versus time. The equation describing the change in concentration in the sampled compartment is fit to the blood or plasma drug concentration versus time data and pharmacokinetic parameters in the model are estimated using nonlinear regression.

A. One-Compartment Model

When the concentration versus time profile follows mono-exponential decline, the data is described by a one-compartment model [69]. In this model, there is immediate equilibration with all peripheral compartments, such that the latter are indistinguishable from the central compartment. The slope describing the decline is equal to k , the elimination rate constant. There is only one volume, $V_c = V_{ss}$, and concentrations can be described by the equation: $C_1 = (\text{Dose}/V_c) \cdot e^{-k \cdot t}$

B. Two-Compartment Model

When the concentration versus time profile displays bi-exponential decline, a model incorporating a peripheral in addition to the central compartment will better describe the data.

The rates of change in concentration in the two compartments are described by two differential equations [69]. Solving these for the concentration in the central (sampled) compartment yields: $C_1 = A \cdot e^{-\alpha \cdot t} + B \cdot e^{-\beta \cdot t}$, where A and B are functions of the dose, α and β are the distribution and the elimination rate constants. It can also be shown that the two half-lives are defined by both clearance and distribution rate constants. Conceptually, this is thus consistent with the terminal half-life determined by non-compartmental methods being a function of CL and V.

Those compartment models described above are with i.v. bolus dosing. With extravascular administration, corresponding models contain an additional extravascular compartment with, in the simplest case, an absorption rate constant describing input into the central compartment [69]. Models with three or greater compartments may be used if the drug concentration versus time data appear better described with additional exponential terms. However, the greater complexity of the model must be supported by the richness of the data, or robust pharmacokinetic parameter estimation becomes impossible.

2.4.2 Nonlinear compartmental modeling

Compartmental models are not just confined to linear systems. It is relatively easy to include a nonlinear process such as saturable metabolism or protein binding. For example, for some drugs one or more metabolism processes may follow Michaelis-Menten kinetics. Elimination is described in equation $dC/dt = -(V_m \times C) / (K_m + C)$, with a nonlinear metabolism process with the parameters V_m (maximum velocity) and K_m (Michaelis constant) [81].

At high concentrations, the denominator $K_m + C$ approaches C and the equation above becomes zero order with $dC/dt = -V_m$. At concentrations much lower than K_m , the denominator $K_m + C$ approaches K_m and the equation above becomes a first order equation with $k' = V_m / K_m$. Nonlinear compartmental models lead to more complex data analysis and dosage regimen

calculation. However, the compartmental approach allows these calculations to be made with good data or accurate estimates of the parameter [81].

Another example of nonlinear elimination is the case of saturable protein binding. For some drugs, present at higher concentrations, the available binding sites on plasma protein may be saturated. Thus, at high concentrations the free fraction may be higher than at lower concentrations. This can lead to faster elimination at higher concentrations when renal elimination by filtration is a major route of elimination. This phenomenon can be analyzed using compartmental models by modifying the elimination process as shown in equation $dC_t/dt = -k_{el} \cdot C_f$, where C_f is the free drug concentration, C_t is the total drug concentration.

2.4.3 Non-compartmental modeling

Noncompartmental models can be used to determine certain pharmacokinetic parameters without deciding on a particular compartmental model. The basic calculations are based on the area under the plasma concentration versus times curve (zero moment) and the first moment curve (AUMC) [84]. Therefore, no assumptions are made based on the shape of the blood or plasma drug concentration versus time curve, as is the case with compartmental methods. Noncompartmental model thus furnish important pharmacokinetic data such as AUC, CL, F, $t_{1/2}$, and V_{ss} in a simple and rapid manner. However, note that in calculating CL, an important assumption must still be made: that the drug undergoes first-order (unsaturable) elimination. In other words, that clearance is constant and the rate of drug elimination from blood or plasma is linearly proportional to its concentration. An important limitation of noncompartmental pharmacokinetic analysis is that it lacks the ability to predict pharmacokinetic profiles when there are alterations in a dosing regimen, which compartmental pharmacokinetic methods afford [84].

Utilization of noncompartmental modeling techniques allows problems to be approached in a more general way. This means there are fewer assumptions that usually can be verified easily with a well-designed study. It is also possible focus on a specific kinetic process (e.g., absorption, distribution, or elimination). When a problem can be approached in a more general way, then stronger predictions about future events can be made.

3 Pharmacokinetic-Pharmacodynamic modeling (PK-PD modeling)

PK–PD modeling is the mathematical approach that links the change in drug concentration over time (pharmacokinetic) to the relationship between the concentration at the effect site and the intensity of the observed response (PD). The resulting integrated PK–PD models allow a description of the complete time course of the effect intensity in response to a given dosing regimen [87].

PK-PD modeling also allows the estimation of PK-PD parameters and the prediction of these derived, clinically relevant parameters as well. PK-PD simulations allow the assessment of the descriptive parameters as functions of dose and dose rate. These simulations can provide the dose–response curve for onset, magnitude, and duration of effect. This information can be valuable in optimizing dose and dosing regimens. Currently, there is growing recognition of the importance of PK-PD studies in all phases of drug development [88-91]. In preclinical studies, PK-PD is used to interpret pharmacokinetic data [91], and via physiologic modeling and allometric scaling, it is also used to extrapolate results from animals to humans [92, 93]. During early clinical testing, PK-PD is used to aid in the interpretation of dose–response and escalation studies. In addition, there are several instances in which PK-PD modeling has been used by regulatory agencies to recommend a dose and/or regimen not originally studied as part of the clinical program [94].

4 Physiologically based pharmacokinetic modeling (PBPK modeling)

The basic idea of physiologically based pharmacokinetic modeling was to extend pharmacokinetic modeling so that quantitative aspects of other biological areas could be incorporated. The major structural elements of the PBPK model are derived from the anatomical structure of the organism; therefore, the model structure is predetermined and basically independent of the drug of interest. Features of PBPK models include 1) mass balance approach to characterize drug disposition, 2) utilize differential equations to describe model systems, 3) rational to consider PBPK approach if focus is on understanding drug disposition in tissues, 4) offer greatest potential to predict drug concentrations under different physiological and pharmacological conditions, and 5) can be scaled-up from animals to humans.

The PBPK model input parameters include both a drug-independent and a drug-specific subset. The first subset comprises data underlying the physiological processes (e.g., blood flow), and the second subset comprises drug-specific biochemical parameters. The latter consists of the drug's *in vivo* intrinsic clearance (CL_{int}) of each organ involved in its elimination, in addition to estimates of the drug's tissue-to-plasma coefficient (P_{tp}) for each model compartment.

The software available for PBPK model user can generally be classified into three classes. The first class comprises general mathematical and engineering modeling software such as MATLAB, STELLA, Berkeley Madonna. The second type of software that can be used for PBPK modeling is the general pharmacokinetic modeling software, which is not specific for PBPK, but intended for general pharmacokinetic applications. For example, ADAPT, NONMEM, and WINNONLIN. The third type of software products, starting to emerge more recently, are the specialized PBPK modeling software packages, such as ACSLXTREME, PK-SIM and PKQUEST. Selecting the type of software for PBPK model development and

application should be based on the modeling purpose (e.g., parameter estimation versus simulation), the sophistication level of the modeler (e.g., using GUI, click-and-drag versus model equations specification) and the specific problem (e.g., linear versus nonlinear or ordinary versus partial differential equation systems, etc.).

During the preclinical phase, the overall pharmacokinetics of potential drug candidates in animals and in humans (through a combination of scaling of physiological parameters and use of *in vitro* data) can be anticipated through the use of PBPK modeling [95]. Accounting for differences in tissue-specific transporters and binding sites, PBPK models help to improve the design of preclinical and clinical studies. Further, the simulated concentration-time profiles in main organs, in addition to experimental plasma profiles, are valuable to identify critical accumulation effects or to allow target-specific pharmacokinetic-pharmacodynamic (PKPD) analyses [96]. Such PBPK/PD evaluations provide crucial information on the potency and safety of drug candidates *in vivo* and bridge PKPD concepts established during the preclinical phase to clinical studies.

5 Where do new drugs come from?

5.1 Natural product sources

Natural products have played a significant role in drug discovery [97]. Natural product derived compounds have led to the discovery of many drugs to treat human disease. This has resulted in the use of a large number of medicinal plants to treat various diseases, and some drugs in Western medicine are based on the traditional use of such drugs. Some are used as pure compounds from the traditional medicinal plant, such as atropine, morphine, quinine and digitoxin, and others as modifications of such compounds, such as aspirin and local anaesthetics. In the areas of cancer and infectious disease, 60 and 75%, respectively, of new drugs, originate

from natural sources [97]. In total, 119 plant-derived compounds are used in Western medicine, and of the world's 25 best-selling pharmaceutical agents, 12 are derived from natural products [97]. That means that the hit rate among natural products is apparently much higher than in libraries derived by random synthesis, in which 10,000 compounds are said to be necessary to develop one new drug [98].

Natural product compounds not only serve as drugs or templates for drugs directly, but in many instances, lead to the discovery of novel biology that provides a better understanding of targets and pathways involved in the disease process. Compounds that interact with novel targets, such as, the protein–protein complexes, B-catenin in the WNT pathway and HIF-1/p300, have validated these anticancer targets and pathways [98]. These compounds create opportunities for further drug targets to be identified and exploited in these pathways.

In order for natural product drug discovery to continue to be successful, new and innovative tools are required. Some of these new tools include the use of advances in genomics, searching for natural product compounds in environments that have not been efficiently mined in the past and applying new screening technologies. The marine environment is a largely untapped source of chemical diversity. The opportunity to discover new species and therefore, new chemical diversity has increased through the application of new tools to explore the marine environment. This new chemical diversity combined with our current understanding of disease processes will improve the ability to discover compounds with therapeutic utility.

Natural products continue as a source for innovation in drug discovery by playing a significant role in the discovery and understanding of cellular pathways that are an essential component in the drug discovery process [99, 100].

5.2 Chemical synthesis sources

Traditionally, chemical syntheses in laboratories duplicate natural processes to produce compounds with pharmacological effect, or modify chemical structure of natural compounds. Frequently, chemical structure modification can eliminate side effects and increase the potency of the drug [100]. Examples include barbiturates, sulfonamides, and aspirin. Unlike compounds of natural origin that can be fairly complex, those synthetic drugs are usually much simpler molecules. With the development of new technology in organic synthetic chemistry, and a deeper understanding of interrelated disciplines, the strategies of synthetic chemistry, as an important part in drug discovery processes, has been changed. More and more hit or lead compounds are produced by chemical synthesis, and chemical library for screening of drug discovery has been established [100].

Prodrugs are compounds which are inactive in themselves, but which are converted in the body to the active drug. They have been useful in addressing problems such as acid sensitivity, poor membrane permeability, drug toxicity, bad taste, and short duration of action [101]. Usually, a metabolic enzyme is involved in converting the prodrug to the active drug, and so a good knowledge of drug metabolism and the enzymes involved allows the medicinal chemist to design a suitable prodrug which turns drug metabolism into an advantage rather than a problem.

Combinatorial synthesis is an automated solid-phase procedure aimed at producing as many different structures as possible in as short a time as possible. The reactions are carried out on very small scale, often in a way that will produce mixtures of compounds in each reaction vial. In a sense, combinatorial synthesis aims to mimic what plants do, i.e. produce a pool of chemicals, one of which may prove to be a useful lead compound. This technique was developed to meet the urgent need for new lead compounds for the ever increasing number of novel targets

discovered by genomic and proteomic project. Now, it is an effective method of producing large numbers of analogues for drug development and for studies into structure activity relationship.

Computer-aided design of lead compound. A detailed knowledge of a target binding site significantly aids in the design of novel lead compounds intended to bind with that target. Leads by design tend to be more effective, more specific, and less toxic than the product manufactured in traditional ways. In cases where enzymes or receptors can be crystallized, it is possible to determine the structure of a protein and its binding site by X-ray crystallography. Molecular modeling software programs can then be used to study the binding site, and to design molecules that will fit and bind to the site-*de novo* drug design. In some cases, the enzyme or receptor cannot be crystallized and so X-ray crystallography cannot be carried out. However, if the structure of an analogous protein has been determined, this can be used as a basis for generating a computer model of the protein.

5.2 Reformulation

The process by which older drugs are modified to make them more attractive is called "reformulation." The reason for reformulation of older drugs is 1) poor biopharmaceutical quality, 2) poor patient compliance associated with the inconvenience of frequent administration, and 3) delivery pattern with poor therapeutic effect [101].

One of the drugs that underwent reformulation was saquinavir, Hoffmann-LaRoche's protease inhibitor. Invirase, the first approved formulation of saquinavir, suffered from poor bioavailability. This drawback considerably weakened saquinavir's activity against HIV and caused the development of drug resistant virus in many people. In response, the manufacturer repackaged the drug into capsules made of soft gelatin (the original capsules were made of hard gelatin) to increase the amount of drug released in the GI tract [101].

Understanding and development of relevant nano-assemblies have grown over the last decade. At least 35 nanotechnology drug reformulations are in development. It is therefore almost certain that new nano-based approaches will be used increasingly. Such technologies may not only bring about a new generation of novel drugs, but will also greatly facilitate the redevelopment of drugs in current use to greater therapeutic efficacy. Exciting advances have been made in breaking the barriers of cancerous tumours that ensure their success by using the nanoparticle as the delivery agent instead of the drug itself.

Alternatively, reformulation is a widely employed Product lifecycle management (LCM) technique. According to a report from Data monitor (Reformulation Strategies — Comparisons of Past and Future Reformulation Strategies, September 2006), reformulation has become an almost ubiquitous product lifecycle management technique. The top 50 manufacturers used reformulation for almost two thirds of product launches during 2002–2005 [101]. It indicates that new markets for old drugs or ways to modify a formulation to allow it to enter a new market could be the key to keeping productivity from stalling as markets for older products dry up, patents expire and profit margins continue to be eroded by market pressures, competitor products and generic alternatives.

REFERENCE

- [1] Houston, J.G.; Banks, M. *Curr. Opin. Biotechnol.*, 1997, 8, 734.
- [2]. Bosse, R.; IIIy, C.; Elands, J.; Chelsky, D. *DDT*, 2000, 15, S42.
- [3] Hertzberg, R.P.; Pope, A.J. *Curr. Opin. Chem. Biol.*, 2000, 4, 445.
- [4] Kariv, I.; Chung, T.D.Y. *Curr. Drug Dev.*, 2001, 3, 28.
- [5] Oldenburg, K.R.; Kariv, I.; Zhang, J.-H.; Chung, T. D.Y.; Lin, S.; In Handbook of Drug Screenig; Seethala, R.; Fernandes, P. Eds.; Marcel Dekker, Inc.: New York, 2001, pp. 525-562

- [6] Rodrigues, A.D. *Med. Chem. Res.*, 1998, 8, 422.
- [7] Selkirk, A.; *Pharm. Sci. Technol. Today*, 1998, 1, 8.
- [8] Panchaganula, R.; Thomas, N.S. *Int. J. Pharm.*, 2000, 201, 131.
- [9] Chaturvedi, P.; Decker, C.J.; Odinecs, A. *Curr. Opin. Chem. Biol.*, 2001, 5, 452
- [10] P.J. Eddershaw *et al.*, ADME/PK as part of a rational approach to drug discovery. *Drug Discov. Today* 5 (2000), pp. 409–414M.H.
- [11] Tarbit and J. Breman, High-throughput approaches for evaluating absorption, distribution, metabolism and excretion properties of lead compounds. *Curr. Opin. Chem. Biol.* 2 (1998), pp. 411–416
- [12] D.A. Smith and H. van de Waterbeemd, Pharmacokinetics and metabolism in early drug discovery. *Curr. Opin. Chem. Biol.* 3 (1999), pp. 373–378
- [13] C.K. Atterwill and M.G. Wing, *In vitro* preclinical lead optimization technologies (PLOTs) in pharmaceutical development. *Toxicol. Lett.* 127 (2002), pp. 143–151
- [14] S.A. Roberts, Drug metabolism and pharmacokinetics in drug discovery. *Curr. Opin. Drug Discov. Dev.* 6 (2003), pp. 66–80J.
- [15] Lin *et al.*, The role of absorption, distribution, metabolism, excretion and toxicity in drug discovery. *Curr. Top. Med. Chem.* 3 (2003), pp. 1125–1154
- [16] S.A. Roberts, Drug metabolism and pharmacokinetics in drug discovery, *Curr. Opin. Drug Discov. Dev.* 6 (2003), pp. 66–80.
- [17] I. Kola and J. Landis, Can the pharmaceutical industry reduce attrition rates?, *Nat. Rev. Drug Discov.* 3 (2004), pp. 711–715
- [18] E.H. Kerns and L. Di, Pharmaceutical profiling in drug discovery, *DDT* 8 (2003), pp. 316–323.

- [19] D.A. Smith and H. van de Waterbeemd, Pharmacokinetics and metabolism in early drug discovery, *Curr. Opin. Chem. Biol.* 3 (1999), pp. 373–378
- [20] Somberg, J. In Drug Development Process: Increasing Efficiency and Cost-Effectiveness; Welling, P.G.; Lasagna, L.; Banakar, U.V. Eds. *Marcel Dekker, Inc.*: New York, 1996, pp. 1-37.
- [21] Kaitin, K. In Speed to Market Achieving Breakthrough Performance; Case Studies in R&D Management; Kaitin, K.I.; Levy, M. Eds. *The American Academy of Arts and Science: Cambridge*, 1997, pp. 6-9.
- [22] Krebs, R. *Curr. Opin. Drug Discov. Dev.*, 1999, 2, 239.
- [23] Lipinski, C. *J. Pharmacol. Toxicol. Meth.*, 2000, 44, 235.
- [24] Venkatesh, S.; Lipper, R.A. *J. Pharmaceut. Sci.*, 1999, 89, 145.
- [25] Caldwell, G. *Curr. Opin. Drug Discov.*, 2000, 3, 30.
- [26] Tarbit, M.H.; Berman, J. *Curr. Opin. Chem. Biol.*, 1998, 2, 411.
- [27] Smith, D.A.; Van de Waterbeemd, H. *Curr. Opin. Chem. Biol.*, 1999, 3, 373.
- [28] Eddershaw, P.J.; Beresford, A.P.; Bayliss, M.K. *DDT*, 2000, 5, 409.
- [29] Masimirembwa, C.M.; Homson, R.; Andersson, T.B. *Comb. Chem. High Throughput Screen.*, 2001, 4, 245.
- [30] Holford N.H., Kimko H.C., Monteleone J.P., C.C. Peck, Simulation of clinical trials, *Annu. Rev. Pharmacol. Toxicol.* 40 (2000) 209–234
- [31] M.E. Burton, M.R. Vasko, D.C. Brater, Comparison of drug dosing methods, *Clin. Pharmacokinet.* 10 (1985) 1–37
- [32] Sheiner L., Wakeld J., Population modelling in drug development, *Stat. Methods Med. Res.* 8 (1999) 183–193

- [33] Ong, S. *et al.* (1996) Immobilized-artificial membrane chromatography: measurements of membrane partition coefficient and predicting drug membrane permeability. *J. Chromatogr. A* 728, 113–128
- [34] Ong, S.; Liu, H.; Pidgeon, C. Immobilized-artificial membrane chromatography: measurements of membrane partition coefficient and predicting drug membrane permeability. *J. Chrom. A.* 1996, 728, 113-128.
- [35] Pidgeon, C.; Ong, S.; Liu, H.; Qiu, X.; Pidgeon, M.; Dantzig, A.H.; Munroe, J.; Hornback, W.J.; Kasher, J.S.; Glunz, L. *et al.* IAM chromatography: An in vitro screen for predicting drug membrane permeability. *J. Med. Chem.* 1995, 38, 590-594
- [36] Artursson, P. *et al.* (2001) Caco-2 monolayers in experimental and theoretical predictions of drug transport. *Adv. Drug Deliv. Rev.* 46, 27–43.
- [37] Hidalgo, I.J. (2001) Assessing the absorption of new pharmaceuticals. *Curr. Top. Med. Chem.* 1, 385–401
- [38] Irvine, J.D. *et al.* (1999) MDCK (Madin-Darby canine kidney) cells: a tool for membrane permeability screening. *J. Pharm. Sci.* 88, 28–33
- [39] Lipinski, C.A. (2001) Avoiding investment in doomed drugs. *Curr. Drug Discov.* April, 17–19
- [40] Menard, C.A. *et al.* (2001) Comparison of Caco-2 permeability data in 24- and 96 well formats. *Book of Abstracts. Lab Automation* January, 2001
- [41] Kansy, M. *et al.* (1998) Physicochemical high throughput screening: parallel artificial membrane permeation assay in the description of passive absorption processes. *J. Med. Chem.* 41, 1007–1010.

- [42] Avdeef, A. *et al.* (2001) Drug absorption *in vitro* model: filter-immobilized artificial membranes studies of the permeability properties of lactones in *Piper methysticum* Forst. *Eur. J. Pharm. Sci.* 14, 271–280
- [43] Korfmacher, W.A. *et al.* (1999) Development of an automated mass spectrometry system for the quantitative analysis of liver microsomal incubation samples: a tool for rapid screening of new compounds for metabolic stability. *Rapid Commun. Mass Spectrom.* 13, 901–907
- [44] Mandagere, A.K. *et al.* (2002) Graphical model for estimating oral bioavailability of drugs in humans and other species from their Caco-2 permeability and *in vitro* liver enzyme metabolic stability rates. *J. Med. Chem.* 45, 304–311
- [45] Rourick, R.A. *et al.* (1996) Predictive strategy for the rapid structure elucidation of drug degradants. *J. Pharm. Biomed. Anal.* 14, 1743–1752
- [46] Li, A.P. (2001) Higher-throughput screening assays with human hepatocytes for hepatotoxicity, metabolic stability, and drug-drug interaction potential. In *Drugs and the Pharmaceutical Sciences, 114 (Handbook of Drug Screening)*, pp. 383–402
- [47] Wang, G. *et al.* (2002) Semi-automated determination of plasma stability of drug discovery compounds using liquid chromatography-tandem mass spectrometry. *J. Chromatogr. B Biomed. Sci. Appl.* 780, 451–457
- [48] Obach, R.S. Prediction of Human Clearance of Twenty- Nine Drugs from Hepatic Microsomal Intrinsic Clearance Data: An Examination of *In Vitro* Half-Life Approach and Nonspecific Binding to Microsomes. *Drug Metab. Dispos.* 1999, 27(11), 1350-1359.
- [49] Kerns, E.H. *et al.* (1997) Buspirone metabolite structure profile using a standard liquid chromatographic-mass spectrometric protocol. *J. Chromatogr. B Biomed. Sci. Appl.* 698, 133–145.

- [50] Lopez, L.L. *et al.* (1998) Identification of drug metabolites in biological matrices by intelligent automated liquid chromatography/tandem mass spectrometry. *Rapid Commun. Mass Spectrom.* 12, 1756–1760
- [51] Shockcor, J.P. (2000) Application of directly coupled LC-NMR-MS to the structural elucidation of metabolites of the HIV-1 reverse transcriptase inhibitor BW935U83. *J. Chromatogr. B Biomed. Sci. Appl.* 748, 269–279
- [52] Van Asperen, J. *et al.* (1998) The pharmacological role of P-glycoprotein in the intestinal epithelium. *Pharmacol. Res.* 37, 429–435
- [53] van de Waterbeemd, H. *et al.* (2001) Property-based design: optimization of drug absorption and pharmacokinetics. *J. Med. Chem.* 44, 1313–1333
- [54] Rodrigues, A.D. and Lin, J.H. (2001) Screening of drug candidates for their drug-drug interaction potential. *Curr. Opin. Chem. Biol.* 5, 396–401
- [55] Gao, F. *et al.* (2002) Optimizing higher throughput methods to assess drugdrug interactions for CYP1A2, CYP2C9, CYP2C19, CYP2D6, rCYP2D6, and CYP3A4 *in vitro* using a single point IC₅₀. *J. Biomol. Screen.* 7, 373–382
- [56] Rodrigues, A.D. and Lin, J.H. (2001) Screening of drug candidates for their drug-drug interaction potential. *Curr. Opin. Chem. Biol.* 5, 396–401
- [57] Chu, I. *et al.* (2000) Validation of higher-throughput high-performance liquid chromatography/atmospheric pressure chemical ionization tandem mass spectrometry assays to conduct cytochrome P450s CYP2D6 and CYP3A4 enzyme inhibition studies in human liver microsomes. *Rapid Commun. Mass Spectrom.* 14, 207–214

- [58] Gao, F. *et al.* (2002) Optimizing higher throughput methods to assess drug-drug interactions for CYP1A2, CYP2C9, CYP2C19, CYP2D6, rCYP2D6, and CYP3A4 *in vitro* using a single point IC50. *J. Biomol. Screen.* 7, 373–382
- [59] Kerns, E.H. *et al.* (1998) Cellular uptake profile of paclitaxel using liquid chromatography tandem mass spectrometry. *Rapid Commun. Mass Spectrom.* 12, 620–624
- [60] Yasushi Ishihama, Toshinobu Miwa, Naoki Asakawa, Drug-plasma protein binding assay by electrokinetic chromatography-frontal analysis, *Electrophoresis* 2002, 23, 951–955
- [61] Olah, T.V. *et al.* (1997) The simultaneous determination of mixtures of drug candidates by liquid chromatography/atmospheric pressure chemical ionization mass spectrometry as an *in vivo* drug screening procedure. *Rapid Commun. Mass Spectrom.* 11, 17–23
- [62] Bajpai, M. and Adkison, K.K. (2000) High-throughput screening for lead optimization: a rational approach. *Curr. Opin. Drug Discov. Dev.* 3, 63–71
- [63] Korfmacher, W.A. *et al.* (2001) Cassette-accelerated rapid rat screen: a systematic procedure for the dosing and liquid chromatography/atmospheric pressure ionization tandem mass spectrometric analysis of new chemical entities as part of new drug discovery. *Rapid Commun. Mass Spectrom.* 15, 335–340
- [64] Muller M: Microdialysis in clinical drug delivery studies. *Adv Drug Deliv Rev* 2000, 45:255-269.
- [65] Hutschala D, Skhirtladze K, Kinstner C, Mayer-Helm B, Muller M, Wolner E, Tschernko EM: In vivo microdialysis to measure antibiotic penetration into soft tissue during cardiac surgery. *Ann Thorac Surg* 2007, 84:1605-1610.

- [66] Legat FJ, Maier A, Dittrich P, Zenahlik P, Kern T, Nuhsbaumer S, Frossard M, Salmhofer W, Kerl H, Muller M: Penetration of fosfomycin into inflammatory lesions in patients with cellulites or diabetic foot syndrome. *Antimicrob Agents Chemother* 2003, 47:371-374.
- [67] Brunner M, Pernerstorfer T, Mayer BX, Eichler HG, Muller M: Surgery and intensive care procedures affect the target site distribution of piperacillin. *Crit Care Med* 2000, 28:1754-1759.
- [68] Burkhardt O, Brunner M, Schmidt S, Grant M, Tang Y, Derendorf H: Penetration of ertapenem into skeletal muscle and subcutaneous adipose tissue in healthy volunteers measured by in vivo microdialysis. *J Antimicrob Chemother* 2006, 58:632-636.
- [69] Farfal S, Klimowicz A, Bielecka-Grzela S: Acyclovir concentrations in the skin of humans after a single oral dose assessed by in vivo cutaneous microdialysis. *Skin Res Technol* 2006, 12:228-234.
- [70] Burkhardt O, Brunner M, Schmidt S, Grant M, Tang Y, Derendorf H: Penetration of ertapenem into skeletal muscle and subcutaneous adipose tissue in healthy volunteers measured by in vivo microdialysis. *J Antimicrob Chemother* 2006, 58:632-636.
- [71] Morgan CJ, Renwick AG, Friedmann PS: The role of stratum corneum and dermal microvascular perfusion in penetration and tissue levels of water-soluble drugs investigated by microdialysis. *Br J Dermatol* 2003, 148:434-443.
- [72] Chaurasia CS, Muller M, Bashaw ED, Benfeldt E, Bolinder J, Bullock R, Bungay PM, DeLange EC, Derendorf H, Elmquist WF et al.: AAPS-FDA workshop white paper: microdialysis principles, application and regulatory perspectives. *Pharm Res* 2007, 24:1014-1025.
- [73] Schmidt S, Banks R, Kumar V, Rand KH, Derendorf H: Clinical microdialysis in skin and soft tissues: an update. *J Clin Pharmacol* 2008, 48:351-364.

- [74] Gan, L.S.L. and Thakker, D.R. (1997) Application of the Caco-2 model in the design and development of orally active drugs: elucidation of biochemical and physical barriers posed by the intestinal epithelium. *Adv. Drug Deliv. Rev.* 23, 77–98
- [75] Tamvakopoulos, C.S. *et al.* (2000) Determination of brain and plasma drug concentrations by liquid chromatography/tandem mass spectrometry. *Rapid Commun. Mass Spectrom.* 14, 1729–1735
- [76] Tiller, P.R. *et al.* (1995) Immobilized human serum albumin: liquid chromatography/mass spectrometry as a method of determining drug-protein binding. *Rapid Commun. Mass Spectrom.* 9, 261–263
- [77] Kariv, I. *et al.* (2001) Development of a high throughput equilibrium dialysis method. *J. Pharm. Sci.* 90, 580–587
- [78] Gumbleton, M. and Audus, K.L. (2001) Progress and limitations in the use of *in vitro* cell cultures to serve as a permeability screen for the blood-brain barrier. *J. Pharm. Sci.* 90, 1681–1698
- [79] Di, L. *et al.* High throughput artificial membrane permeability assay for blood-brain barrier. *Eur. J. Med. Chem.* (2002). 47:371-374
- [80] Smith M. , Omid Y. and Gumbleton M., Primary porcine brain microvascular endothelial cells: Biochemical and functional characterisation as a model for drug transport and targeting, *Journal of Drug Targeting*, 2007, Vol. 15, No. 4, 253-268
- [81] Janiszewski, J.S. *et al.* (2001) A high-capacity LC/MS system for the bioanalysis of samples generated from plate-based metabolic screening. *Anal. Chem.* 73, 1495–1501

- [82] J. H. Lin, Applications and Limitations of Interspecies Scaling and *In Vitro* Extrapolation in Pharmacokinetics, DRUG METABOLISM AND DISPOSITION, Vol. 26, Issue 12, 1202-1212, December 1998
- [83] Le Bigot JF, Begue JM, Kiechel JR and Guillouzo A (1987) Species differences in metabolism of ketotofen in rat, rabbit and human: Demonstration of similar pathways *in vivo* and in cultured hepatocytes. *Life Sci* 40: 883-890
- [84] Guengerich F. P., In Vitro techniques for studying drug metabolism, Journal of Pharmacokinetics and Pharmacodynamics, Volume 24, Number 5 / October, 2001
- [85] Ekins S., Ring B. J., Grace J., McRobie-Belle D. J. and Wrighton S. A., Present and future in vitro approaches for drug metabolism, Journal of Pharmacological and Toxicological Methods, Volume 44, Issue 1, July-August 2000, Pages 313-324
- [86] Lin JH and Lu AYH (1997) Role of pharmacokinetics and metabolism in drug discovery and development. *Pharmacol Rev* 49: 403-449
- [87] H. Derendorf, and B. Meibohm. Modeling of pharmacokinetic/ pharmacodynamic (PK–PD) relationships: concepts and perspectives. *Pharm Res*. 16:176–185 (1999)
- [88] Van Peer A, Snoeck E, Huang ML, Heykants J. Pharmacokinetic-pharmacodynamic relationships in phase I/phase II of drug development. *Eur J Drug Metab Pharmacokinet* 1993;18:149.
- [89] Steimer JL, Ebelin ME, Van Bree J. Pharmacokinetic and pharmacodynamic data and models clinical trials. *Eur J Drug Metab Pharmacokinet* 1993;18:161.
- [90] Lieberman R, McMichael J. Role of pharmacokinetic-pharmacodynamic principles in rational and cost-effective drug development. *Ther Drug Monit* 1996;18(4):423.

- [91] Masri HA, Thomas RS, Benjamin SA, Yang RS. Physiologically based pharmacokinetic/pharmacodynamic modelling of chemical mixtures and possible applications in risk assessment. *Toxicology* 1995;105(2–3):275.
- [92] Schaick EA, de Greef HJ, Ijzerman AP, Danhof M. Physiological indirect effect modelling of the antilipolytic effects of adenosine A1- receptor agonists. *J Pharmacokinet Biopharm* 1997;25(6):673.
- [93] Boxenbaum H, DiLea C. First-time-in-human dose selection: allometric thoughts and perspectives. *J Clin Pharmacol* 1995;35:957.
- [94] Gabrielsson J, Weiner DL. Methodology for pharmacokinetic/pharmacodynamic data analysis. *PSTT* 1999;2(6):244
- [95] Morgan P., The use of preclinical pharmacokinetic and pharmacodynamic data to predict clinical doses: current and future perspectives, *International Congress Series*, Volume 1220, August 2001, Pages 1-12
- [96] Espié P., Tytgat D., Sargentini-Maier M., Poggesi I., and Watelet J., Physiologically based pharmacokinetics (PBPK) *Drug Metabolism Reviews*, August 2009, Vol. 41, No. 3, Pages 391-407
- [97] Koehn FE, Carter GT (2005) The evolving role of natural products drug discovery. *Nat Rev* 4:206–220
- [98] Newman DJ, Cragg GM, Snader KM (2000) The influence of natural products upon drug discovery. *Nat Prod Rep* 17:215–234
- [99] Butler MS (2004) The role of natural product chemistry in drug discovery. *J Nat Prod* 67:2141–2153

[100] Butler MS (2005) Natural products to drugs: natural product compounds in clinical trials.
Nat Prod Rep 22:162–195

[101] MacDiarmid S, Sandage BW Jr, Malhotra BK, The effects of reformulation: improved
therapeutic index. Curr Urol Rep. 2008 Nov;9(6):465-71

CHAPTER 3

PHARMACOKINETICS AND TISSUE DISTRIBUTION OF PSEUDOTEROSIN A IN MICE UTILIZING A NEW HPLC-ULTRAVIOLET DETECTION METHOD WITH DERIVATIZATION *

*Bo Zheng, Lyndon M. West, Catherine A. White. To be submitted to *Journal of Chromatography B*

ABSTRACT

Pseudopterosin A, a gorgonian derived diterpene glycoside, is known to possess anti-inflammatory, analgesic and antioxidant activity. A simple, rapid and sensitive method for determination of pseudopterosin A (PsA) in mouse plasma, liver, brain, and kidney using pre-column derivatization and HPLC-ultraviolet detection is presented. The lower limit of quantification for PsA in plasma and tissues was 0.05 µg/ml. The method showed good linearity over the range of 0.05 – 60 µg/mL PsA in plasma and tissues, with correlation coefficient (R^2) values higher than 0.998. The precision and accuracy for intra-day and inter-day measurements were less than 10%. The absolute recoveries of PsA from all matrices were greater than 93%. Stability tests including freeze and thaw of specimens were also investigated. Pharmacokinetic study of PsA following administration of a 50 mg/kg i.v. dose with this validated method was performed. PsA distribution and elimination half lives in mice were 0.05 hr and 3.21 hr, respectively. Volume of distribution at steady state of PsA was 10.09 L/kg, clearance was 3.48 L/hr·kg. The half-life of PsA in tissues ranged from 2.91 to 3.98 hr. The AUC values for all tissues were higher than that of plasma. Relative exposure for these tissues to PsA ranged from 1.27 to 1.36. The pharmacokinetic profile indicated that PsA had a rapid tissue uptake and extensive tissue distribution. Pharmacokinetic characteristics in brain also documented PsA can cross the blood-brain barrier easily and achieve high concentrations that could be attributed to its high lipophilicity.

Keywords: Pseudopterosin A, HPLC, Pharmacokinetics, Derivatization, Mice, Tissue distribution

INTRODUCTION

Pseudopterosins are an interesting group of diterpene glycosides first isolated from specimens of the gorgonian coral, *Pseudopterogorgia elisabethae*, collected in the Bahamas [1]. Pseudopterosin A (PsA, Figure 3.1) have been shown to possess potent anti-inflammatory and analgesic (pain relief) properties [1-5]. It blocks eicosanoid release by inhibiting phospholipase A2 (PLA2), 5-lipoxygenase (5-LO) and cyclooxygenase (COX), degranulation of leukocytes and the consequent liberation of lysosomal enzymes [5]. The compound appears to be pharmacologically distinct from other non-steroidal anti-inflammatory drugs (NSAIDs) and their mechanism of action appears to be novel as well. A PsA extract is currently used as an additive to prevent skin irritation in cosmetic preparations. The Ps A were licensed to a pharmaceutical company to evaluate the semisynthetic pseudopterosin derivative in clinical trials as topical anti-inflammatory agent for contact dermatitis [6-11]. Regrettably, the studies were not pursued because the company declared bankruptcy in the late 1990s [6, 8].

Recent research from our laboratory has shown that Ps A reduce the oxidative stress induced loss of quantum photosynthetic yield in zooxanthellae (the algal symbionts of *P. elisabethae*) quantified using pulse amplitude-modulated (PAM) fluorometry. PsA can reduce significantly the oxidation of the probe dichlorofluorescein diacetate (DCFH-DA) which has been used as a substrate for measuring intracellular oxidant production in a zooxanthellae/micro-plate based assay [12].

Data from experimental models and human brain studies suggest oxidative stress may play an important role in neuronal degeneration in diseases such as Parkinson's disease, Alzheimer's disease, and amyotrophic lateral sclerosis [4]. The brain is particularly vulnerable to

oxidative processes because it has a high glucose-driven metabolic rate, has low levels of antioxidant defense enzymes, contains high concentrations of polyunsaturated fatty acids, which are potential substrates for lipid peroxidation and is rich in enzymatically active transition metals, which can potentially catalyze radical formation [13]. High-dose α -tocopherol supplementation (5 g/kg) was associated with increased median and maximum life span and improved brain mitochondrial function in male mice from a short-lived strain [14]. Several studies have suggested that these increases in oxidative stress vulnerability and the resulting neuronal loss can be reduced through dietary supplementation of plant extracts that prevent brain atrophy as well as learning and memory impairments [15-17]. It has been demonstrated that certain phenolic antioxidants attenuate neuronal cell death induced by oxidative stress [18, 19]. The PsA have displayed potent antioxidant activity in both solution and cell based assays and might therefore be a promising drug class in the treatment of neurodegenerative diseases in which oxidative stress plays an important role. Convincing evidences existing show that different classes of antioxidants, mainly those that belong to the family of direct antioxidants, act as neuroprotectants *in vitro* [4]. Vitamin E remains to be one of the most potent chain-breaking antioxidant structures. However, its passage through the blood brain barrier (BBB) is limited. Consequently, the identification of structures with much better blood brain barrier penetration and increased antioxidant activity may, ultimately, lead to the development of novel neuroprotective drugs.

To understand tissue distribution and pharmacokinetics of PsA, we have developed a sensitive, accurate and reproducible method using reversed phase high-performance liquid chromatography (HPLC) and UV detection. The method was successfully applied to evaluate the pharmacokinetics of PsA following administration of a 50 mg/kg i.v. dose in a mouse model.

MATERIALS AND METHODS

Materials

Pseudopterosin A (PsA) was isolated from *Pseudopterogorgia elisabethae* collected from Burrows Cay, Bahamas. The chemical structure of pseudopterosin A was identified by nuclear magnetic resonance and mass spectrometry. Acetonitrile and Ethyl acetate (HPLC grade) was obtained from Fisher Scientific Inc. The derivatization reagent, 4-chloro-7-nitrobenzofurazan (NBD-Cl) and internal standard, 17 β -estradiol (IS) were purchased from Sigma Aldrich. Other reagents were of an analytical grade.

Preparation of stocks, calibration standards and quality control samples

Stock solutions of 1.0 mg/mL PsA, 17 β -estradiol and 5.0 mg/mL 4-chloro-7-nitrobenzofurazan (NBD-Cl) were individually prepared in acetonitrile. Standard solutions of PsA were prepared by mixing and diluting the appropriate amounts from the individual stock solutions. The final concentrations of the standard solutions were 600, 200, 100, 50, 10, 5, and 0.5 μ g/mL. A 2.5 mg/mL standard solution of 4-chloro-7-nitrobenzofurazan was prepared with acetonitrile from 5 mg/mL stock. A 100 μ g/mL standard solution of 17 β -estradiol was prepared with acetonitrile from 1 mg/mL stock. The quality control samples (QCs) were prepared in duplicate from separate stock solutions. High-, mid- and low-concentration quality control samples contained 400, 10 and 1 μ g/mL of PsA were prepared in a manner similar to that used for the preparation of the calibration standards. Stock solutions were kept refrigerated when not in use and replaced on a bi-weekly basis. Fresh standard solutions were prepared for each day of analysis or validation.

Calibration curves

Blank plasma, liver, brain, and kidney tissue were collected from untreated anesthetized mice. The tissues were homogenized with same volumes of deionized water (w/v) using an Ultra-Turbax T8 tissue grinder (IKA Labortechnik, Germany). Plasma calibration points were prepared by spiking 100 μL of the biological matrices with 10 μL of each PsA and 17β -estradiol standard solution. Tissue calibration points were prepared by spiking 200 μL of the biological matrices with 10 μL of each PsA and 17β -estradiol standard solution. The calibration curves of all matrices were in the range of 0.05 – 60 $\mu\text{g/mL}$, with an internal standard concentration in each sample of 10 $\mu\text{g/mL}$. After each matrix was spiked, it underwent sample preparation before analysis.

Sample Extraction

After spiking with 10 μL of 17β -estradiol (100 $\mu\text{g/mL}$), 100 μL plasma or 200 μg of tissue homogenate (prepared as above) was mixed with 300 μL of acetonitrile and vortex-mixed for 15 s. The samples were then extracted with 0.6 mL of Ethyl acetate. After centrifugation for 10 min at $2000\times g$, the upper organic layer was removed and evaporated to dryness under reduced pressure in a vacuum centrifuge. The residue obtained was reconstituted in 80 μL acetonitrile with ultrasonic treatment for 1 min and the derivatization was performed as follows.

Derivatization reaction

Ten μL of 25 nM 18-crown-6 (dissolved in dehydrated ACN) and 15 mM potassium carbonate were added and vortex-mixed for 1 min. Then, 10 μL NBD-Cl (2.5 mg/mL) was added and vortex-mixed. The mixture was allowed to react for 30 min at room temperature. After the color of the mixture changed from colorless to deep yellow, the mixture was set on ice to stop the derivatization reaction. Twenty μL injection volumes were used for HPLC analysis.

Chromatographic system

The HPLC measurements were carried out using a Shimadzu LC-20AT liquid chromatography coupled to a UV-SPD-M20A diode array detector. Data acquisition was performed using EZStart chromatography software package version 7.4. The chromatographic separation of NBD-Cl –derivative of PsA was achieved using a Phenomenex Gemini 5 μ C18 110Å column with a Phenomenex Security Guard C18 guard column (Torrance, CA, USA).

Chromatographic conditions

The Mobile phase: A: 20 mM AcONH₄ (pH = 7.4) : ACN (2:1); B: CAN. Running program: 0 – 5 min, 80% – 90% B; 5 – 7 min, 90% B; 7 – 12 min, 90 – 100% B; 12 – 15 min, 100 – 80% B. The mobile phase flow rate was 1.0 mL/min and the UV detection wavelength was set at 378 nm. Under the chromatographic conditions described, NBD-Cl derivatives of PsA and 17 β -estradiol eluted at 7.3 and 5.5 min, respectively.

Bioanalytical method validation

Linearity, precision and accuracy

The linearity of the HPLC method for the determination of PsA was evaluated by a calibration curve in the range of 0.05–60 μ g/mL or μ g/g. The calibration curve was obtained by plotting the ratio of peak area of each analyte to internal standard versus PsA theoretical concentration. Least squares linear regression analysis was used to determine the slope, intercept and correlation coefficient. The calibration curve required a correlation coefficient (r^2) of 0.99 or better, which was considered appropriate for a validated method. To evaluate precision, at least five QCs at each of the three different concentrations were processed and injected on a single day (intra-day) and on different days (inter-day). The variability of PsA determination was expressed as the coefficient of variation (%CV), which should be $\leq 15\%$ for all concentrations. Accuracy

was expressed as % bias of theoretical versus calculated concentrations, and should be within limits of $\pm 15\%$ for all concentrations of PsA.

Recovery

The absolute recoveries of PsA from plasma and tissues were determined at different standard concentrations by spiking the drug into the corresponding fresh blank plasma or tissues. The percentage of recovery was calculated by comparing the peak area of extracted samples with samples in which the same amount of compounds were diluted with acetonitrile, took derivatization reaction and injected directly. The recoveries at three QC concentration levels of PsA in plasma and tissues were examined at least five times.

Pharmacokinetic experiments in mice

Male NIH Swiss mice (weighing 25-30 g) were obtained from Harlan Laboratories, Inc. The mice were acclimated (5 mice/cage) for at least 7 days in an AAALAC (Association for Assessment and Accreditation of Laboratory Animal Care) approved animal care facility after arrival. All experimental protocols were approved by the Institutional Animal Care and Use Committee at the University of Georgia. The mice were fasted 12 h before receiving PsA and provided feed 4 h after drug administration. All mice received an IV bolus dose of PsA (50 mg/kg) via the tail vein. The mice ($n = 3$ per time point) were sacrificed under anesthesia, blood samples were collected at each time point (2, 5, 10, 15, 30, 60, 120, 180, 240, 360, 480, 720 min) into heparinized microcentrifuge tubes. Plasma was prepared by centrifugation of blood at 1000 g for 15 min at 4°C and stored at -80°C until analysis. Tissues (brain, liver and kidney) were also collected and homogenized (with 1:1 water for tissues) and stored at -80°C until analysis. Plasma, liver, brain and kidney were processed and analyzed as described above. A calibration

curve from each matrix was prepared on the day of analysis to calculate the concentrations of PsA present in the samples. The concentration–time profiles of PsA in all matrices were plotted.

The plasma data was subjected to compartmental analysis using *WinNonlin* 5.2. (Pharsight, Mountain View, CA, USA). A two-compartment intravenous bolus model with first-order elimination was used to fit the plasma data. A $1/y^2$ -weighting scheme was used throughout the analysis. Pharmacokinetic parameters such as half life, volume of distribution, clearance and area under curve were generated. Pharmacokinetic analysis of PsA concentrations in tissues was performed using noncompartmental methods via software *WinNonlin* 5.2. Pharmacokinetic parameters such as half life, area under curve were generated. Relative exposure (RE) of each tissue was calculated as $AUC_{\text{tissue}} / AUC_{\text{plasma}}$.

RESULTS AND DISCUSSION

The optimal derivatization of Pseudopterosin A and IS with 4-chloro-7-nitrobenzofurazan

PsA has very weak UV absorption at 287 nm. The LLOD of PsA in pure acetonitrile is just 1 $\mu\text{g/mL}$, the LLOQ in biological matrices even higher to 5 $\mu\text{g/mL}$ or $\mu\text{g/g}$. By pre-column derivatization with NBD-Cl, the LLOQ of PsA in biological matrices could be lowered to 0.05 $\mu\text{g/mL}$ or $\mu\text{g/g}$. In order to optimize derivatization procedure, reaction conditions were varied and the reaction mixtures were analyzed by HPLC. The presence or absence of catalyst, different temperature and time of reaction were also tested in a series of experiments. It was found that 30 min reaction time under room temperature, with 18-crown-6 and potassium carbonate could achieve the highest derivative peak of PsA. After 30 min reaction, the reaction could be stopped by lowering the temperature below 4°C. The derivatives of PsA and internal standard were stable for over 3 days at 4°C. The derivatization scheme for PsA and IS with NBD-Cl is shown in Figure 3. 2.

Chromatogram

The chromatograms of blank biometrics sample, 1 µg/mL or µg/g PsA quality control biometrics sample, LLOQ of each biometrics and real samples 30 min after a 50 mg/kg iv dosing with PsA are shown in Figure 3.3 (plasma), Figure 3.4 (liver), Figure 3.5 (brain) and Figure 3.6 (kidney). Blank biometrics showed no peaks of interfering endogenous compounds around the retention time of PsA and internal standard. In addition, the retention time (7.3 min) of PsA was suitable for routine analysis.

Method validation

A linear relationship was found between peak areas of PsA in plasma, brain, liver and kidney theoretical concentrations within the range of 0.05 – 60 µg/mL. The correlation coefficient of linear regression equations for calibration curves in plasma, brain, liver and kidney were larger than 0.99 (Table 3.1). The coefficient of variations of slope for PsA were found to be <15%, which indicated a high precision of the present assay. The absolute recovery of PsA after sample preparation ranged from 93.76 to 98.78% and %CV of recovery was below 15% for each concentration (Table 3.2).

The intra- and inter-day variability of plasma, brain, liver and kidney assay are listed in Table 3.3. The HPLC method for the determination of PsA was reliable and reproducible since both %CV and %bias were below 15% for all estimated concentrations of PsA. The LLOQ was evaluated by analyzing plasma samples spiked with the analyte at a final concentration of 0.05 µg/mL at which the signal-to-noise (S/N) ratio was 10 (Figure 3.3c, Figure 3.4c, Figure 3.5c, Figure 3.6c,). These results suggested that the reproducibility and recovery were acceptable over the range of concentrations studied.

Pharmacokinetic study of Pseudopterosin A (PsA) in mice

The concentration–time profiles of PsA in all matrices are shown in Figure 3.7. The plasma PsA concentrations decline in biexponential fashion after IV administration. In Figure 3.8, the mean plasma concentration-time profile after IV administration of PsA was fitted to a two-compartment model. The pharmacokinetic parameters generated from two-compartmental analysis of the plasma data are presented in Table 3.4. Distribution and elimination half lives were 0.05 hr and 3.21 hr respectively, which indicates that PsA is distributed rapidly into mouse tissues after IV administration. The volume of distribution at steady state of PsA was 10.09 L/kg (volume of total body water of mice is 0.43 L/kg [20]), indicating that PsA is distributed extensively in mice tissues. That could be attributed, in part, to its high lipophilicity. Clearance is 3.48 L/hr/ kg, which suggests that this compound is cleared rapidly from the body (value of blood flow of liver and kidney in mouse are 4.46 L/hr/kg and 2.52 L/hr/kg, respectively [21]).

The pharmacokinetic parameters for tissues are given in Table 3.5. The PsA in liver and brain rapidly reached the peak concentration of 10.06 and 10.02 $\mu\text{g/g}$, at 0.17 and 0.5 hr respectively. The concentration-time profiles of brain and liver declined in a bi-exponential fashion after reaching peak concentration, indicating two-compartment model behavior in brain and liver. For liver and brain, $\text{CL}_{\text{Plasma to Tissue}}$ was equivalent to $\text{CL}_{\text{Tissue to Plasma}}$, indicating a rapid equilibrium was achieved between plasma and liver or brain. In contrast, the concentration-time profile of PsA in kidney indicated that the kidney does not achieve a rapid equilibrium with plasma (for kidney, $\text{CL}_{\text{Plasma to Tissue}} \gg \text{CL}_{\text{Tissue to Plasma}}$, which suggests the possible existence of CL_{int} in kidney). The kidney concentrations peaked later ($T_{\text{max}}=1.5$ hr) and were significantly lower ($C_{\text{max}}=3.00\mu\text{g/g}$) than those observed in the brain and liver. PsA concentration in liver, brain and kidney were in excess of that in plasma 10 min, 15 min and 60 min after IV administration, respectively. After IV administration, PsA concentration in kidney at 90 min was

higher than those observed in plasma and other tissues. All tissues had higher concentration of PsA than plasma during the elimination phase. The PsA terminal half life in tissues ranged from 2.91 hr (brain) to 3.98 hr (kidney). The terminal half live of liver and brain were equivalent to the plasma half life. All tissue AUCs were larger than plasma AUC (14.35 hr ug/g), yielding $RE > 1.0$. Among 3 tissues, brain had the largest AUC (19.49 hr ug/g), which indicates that PsA can cross blood brain barrier easily and distribute into brain. .

CONCLUSIONS

An HPLC method with a new pre-column derivatization was developed using NBD-Cl as the derivatization reagent for the determination of PsA in mouse plasma, liver, brain and kidney. After a pre-column derivatization, both the detection limit and the chromatographic behavior of each drug were improved significantly. This method was accurate, sensitive, and simple. It has been successfully applied to the pharmacokinetic study of PsA in mice, and the pharmacokinetic characteristics were revealed. The plasma PsA concentrations declined in biexponential fashion after IV administration. The large V_{ss} and $REs > 1.0$ for PsA indicates extensive tissue distribution. The high concentrations achieved in the brain indicate that PsA can cross the blood-brain barrier easily. This is due, in part, to the high octanol-water partition coefficient ($\log P \approx 4.3$) for PsA [11].

ACKNOWLEDGEMENTS

We would like to thank Prasoon Gupta for the isolation and purification pseudopterosin A.

REFERENCES

- [1] A.S. Look, W. Fenical, R.S. Jacobs, J. Clardy, Proc. Natl. Acad. Sci. USA. 83 (1986) 6238.
- [2] W.S. Ettuati, R.S. Jacobs, Mol. Pharmacol. 31 (1987) 500.
- [3] C.E. Moya, R.S. Jacobs, Comp. Biochem. Physiol. C: Pharmacol. Toxicol. 143 (2006) 436.
- [4] A. Ata, R. G. Kerr, C.E. Moya, R.S. Jacobs, Tetrahedron. 59 (2003) 4215.
- [5] A.M. Mayer, P.B. Jacobson, W. Fenical, R.S. Jacobs, K.B. Glasei, Life Sci. 62 (1998) PL401.
- [6] H. Gross, G.M. König, Phytochemistry Reviews. 5 (2006) 115.
- [7] H.B. Haimes, S.S. Glasson, P.M. Harlan, R. Jacobs, W. Fenical, P.A. Jimenez, Inflamm. Res. 44 (1995) W13.
- [8] D.J. Faulkner, Marine pharmacology. Ant. van Leeuw. 77 (2000) 135.
- [9] B. Haefner, Drug discovery today. 8 (2003) 536.
- [10] H. Correa, A.L. Valenzuela, L.F. Ospina, C. Duque, J. Inflamm. (Lond). 6 (2009) 5.
- [11] D.S. Scherl, J. Afflitto, A. Gaffar, Journal of Clinical Periodontology. 26 (2003) 246.
- [12] M.S. Mukherjee. Inter- and intra- species variation in secondary metabolites from Caribbean octocorals of the genus *Pseudopterogorgia*: antioxidant activity and a potential ecological role. Doctoral Dissertation, University of Georgia, Athens, December 2008.
- [13] B. Halliwell, and J.M.C. Gutteridge (1989). Free Radicals in Biology and Medicine. (2nd Edit ed.), Clarendon Press, Oxford.
- [14] A. Navarro, C. Gomez, M.J Sanchez-Pino, H. Gonzalez, M.J. Bandez, A.D. Boveris, A. Boveris. Am. J. Physiol. Regul. Integr. Comp. Physiol. 289 (2005) R1392.
- [15] S. Kanowski, W.M. Herrmann, K. Stephan, W. Wierich, R. Hörr. Pharmacopsychiatry. 29 (1996) 47.

- [16] T. Moriguchi, H. Saito, N. Nishiyama. Clin. Exp. Pharmacol. Physiol. 24 (1997) 235.
- [17] N. Nishiyama, T. Moriguchi, H. Saitu. Exp. Gerontol. 32 (1997) 149.
- [18] H. Schroeter, R.J. Williams, R. Matin, L. Iversen, C.A. Rice-Evans. Free. Radic. Biol. Med. 29 (2000) 1222.
- [19] K.A. Youdim, J.A. Joseph. Free Radic. Biol. Med. 30 (2001) 583.
- [20] B Künnecke, P Verry, A Bénardeau, M Kienlin. Obesity Research 12 (2004), 1604–1615
- [21] R Brown, M Delp, S Lindstedt, L Rhomberg, R Beliles. Toxicology and industrial health, Vol. 13, No. 4, (1997) 407.

Table 3.1. Linear regression equations generated from validation data for each matrix; slope (mean \pm s.d.), correlation coefficient (mean \pm s.d.)

Matrix	Slope	R ²
Plasma	8.63 \pm 0.52	0.9998 \pm 0.07
Brain	8.62 \pm 0.78	0.9996 \pm 0.07
Liver	8.70 \pm 0.92	0.9980 \pm 0.10
Kidney	8.54 \pm 1.0	0.9984 \pm 0.12

Table 3.2. Absolute recovery (mean \pm S.D.) of the method for determining the concentration of PsA in plasma, brain, liver and kidney (n = 15)

Concentration ($\mu\text{g/mL}$ or $\mu\text{g/g}$)	Plasma	Brain	Liver	Kidney
0.05	95.5 ± 3.2	94.2 ± 5.7	93.7 ± 5.8	95.0 ± 3.7
0.1	95.7 ± 2.1	94.7 ± 5.4	94.2 ± 3.3	96.1 ± 2.8
1	98.5 ± 3.5	96.3 ± 3.6	95.3 ± 7.1	97.4 ± 3.1
40	98.8 ± 4.7	96.5 ± 4.0	96.1 ± 2.6	98.1 ± 2.0

Table 3.3. Intra-day (n = 5) and inter-day (n = 15) precision and accuracy of PsA measurement in each matrix

Biological matrix	T.C. (ug/ml or Ug/g)	Intra-day			Inter-day		
		E.C. (ug/ml or Ug/g)	Precision (% CV)	Accuracy (% error)	E.C. (ug/ml or Ug/g)	Precision (%CV)	Accuracy (% error)
Plasma	0.1	0.10	6.64	7.12	0.11	7.91	8.83
	1	1.02	5.35	5.63	1.03	5.23	4.62
	40	41.3	4.98	3.54	41.1	4.05	2.96
Brain	0.1	0.10	5.37	4.73	0.10	4.61	4.81
	1	1.02	4.09	5.25	1.03	4.37	4.89
	40	40.6	5.58	4.39	39.5	3.32	3.21
Liver	0.1	0.10	6.98	5.53	0.11	7.15	4.93
	1	1.02	5.21	5.14	1.04	5.56	5.04
	40	40.6	6.91	4.88	39.7	5.12	4.42
Kidney	0.1	0.11	5.04	6.72	0.10	4.89	3.87
	1	1.01	4.52	5.87	1.02	3.95	5.65
	40	38.5	4.34	3.72	40.5	3.51	3.61

Table 3.4. Plasma Pharmacokinetic Parameters for PsA (estimate \pm standard error)

Parameter	Value
Distribution Half-life (hr)	0.05 ± 0.005
Elimination Half-life (hr)	3.21 ± 0.30
AUC (hr·mg/ L)	14.4 ± 0.95
Cl _T (L/hr·kg)	3.48 ± 0.23
V _{ss} (L/kg)	10.1 ± 1.35
C _{max} (mg/L)	85.5 ± 7.64

Table 3.5. Brain, Liver, and Kidney Pharmacokinetic Parameters and Relative Exposures for PsA.

Parameter	Brain	Liver	Kidney
Half-life (hr)	2.91	3.16	3.98
AUC (hr·ug/ g)	19.5	18.2	18.4
Cmax (μg/g)	10.0	10.1	3.00
Tmax (hr)	0.5	0.17	1.5
Relative Exposure*	1.36	1.27	1.28
Cl _{Plasma to Tissue} (L/hr·kg)	0.017	0.074	0.061
Cl _{Tissue to Plasma} (L/hr·kg)	0.015	0.065	0.005

*Relative Exposure = $AUC_{tissue}/AUC_{plasma}$

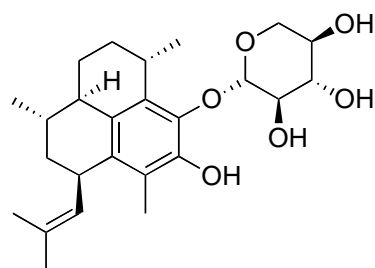


Figure 3.1. Chemical structure of PsA.

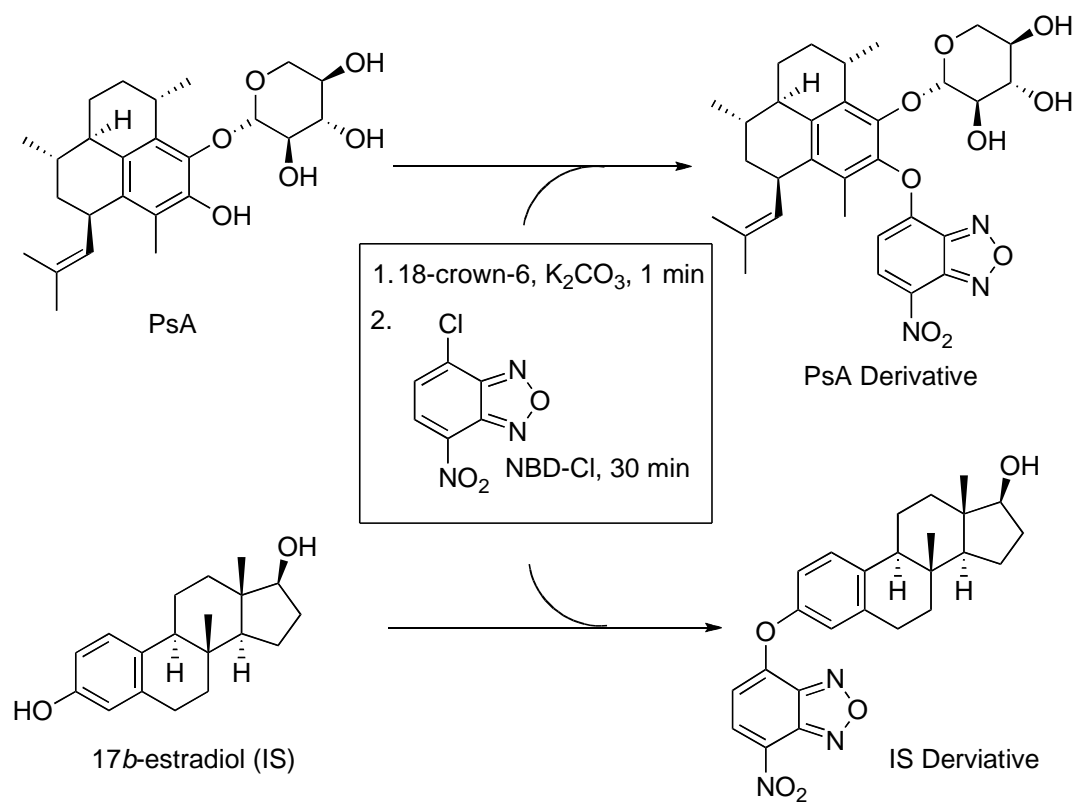


Figure 3.2. Derivatization scheme for PsA and IS with NBD-Cl.

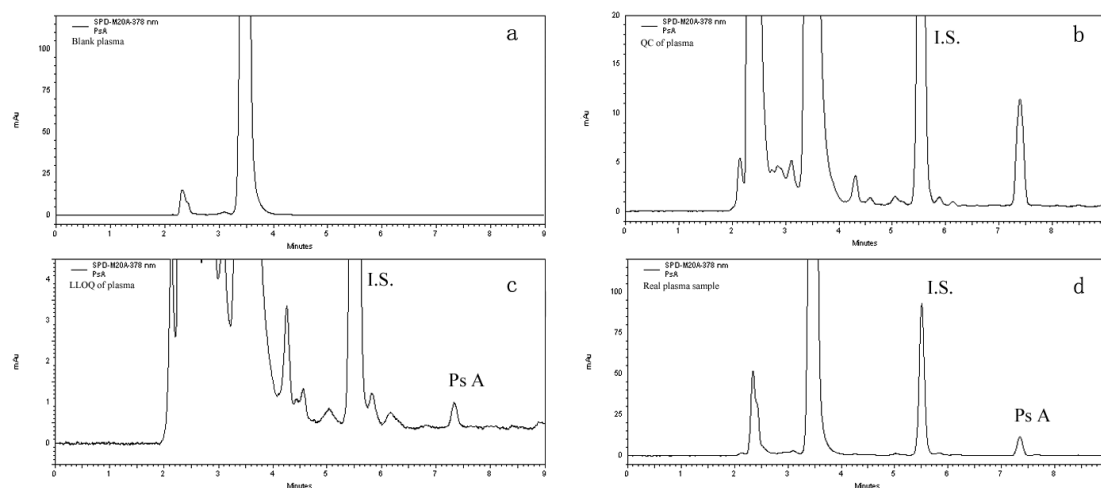


Figure 3.3. Representative HPLC chromatograms: (a) blank plasma sample, (b) a 1 µg/mL PsA quality control plasma sample, (c) the LLOQ of Ps A (0.05 µg/mL) in plasma and (d) a mouse plasma sample 30min after a 50 mg/kg dose of PsA.

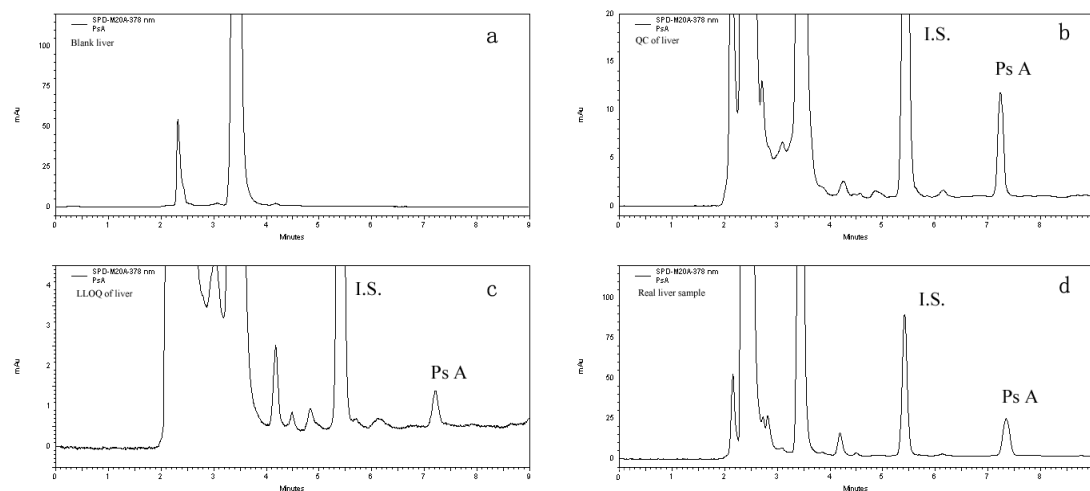


Figure 3.4. Representative HPLC chromatograms: (a) blank liver sample, (b) a 1 $\mu\text{g/ml}$ PsA quality control liver sample, (c) the LLOQ of PsA (0.05 $\mu\text{g/mL}$) in liver and (d) a mouse liver sample 30 min after a 50 mg/kg dose of PsA.

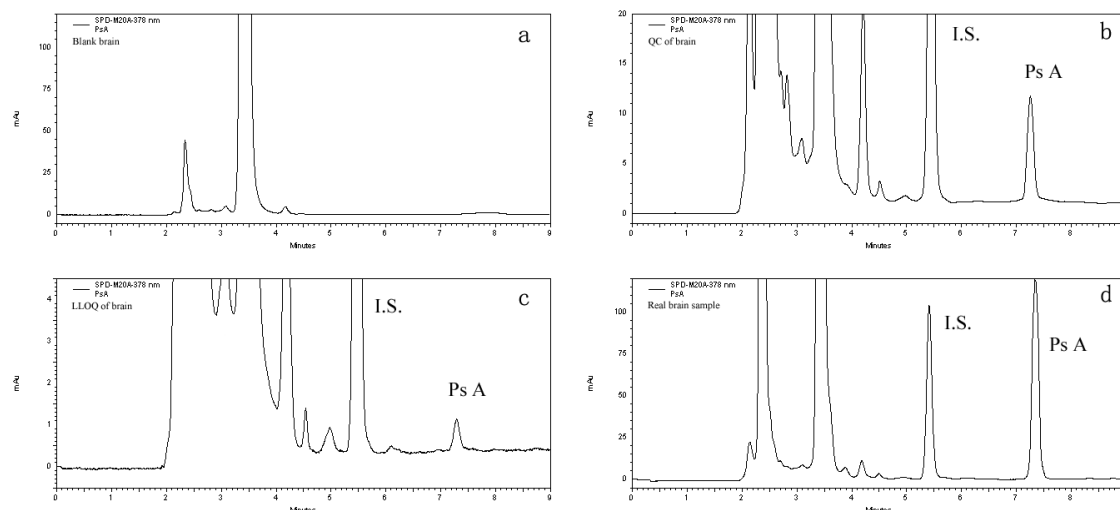


Figure 3.5. . Representative HPLC chromatograms: (a) blank brain sample, (b) a 1 µg/mL PsA quality control brain sample, (c) the LLOQ of PsA (0.05 µg/ml) in brain and (d) a mouse brain sample 30 min after a 50 mg/kg dose of PsA.

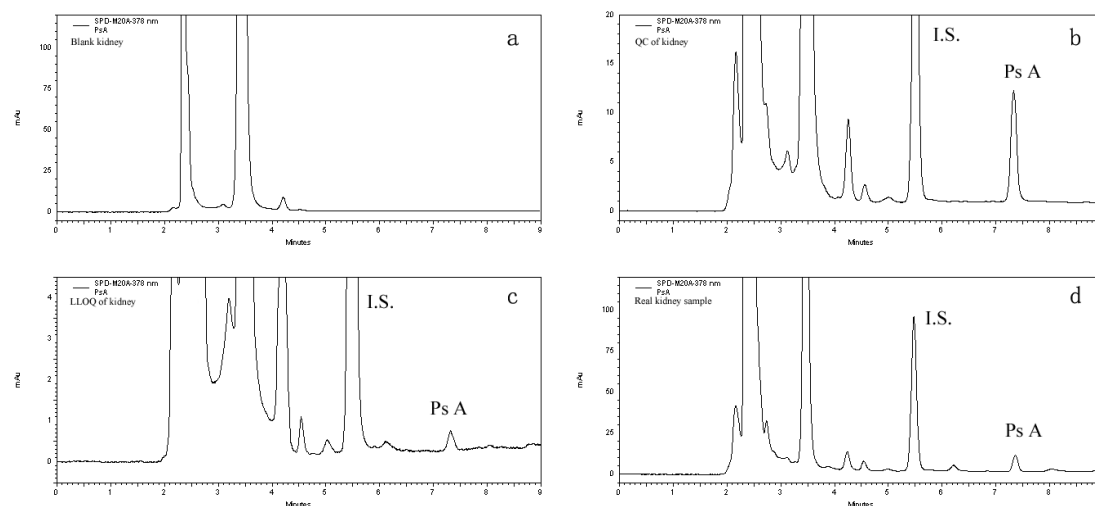


Figure 3.6. Representative HPLC chromatograms: (a) blank kidney sample, (b) a 1 µg/mL PsA quality control kidney sample, (c) the LLOQ of PsA (0.05µg/mL) in kidney and (d) a mouse kidney sample 30 min after a 50 mg/kg dose of Ps A.

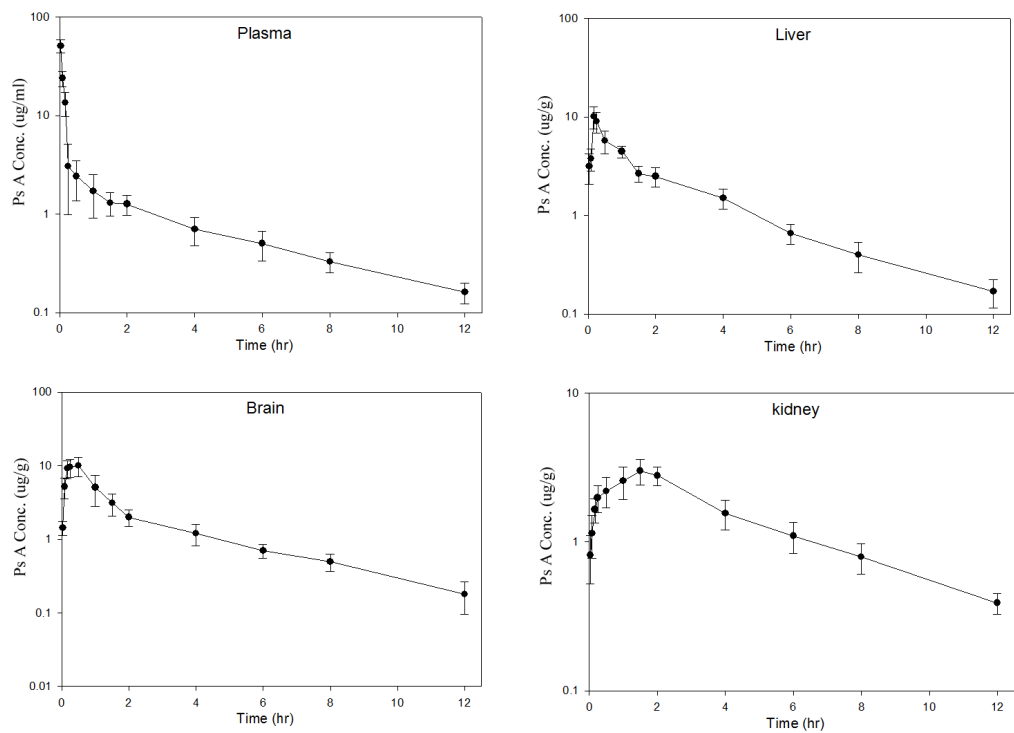


Figure 3.7. Concentration vs. time profiles of PsA in plasma, liver, brain and kidney after 50 mg/mL i.v. bolus doses of PsA.

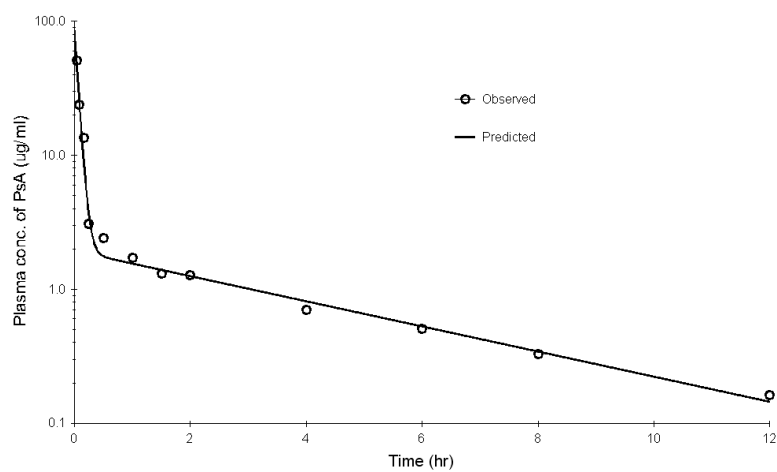


Figure 3.8. The mean plasma concentration-time profile after IV administration of PsA was fitted to a two-compartment model.

CHAPTER 4
PHARMACOKINETICS OF A MIDAZOLAM GEL FOLLOWING INTRANASAL
DELIVERY IN DOGS*

*Bo Zheng, Simon Platt, Deborah Strong Elder, Catherine A. White. To be submitted to *The AAPS Journal*

ABSTRACT

Status epilepticus (SE) is a medical emergency requiring immediate therapy. Benzodiazepines, such as midazolam, form the cornerstone of the early therapy for status epilepticus. Midazolam has marked anticonvulsive effects in humans and animals, being more effective than comparable doses of diazepam. Intranasal anticonvulsants have been successfully used to treat human status epilepticus. Rapid absorption and attainment of therapeutic drug levels have been demonstrated for intranasal diazepam and midazolam in dogs and human; however, the parenteral formulations are impractical to use in patients because of safety and dosing issues. These problems could be avoided by the use of midazolam formulated as a bioadhesive gel. Bioadhesive gel formulations that utilize unique polymers such as methylcellulose, have been shown to improve adherence time, transmucosal absorption and bioavailability of drugs to the nasal mucosa when administered intranasally. We developed a methylcellulose gel formulation of midazolam that was anticipated to have a large impact on the treatment of canine status epilepticus by veterinarians and pet owners and to reduce the complications associated with prolonged seizures. In this study, we compared the pharmacokinetics of a novel midazolam gel formulation given intranasally to the pharmacokinetics of parenteral midazolam given intranasally, intravenously and rectally in dogs.

INTRODUCTION

Status epilepticus (SE), a life-threatening condition in which the brain is in a state of persistent seizure, is a medical and neurological emergency ^[1-3]. Most seizures are brief and resolve without treatment. Prompt intervention is recommended when any seizure lasting longer than 5 minutes represents status epilepticus ^[4-6]. Status epilepticus is a common and devastating problem in many breeds of dog that can cause central nervous system dysfunction such as trauma, inflammation, neoplasia and metabolic disorder ^[29]. A large proportion of dogs with status epilepticus has no underlying disease and is documented to have idiopathic or ‘cryptogenic’ epilepsy ^[7]. Such dogs may experience multiple episodes of status epilepticus during their life, which is both a major health issue for the patient and has a significant financial impact on the owner ^[8]. Thus, treatment needs to be given as quickly as possible to avoid potential brain damage. In planning home therapy, the safety, ease of administration, choice of drug, route of therapy, the practicability by the user are important issues. Various drugs administered through different routes have been tried in the management of acute seizures.

Benzodiazepines (diazepam, lorazepam and clonazepam) are potent, fast-acting anticonvulsants and in animal screening tests, have a broad spectrum of anticonvulsant activity inhibiting seizure activity effectively at low doses. Since 1965, benzodiazepines (BZDs) have been used widely in the management of epilepsy in both children and adults. At present, seven different benzodiazepines are used in various countries as anticonvulsant drugs ^[9].

Benzodiazepines (BZDs) form the cornerstone of the early therapy for status epilepticus.

Because of their high lipophilicity, rapid brain penetration, and brain receptor binding, benzodiazepines administered either intravenous (i.v.) or rectally are often first-line agents for acute seizure management. Currently, intravenous (i.v.) diazepam or midazolam is used in

veterinary medicine for the immediate treatment of status epilepticus. Intranasal benzodiazepines are the anticonvulsant drugs (AEDs) of first choice for treating status epilepticus in most emergency rooms. However, intravenous administration of any drug during status epilepticus is difficult and dangerous for both the care-giver and the patient. It is also not feasible as a drug administration route when the patient is not in a hospital environment. Unfortunately, properties of some benzodiazepines limit administration into few routes. For example, oral administration is unpractical because of swallowing problem diazepam must be given intravenously (i.v.) or rectally because absorption is slow and erratic if given via the intramuscular route ^[10, 11]. Lorazepam may be administered via the i.v., intramuscular, or transmucosal route ^[12, 13].

Midazolam (Figure 4.1) is an ultra short-acting benzodiazepine derivative that has potent anxiolytic, amnestic, hypnotic, anticonvulsant, skeletal muscle relaxant, and sedative properties ^[8]. Because chemical structure of midazolam changes with different pH, midazolam is water-soluble in acidic solution but becomes lipophilic at physiological pH allowing it to cross the cell membrane, which is associated with a very favorable hemodynamic and pharmacokinetic profile ^[15-17]. Midazolam has a marked anticonvulsive effect in humans and animals, being more effective than comparable doses of diazepam, which is more commonly utilized in veterinary medicine ^[18]. Midazolam also lacks direct effects on autonomic functions and cardiovascular system, demonstrating excellent local tolerance and a low acute toxicity profile ^[19]. Within the central nervous system, midazolam has twice the affinity for the benzodiazepine receptor and possesses up to four times the hypnotic potency of diazepam ^[20]. Midazolam has a unique pH-dependent biphasic molecular structure that allows multiple administration approaches. In the parenteral preparation, midazolam has a pH of 3.5 and is a water-soluble, relatively nonirritating solution that allows multiple administration approaches. At physiologic pH, midazolam is highly

lipophilic, which facilitates transport across the blood brain barrier and accounts for its rapid onset of action.

Although i.v. and intramuscular administrations of midazolam are the most effective sedative approach, injections are impractical to administer during SE ^[21, 22]. The oral route is more acceptable to animals and human, but drug absorption and onset of action are significantly delayed with peak concentration in plasma at 120 min ^[22]. Moreover, the first pass hepatic metabolism, associated with orally administered midazolam, results in inactivation of up to 70% of the dose prior to reaching the systemic circulation ^[23]. Thus, other routes of administration of midazolam such as sublingual, rectal and nasal that avoid injection sequelae and the first-pass effect, require investigation. The development of anticonvulsants (such as diazepam) rectal gel is made in recognition of the need for non-injection-based delivery. However, the slower onset of action, less efficacy at controlling seizures make rectal delivery less popular with animals and caregivers ^[24].

The nasal cavity is covered by a thin mucus layer, a monolayer ciliated epithelium, with an abundant underlying blood supply ^[25]. These conditions are ideal to permit passive diffusion (transcellular) of medications with certain chemical characteristics across cell membranes and into the bloodstream. Some medications also transit to the bloodstream by passing through the tight-cell junctions between cells (paracellular). Intranasal administration of antiepileptic medications, in particular benzodiazepines, has been studied with various preparations. Intranasal administration of anticonvulsants have been used successfully in human status epilepticus ^[26, 27], particularly for children, proving additionally safe and relatively easy to administer. Intranasal administration of anticonvulsants has been recommended as an alternative drug delivery technique for prompt treatment. For animals, rapid absorption and attainment of

therapeutic drug level have been demonstrated for intranasal diazepam and midazolam in dogs [28]. Plasma and cerebrospinal fluid (CSF) concentrations following nasal administration demonstrate the advantage of midazolam's unique molecular properties when using the nasal approach [29].

Residence time at the site of absorption is one factor that limits the onset time and bioavailability of drugs administered nasally. Some efforts to increase the bioavailability of nasally administered drugs have attempted to increase the residence time in the nasal cavity. One method to lengthen nasal residence time has been to include a bioadhesive in the formulation. Bioadhesive gel formulations utilizing unique polymers have been shown to improve adherence time, transmucosal absorption and bioavailability of drugs to the nasal mucosa when administered intranasally [30]. Methylocellulose is very high molecular weight polymer, and has been used for development of bioadhesive controlled-release drug delivery systems owing to their bioadhesive properties [31]. Within the last 3-4 years, the pharmacokinetics of nasal gel formulations of several drugs, including insulin, metoclopramide and sumatriptan, has been determined [32-34]. These gel formulations improve bioavailability and residence time of the drugs under investigation.

We hypothesized that intranasal administration of a novel gel midazolam formulation would have improved increased bioavailability and C_{max} to that of intranasal, intravenous and rectally administered parenteral midazolam. We developed a methylocellulose gel formulation of midazolam that was anticipated to have a large impact on the treatment of canine status epilepticus by veterinarians and pet owners and to reduce the complications associated with prolonged seizures. In this study we compared the pharmacokinetics of a novel midazolam gel

formulation given intranasally to pharmacokinetics of parenteral midazolam given intranasally, intravenously and rectally in dogs.

METHOD

Drug Formulation

Commercially available midazolam hydrochloride (Bedford Laboratories, Bedford, Ohio) was purchased for comparative IV and rectal administration. The 50 mg/ml IN midazolam formulation were prepared aseptically, creating a sterile product, following the USP standards. The IN formulation, an aqueous solution, was made to a final volume of 10 ml using purified USP grade water containing 0.5 g of midazolam, 0.2% sodium hydroxide, 0.08% Hydrochloric Acid and 0.01% Benzalkonium chloride combined with 0.4% methycellulose (Methocel®) powder. The pH of the formulation was 2.98. The formulation was delivered in 0.1ml sprayed actuations providing 5 mg of midazolam. The concentration of the formulation was adjusted to ensure that each dog receives the same dose. (Note: the delivery device was calibrated to ensure each dog received the same dose, 5 mg per 0.1 mL.)

Drug Administration

The use of animals was approved by the University of Georgia Institutional Animal Use and Care Committee (IACUC) and was conducted in accordance with the Animal Welfare Act and the National Institutes of Health Guide for the Care and Use of Laboratory Animals. This study was performed in 10 healthy dogs. The dogs were housed one animal per cage in the College of Veterinary Medicine of University of Georgia. The living environment of the animals was controlled with 12 h of light per day, a constant temperature of 70-75° F, daily feeding and tap water. The dogs underwent a physical and basic lab tests prior to the study and all dogs were fasted for 12 h before dosing. The dogs were randomly divided on the first day

of the study into 4 groups of two and remained in these groups throughout the study.

Commercially available parenteral midazolam hydrochloride (Bedford Laboratories, Bedford, Ohio) was administered IV to 2 dogs, rectally to 2 dogs and IN to 2 dogs at a dose of 0.2 mg/kg, all using a syringe delivery. Intravenous administration was via a cephalic vein catheter, which was flushed with 0.5 cc heparinized saline solution after the injection. Rectal administration was via the use of rectal catheter attached to the syringe that was flushed with 5 cc of sterile saline after administration. Intranasal administration of the parenteral formulation was performed using a 3 cc syringe depositing approximately half of the dose into each nostril, over a 20 second time period. The dogs' heads were held up at approximately 30° for one minute to prevent loss of the midazolam to the exterior. A gel formulation (methylcellulose) of midazolam was delivered intranasally (0.2 mg/kg) using a metered syringe device to 2 dogs. The protocol was repeated following a 14-day washout period 4 additional times so that each dog received all 4 treatments.

Physiologic monitoring of study dogs

All the dogs had their heart rates measured with auscultation and pulse palpation before and over the 30 minutes after administration of the drug, every 5 minutes. Each dog had its respiratory rate calculated by monitoring thoracic cage excursions at the above time periods. Each dog had its blood pressure recorded indirectly before, 15 and 30 minutes after the drug administration.

Sample collection

Venous blood samples (2.0 ml) were collected from the jugular veins and placed into lithium heparin tubes before and 3, 6, 9, 12, 15, 20, 30, 60, 120, 240 and 480 minutes after the administration of the midazolam. The blood samples were stored on ice for a maximum of 2 hours

at which time they were centrifuged at 3000g to harvest the plasma, which were stored in polypropylene vials at -70°C until the assay is performed at the end of the study.

Determination of plasma concentration of midazolam

Preparation of stock and standard solutions

A stock solution of 1.0 mg/ml midazolam was prepared in methanol. Standard solutions of midazolam were prepared by serial dilution. The final concentrations of the standard solutions were 100, 50, 25, 10, 5, 2.5, 1, 0.5 and 0.1 µg/ml. The stock solution was kept refrigerated when not in use and replaced on a bi-weekly basis. Fresh standard solutions were prepared for each day of analysis.

Preparation of calibration curves

Plasma calibration points were prepared by spiking 400 µl of the blank plasma with 40 µl of each midazolam standard solution. The calibration curve of the plasma was in the range of 0.01 - 10 µg/mL with individual calibration points of 10, 5, 1, 0.5, 0.1, 0.05 and 0.01 µg/mL.

Preparation of samples

Plasma concentrations of midazolam were analyzed using a high-performance liquid chromatography method with UV detection at 220nm. Plasma aliquots of 0.4 ml were mixed with 400 ng of the internal standard diazepam and 0.1 ml sodium hydroxide (0.5 M). Following liquid-liquid extraction with 1 ml cyclohexane-dichloromethane (55/45, v/v), the organic layer was evaporated. The residue was dissolved in 100 µl water-acetonitrile (95/5, v/v) and 50 µl were injected onto the chromatograph.

Chromatographic system

An agilent 1100 series HPLC coupled with a UV detector was used for biosample analysis. Separation was achieved on an Inertsil ODS-3 C-18 250x4.6mm 5 µM column (Varian,

Inc) with C-18 guard column. The isocratic mobile phase was 25 mM KH_2PO_4 buffer (pH = 7.0) : acetonitrile (56:44). Mobile phase flow rate was 1ml/min. The UV detector wavelength was set as 220nm.

HPLC analytical method validation

The linearity of the HPLC method for the determination of midazolam was evaluated by a calibration curve in the range of 0.05–10 $\mu\text{g/mL}$ or $\mu\text{g/g}$. The calibration curve was obtained by plotting the ratio of peak area of each analyte to internal standard versus midazolam theoretical concentration. Least squares linear regression analysis was used to determine the slope, intercept and correlation coefficient. The calibration curve required a correlation coefficient (r^2) of 0.99 or better which was considered appropriate for a validated method ^[35]. To evaluate precision, at least five quality control samples at each of the three different concentrations were prepared and injected on a single day (intra-day) and on different days (inter-day). The variability of midazolam determination was expressed as coefficient of variation (%CV), which should be $\leq 15\%$ for all concentrations. Accuracy was expressed as % bias of theoretical versus calculated concentrations, and it should be within limits of $\pm 15\%$ for all concentrations of midazolam. The absolute recoveries of midazolam from plasma were determined at different standard concentrations by spiking the drug into the corresponding fresh blank plasma. The percentage of recovery was calculated by comparing the peak area of extracted samples with samples in which the same amount of compounds were diluted with acetonitrile and injected directly. The recoveries at three quality control concentration levels of midazolam in plasma were examined at least five times.

Pharmacokinetic analysis

Pharmacokinetic parameters were determined from the plasma midazolam concentration-time profiles. Plasma concentration-time data were analyzed with WinNonlin (Pharsight, version 5.2) utilizing both compartmental and non-compartmental methods. Peak concentration (C_{\max}), time to achieve peak concentration (T_{\max}), bioavailability (F), clearance (CL), volume of distribution (Vd), elimination half life ($t_{1/2}$) and area under the concentration curves (AUC) were determined using compartmental or noncompartmental method.

Statistical analysis

A repeated measures analysis of variance (ANOVA) was used to compare the concentrations among groups and time-points. A 2-factor model was used which includes time, group and time-by-group interaction factors. A repeated measure ANOVA was used to compare peak concentrations, time to peak, bioavailability and area-under-the-curve among groups. A single factor model which includes a group factor was used to compare pharmacokinetic parameters between groups. An unstructured covariance structure was used in all repeated measure models. Hypothesis test was 2 sided with $\alpha < 0.05$. Statistical analysis was performed in SAS 9.1.3.

RESULTS

Chromatography method development

The chromatography of blank dog plasma, dog plasma spiked 0.2 ug/ml midazoalm, LLOQ (0.01 ug/ml) of plasma, and real dog plasma sample 30 min after intravenous administration are represented by Figure 4.2. Calibration curves were linear over the range of 0.01-10 $\mu\text{g/ml}$ ($r^2 > 0.99$). Inter and intra-day coefficients of variation were less than 7%. The lowest limit of quantification was 0.01 $\mu\text{g/ml}$. Absolute recovery was larger than 95%.

Pharmacokinetic analysis

The mean plasma concentration-time profiles of midazolam following 0.2 mg/kg administration of intravenous bolus, intranasal, rectal, and intranasal gel syringe are presented in Figure 4.3. The pharmacokinetic parameters generated from WINNONLIN for each route of administration are given in Table 4.1. The plasma midazolam concentrations decline in biexponential fashion after intravenous administration that is consistent with a previous study [35]. The concentration-time profile of intranasal, rectal and intranasal gel treatment displayed absorption and elimination phases. Midazolam was rapidly absorbed into the systemic circulation after intranasal gel administration, with a mean peak concentration of $0.45 \pm 0.09 \mu\text{g/ml}$ reached at $11.7 \pm 2.63 \text{ min}$. Intranasal and rectal administration reached peak concentration of 0.21 ± 0.02 and $0.15 \pm 0.01 \mu\text{g/ml}$, at $17.5 \pm 2.64 \text{ min}$ and $39.0 \pm 14.5 \text{ min}$ which is consistent with previous studies [36, 37]. The T_{max} and C_{max} of midazolam after intranasal gel administration were significantly shorter and greater than those after intranasal and rectal dosing ($p < 0.05$), which indicate that intranasal gel treatment resulted in faster and increased absorption of midazolam in the nasal cavity. The elimination phase was similar for all treatment groups. The volume of distribution of midazolam was 0.5 L/kg which was less than total body water ($0.56 \pm 0.03 \text{ L/kg}$) but much larger than the extracellular water ($0.24 \pm 0.03 \text{ L/kg}$) [38] of dogs indicating that midazolam was extensively distributed in both extracellular and intracellular fluids in dogs. This was less than a volume distribution of $1\text{-}3 \text{ L/kg}$ [39] reported in human. The systemic clearance of midazolam in dog was $3.0 \pm 0.6 \text{ ml/min/kg}$ which is less than that reported for human ($6.7\text{-}8.3 \text{ ml/min/kg}$) [40]. The half life, V_d and CL following intranasal administration, rectal administration and intranasal gel administration were consistent with those of intravenous administration which indicate that administration and formulation difference did not alter the intrinsic pharmacokinetic behavior of midazolam. Bioavailability of intranasal and rectal

administration of midazolam were 54.0% and 50.6%, respectively which is consistent with previously published data ^[29, 41, 42]. A significant increased bioavailability (74.4%) was observed after intranasal midazoam gel administration.

DISCUSSION

Mizazolam, a water-soluble benzodiazepine, can be effective in the treatment of status epilepticus. The nasopharyngeal mucosal surface is relatively large and well vascularized, allowing for a rapid absorption of midazolam. Nasal absorption also avoids the high first-pass metabolism of midazolam after oral administration ^[29]. Early studies have proved that intranasal midazolam can safely and effectively suppress epileptic activity in human and animals. Intranasal midazolam is as effective as intravenous diazepam and more effective than rectal diazepam, which prompted its potential use in the management of acute seizures ^[7, 25]. The greatest benefit of intranasal midazolam is for the treatment of seizures in the community. Although intranasal administration of midazolam has many advantages, some disadvantages such as the short residence time and incomplete absorption still limit its clinical popularity. Since an adhesive gel formulation could significantly prolong a drug's residence time at the absorption site and improve the bioavailability of drug, it has increased the popularity of the route of administration. In this study, we developed an intranasal gel formulation that was delivered by syringe into dog nasal cavity. Four administration routes (intravenous, intranasal, rectal and intranasal gel) were utilized to determine if there were increased bioavailability and C_{max} of the new intranasal gel formulation of midazolam. Data from this study demonstrated rapid absorption of midazolam from this intranasal gel formulation, with a mean T_{max} of 11.7 min, from the nasal cavity and into the systemic circulation. Intranasal and rectal routes of administration using a commercial midazolam solution demonstrated slower absorption and

lower bioavailability. Our data were consistent with that of early studies, in either healthy volunteers or dogs that reported that peak concentrations after intranasal and rectal administration of midazolam occurred within 20 min and 30 min ^[43-45]. The bioavailability of midazolam was improved significantly from approximately 50% (intranasal and rectal administration) to 74.4%. This increase indicated that administered midazolam intranasal gel formulation could reduce time to cessation of seizures with desirable pharmacokinetic profiles such as rapid absorption and high bioavailability.

REFERENCE

- [1]. Bassin S, Smith TL, Bleck TP 2002. Clinical review: Status epilepticus. *Crit Care* 6(2):137-142
- [2]. Lowenstein DH 2005. Treatment options for status epilepticus. *Curr Opin Pharmacol* 5(3):334-339.
- [3]. Lowenstein DH 2006. The management of refractory status epilepticus: An update. *Epilepsia* 47 Suppl 1:35-40
- [4]. Lowenstein DH, Bleck T, Macdonald RL 1999. It's time to revise the definition of status epilepticus. *Epilepsia* 40(1): 120-122
- [5]. Delorenzo RJ, Garnett LK, Towne AR, Waterhouse EJ, Ko D 1999. Comparison of status epilepticus with prolonged seizure episodes lasting from 10-29 minutes. *Epilepsia* 40 (2):164-169
- [6]. Shinnar S, Berg AT, Shinnar R 2001. How long do the new-onset seizures in children last? *Ann Neurol* 49 (5):659-664

- [7]. Platt SR, Haag M 2002. Canine status epilepticus: A retrospective study of 50 cases. *J Small Anim Pract* 43(4): 151-153
- [8]. Bateman SW, Parent JM 1999. Clinical findings, treatment, and outcome of dogs with status epilepticus or cluster seizures: 156 cases (1990-1995). *Vet Med Assoc* 215(10):1463-1468.
- [9]. Olaf Henriksen 2007 An Overview of Benzodiazepines in Seizure Management. *Epilepsia* Volume 39 Issue S1, Pages S2 - S6
- [10]. Magnussen I, Oxlund HR, Alsbirk KE, Arnold E. Absorption of diazepam in man following rectal and parenteral administration. *Acta Pharmacol Toxicol (Copenh)* 1979; 45:87 - 90.
- [11]. Hung OR, Dyck JB, Varvel J, Shafer SL, Stanski DR. Comparative absorption kinetics of intramuscular midazolam and diazepam. *Can J Anaesth* 1996;43:450 - 5.
- [12]. Yager JY, Seshia SS. Sublingual lorazepam in childhood serial seizures. *Am J Dis Child* 1988; 142: 931- 2.
- [13]. Wermeling DP, Miller JL, Archer SM, Manaligod JM, Rudy AC. Bioavailability and pharmacokinetics of lorazepam after intranasal, intravenous, and intramuscular administration. *J Clin Pharmacol* 2001; 41: 1225- 31.
- [14]. Mandrioli R, Mercolini L, Raggi MA (October 2008). Benzodiazepine metabolism: An analytical perspective. *Curr. Drug Metab.* **9** (8): 827–44
- [15]. Nordt SP, Clark RF 1997. Midazolam: A review of therapeutic uses and toxicity. *J Emerg Med* 15(3): 357-365
- [16]. BebinM, Bleck TP 1994. New anticonvulsant drugs. Focus on flunarizine, fosphenytoin, midazolam and stiripentol. *Drugs* 48 (2): 153-171

- [17]. Hung OR, Dyck JB, Varvel J, Shafer SL, Stanski DR 1996. Comparative absorption kinetics of intramuscular midazolam and diazepam. *Canadian Journal of Anaesthesia* 43 (5):450-455
- [18]. GalvinGM, Jelinek GA 1987. Midazolam: A effective intravenous agent for seizure control. *Arch Emerg Med* 4(3):169-172
- [19]. Pieri L 1983. Preclinical pharmacology of midazolam. *British Journal of Clinical pharmacology* 16 Suppl 1:17S-27S
- [20]. Reves JG, Fragen RJ, Vinik HR, Greenblatt DJ 1985. Midazolam: pharmacology and uses. *Anesthesiology* 62(3):310-324
- [21]. Lahat E, Goldman M, Barr J, Bistrizter T, Berkovitch M. Comparison of intranasal midazolam with intravenous diazepam for treating febrile seizures in children: prospective randomised study. *Br Med J*. 2000;321:83–86
- [22]. Scott RC, Besag MC, Nevill BGR. Buccal midazolam and rectal diazepam for the treatment of prolonged seizures in childhood and adolescence: A randomised trial. *Lancet*. 1999;353: 623–626
- [23]. Mandema JW, Tuk B, Van Steveninck AL, Breimer DD, Cohen AF, Danhof M. Pharmacokinetic-pharmacodynamic modeling of the central nervous system effects of midazolam and its main metabolite alpha-hydroxymidazolam in healthy volunteers. *Clin Pharmacol Ther*. 1992;51:715–728
- [24]. Bhattacharyya M, KalraV, Gulati S. Intranasal midazolam vs rectal diazepam in acute childhood seizures. *Pediatric Neurology*. 2002 Vol.34 No.5: 355-359
- [25]. Illum L. Nasal Clearance in Health and Disease. *J Aerosol Med* 2006;19: 92–99

- [26]. Kendall JL, Reynolds M, Goldberg R. Intranasal midazolam in patients with status epilepticus. *Ann Emerg Med*, 1997, 29 (3):415-417
- [27]. Platt SR, Randel SC, Scott KC, Chrisman CL, Hill RC, Gronwall RR. Comparison of plasma benzodiazepine concentrations following intranasal and intravenous administration of diazepam to dogs. *American Journal of Pharmaceutical Sciences*, 2000, 80(12): 1125-1129
- [28]. Platt SR, Randel SC, Scott KC, Chrisman CL, Hill RC, Gronwall RR 2000. Comparison of plasma benzodiazepine concentrations following intranasal and intravenous administration of diazepam to dogs. *American Journal of Pharmaceutical Sciences* 80(12): 1125-1129
- [29]. Rey E, Delaunay L, Pons G, Murat I, Richard MO, Saint-Maurice C, Olive G 1991. Pharmacokinetics of midazolam in children: comparative study of intranasal and intravenous administration. *European Journal of Clinical Pharmacology* 41(4):355-357
- [30]. Charlton ST, Davis SS, Illum L. Evaluation of bioadhesive polymers as delivery systems for nose to brain delivery: in vitro characterisation studies. *J Control Release*. 2007 Apr 2;118(2):225-34. Epub 2006 Dec 23.
- [31]. Jagdale SC, Agavekar AJ, Pandya SV, Kuchekar BS, Chabukswar AR. Formulation and evaluation of gastroretentive drug delivery system of propranolol hydrochloride. *AAPS PharmSciTech*. 2009;10(3):1071-9. Epub 2009 Aug 12.
- [32]. Varshosaz J, Sadrai H, Heidari A. Nasal delivery of insulin using bioadhesive chitosan gels. *Drug Deliv*. 2006 Jan-Feb;13(1):31-8.
- [33]. Zaki NM, Awad GA, Mortada ND, Abd Elhady SS. Enhanced bioavailability of metoclopramide HCl by intranasal administration of a mucoadhesive in situ gel with modulated rheological and mucociliary transport properties. *Eur J Pharm Sci*. 2007 Dec;32(4-5):296-307. Epub 2007 Aug 31.

- [34]. Majithiya RJ, Ghosh PK, Umrethia ML, Murthy RS. Thermoreversible-mucoadhesive gel for nasal delivery of sumatriptan. *AAPS PharmSciTech*. 2006 Aug 4;7(3):67.
- [35]. Knoester PD, Jonker DM, Van Der Hoeven RT, Vermeij TA, Edelbroek PM, Brekelmans GJ, de Haan GJ. Pharmacokinetics and pharmacodynamics of midazolam administered as a concentrated intranasal spray. A study in healthy volunteers, *Br J Clin Pharmacol*, 2002;53(5):501-7
- [36]. Henry RJ, Ruano N, Casto D, Wolf RH. A pharmacokinetic study of midazolam in dogs: Nasal drop vs. atomizer administration. *Pediatr Dent*. 1998 Sep-Oct;20(5):321-6
- [37]. Lui CY, Amidon GL, Goldberg A. Intranasal absorption of flurazepam, midazolam, and triazolam in dogs *J Pharm Sci*. 1991 Dec;80(12):1125-9
- [38]. Zweens J, Frankena H, Rispens P, Zijlstra WG. Determination of extracellular fluid volume in the dog with ferrocyanide. *Pflugers Arch*. 1975 Jun 26; 357(3-4): 275-90
- [39]. R J Wills, K C Khoo, P P Soni, and I H Patel. *Br J Clin Pharmacol*. 1990 February; 29(2): 269–272
- [40]. K C Khoo, R J Wills, I H Patel. *Br J Clin Pharmacol*. 1992 April; 31(1): 319–323
- [41]. Schwagmeier R, Alincic S, Striebel HW 1988. Midazolam pharmacokinetics following intravenous and buccal administration. *British Journal of Clinical Pharmacology* 46(3): 203-206
- [42]. Wermeling DP, Record KA, Kelly TH, Archer SM, Clinch T, Rudy AC 2006. Pharmacokinetics and pharmacodynamics of a new intranasal midazolam formulation in healthy volunteers. *Anesthesia and Analgesia* 103(2):344-349.
- [43]. Bjorkman, S., Rigemar, G., Idvall, J., 1997. Pharmacokinetics of midazolam given as an intranasal spray to adult surgical patients. *Br. J. Anaesth*. 79, 575—580

- [44]. Fişgin T, Gurer Y, Teziç T, Senbil N, Zorlu P, Okuyaz C, Akgün D. Effects of intranasal midazolam and rectal diazepam on acute convulsions in children: Prospective randomized study. *J Child Neurol.* 2002;17(2):123-6.
- [45]. Alp H, Orbak Z, Güler I, Altinkaynak S. Efficacy and safety of rectal thiopental, intramuscular cocktail and rectal midazolam for sedation in children undergoing neuroimaging. *Pediatr Int.* 2002; 44(6):628-34.

Table 4.1. Pharmacokinetic parameters (mean \pm SD) generated from WinNonlin analysis of plasma data collected after intravenous, intranasal, rectal and intranasal gel spray administration of Midazolam.

	i.v.	i.n.	rectal	i.n. gel spray
C_{max} (ug/ml)	2.97 \pm 0.73	0.21 \pm 0.02	0.15 \pm 0.01	0.45 \pm 0.09
T_{max} (min)	-	17.50 \pm 2.64	39.0 \pm 14.5	11.7 \pm 2.63
AUC_{0$\rightarrow$$\infty$} (min ug/ml)	71.1 \pm 13.6	37.6 \pm 5.31	34.9 \pm 3.94	50.3 \pm 7.53
Half life (min)	121 \pm 25.7	118 \pm 18.8	116 \pm 15.6	120 \pm 22.8
Clearance (ml/min/kg)	2.98 \pm 0.61	2.92 \pm 0.55	2.73 \pm 0.56	2.91 \pm 0.57
MRT (min)	134 \pm 18.5	165 \pm 23.8	180 \pm 14.4	164 \pm 20.3
Vd (L/kg)	0.50 \pm 0.18	0.50 \pm 0.13	0.47 \pm 0.11	0.50 \pm 0.10
F (%)	-	54.0 \pm 9.51	50.6 \pm 11.3	74.4 \pm 23.2

In the case of IV administration, Cmax was represented by the extrapolated C0.

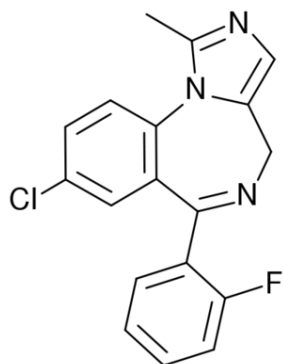


Figure 4.1. Chemical structure of Midazolam

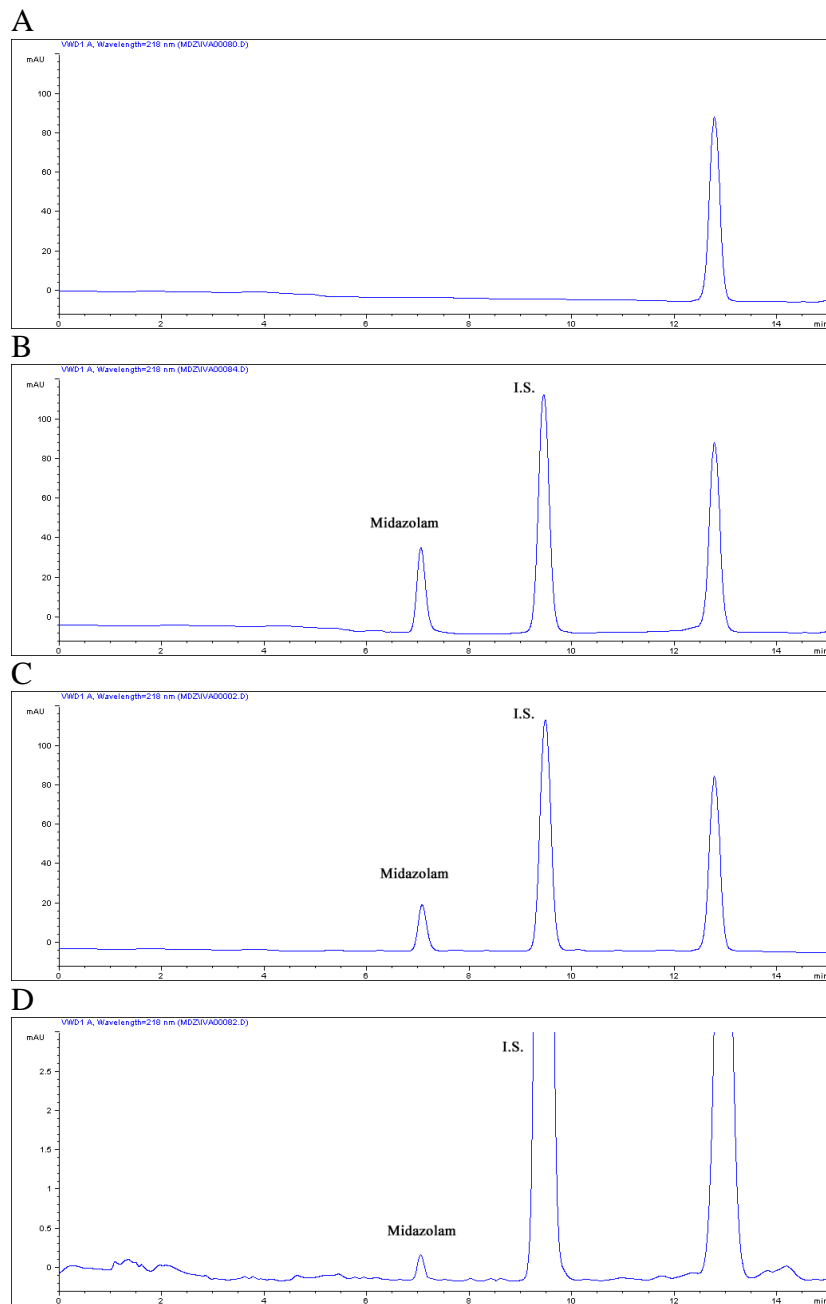


Figure 4.2. Chromatography of blank plasma (A), plasma sample spiked 0.2ug/ml midazolam (B), real plasma sample 30 min after i.v. administration of midazolam (C), LLOQ (0.01 ug/ml) of plasma (D)

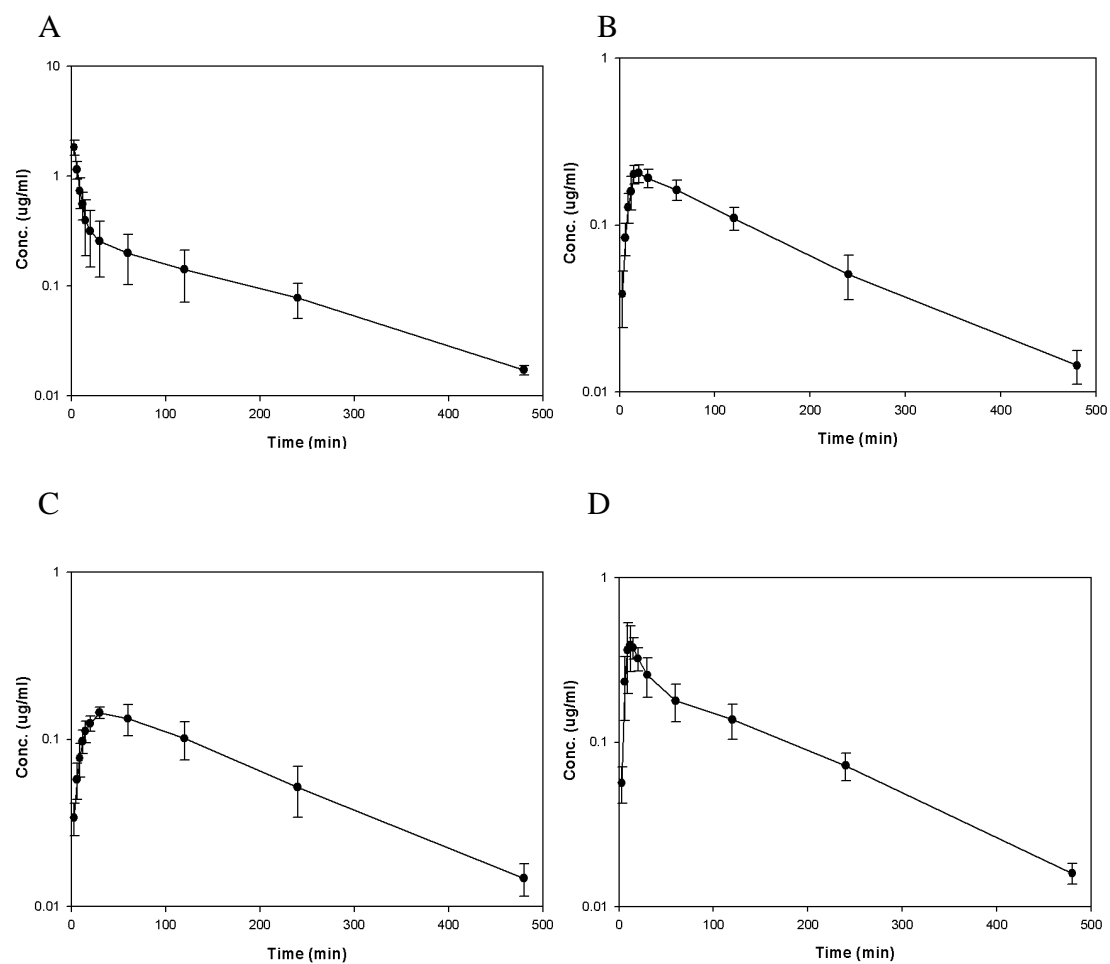


Figure 4.3. Concentration- time profile of i.v. 0.2 mg/kg midazolam administration (A), i.n. 0.2 mg/kg midazolam administration (B), rectal 0.2 mg/kg midazolam administration (C), i.n. gel spray 0.2 mg/kg midazolam administration (D)

CHAPTER 5

PHARMACOKINETICS OF L- β -5-BROMOVINYL-(2-HYDROXYMETHYL)-1, 3- (DIOXOLANYL) URACIL IN RODENTS*

*Bo Zheng, David C.K. Chu, Robert D. Arnold, Catherine A. White. To be submitted to *The AAPS Journal*

ABSTRACT

L- β -5-Bromovinyl-(2-hydroxymethyl)-1,3-(dioxolanyl)uracil (L-BVOddU) has activity both in vitro and in vivo against herpes simplex virus type 1 (HSV-1) and varicella zoster virus (VZV). The purpose of this study was to investigate the pharmacokinetic and tissue distribution at steady state of L-BVOddU in rats and mice, respectively. An HPLC method for the quantification of L-BVOddU in mouse plasma, brain, liver, heart, lung, spleen, kidney, skin and rat plasma was developed and utilized in this study. Mice received 150 mg/kg/day or 8 mg/kg/day orally for 21 day in order that the concentration of L-BVOddU in tissues and plasma reached steady state. Rats received either a 100 mg/kg intravenous dose or a 100 mg/kg oral dose of L-BVOddU. Samples were obtained at serial time points up to 48 hr. Pharmacokinetic parameters were determined using WinNonlin. Acceptable intra-day and inter-day assay precision (<15%) and accuracy (<15%) were observed over a linear range of 0.1-150 ug/ml in all biomatrices ($r^2 = 0.993-0.998$). The recoveries of L-BVOddU ranged from 82.1-98.1%. Ratios of tissue to plasma concentration of L-BVOddU in most tissues were greater than 1 at steady state with both high and low doses, whereas that of L-BVOddU in brain was less 1 with both doses. The $t_{1/2}$, V_d and CL of L-BVOddU in rats were 9.13 hr, 0.55 L/kg, and 43.6 ml/ hr/kg, respectively. The oral bioavailability of L-BVOddU in rat was 26.8 %. It was determined that 95.0-98.1% L-BVOddU was bound to rat plasma proteins over the concentration range of 5-500 ug/ml.

Key words: L-BVOddU, pharmacokinetics, bioavailability, tissue distribution

INTRODUCTION

(E)-5-(2-bromovinyl)-2'-deoxyuridine (D-BVDU) and its derivatives are a group of antiviral agents which are highly active and selective against varicella-zoster virus (VZV) and herpes simplex virus type 1 (HSV-1) ^[1-4]. They owe this high selectivity and activity profile to a specific phosphorylation by the virus-encoded thymidine kinase followed by a potent interaction with the viral DNA polymerase ^[5]. The triphosphate metabolites of these compounds are the active moieties that can interact with the viral DNA polymerase, either as a competitive inhibitor with respect to the natural substrate (dTTP), or as an alternative substrate, allowing the incorporation of BVDU-TP (as BVDU-MP) in the growing DNA chain ^[1-4].

L- β -5-Bromovinyl-(2-hydroxymethyl)-1,3-(dioxolanyl)uracil (L-BVOddU, Figure 5.1), initially synthesized by Bednarski et al. ^[6], has demonstrated antiviral activity against HSV-1 but not HSV-2. L-BVOddU also can inhibit varicella zoster virus (VZV) with an EC₅₀ value of approximately 0.07 ng /ml ^[7]. It has also been reported that L-BVOddU has selective anti-VZV activity with a potency about 80-fold greater than acyclovir (ACV) ^[8]. The metabolism of L-BVOddU is different from that of other anti-VZV nucleoside analogs. Some studies have demonstrated that L-BVOddU is converted into its phosphorylated form by only thymidine kinase of varicella zoster virus and the anti-VZV activity of L-BVOddU is thymidine kinase of varicella zoster virus dependent ^[8]. This is consistent with the findings that bromovinyl nucleoside analogs, such as BVDU and BV-araU, are preferential substrates of the viral thymidine kinase ^[2]. L-BVOddU is the first L-nucleoside that shows potent anti-VZV activity in cell culture. Although L-configuration nucleosides are not always more potent than their D counterparts because they contain the same base and sugar, L-BVOddU is more potent than D-BVOddU, whereas D-BVDU is more potent than L-BVDU. The major side effect of BVDU and

its derivatives is that they can be cleaved by intestinal mucosa flora to produce bromovinyl uracil (BVU). BVU is a strong inhibitor of dihydropyrimidine dehydrogenase (DPD). DPD is an enzyme involved in the degradation of 5-fluorouracil (5-FU), a commonly used anticancer drug.

Therefore, if taken together with 5-FU during anticancer chemotherapy, BVU and its derivatives may cause toxic accumulation of 5-FU and result in death. It was reported that cleavage of L-BVOddU into BVU by mammalian DPD was not detected in *in vitro* metabolism study^[9]. This may give L-BVOddU great clinical potential and a special advantage when used in combination with cancer chemotherapy agents like 5-FU.

It is well known that nucleosides represent a class of anticancer agents. Although it was generally thought that the non-naturally occurring L-nucleoside counterparts might not have biological activity, it has been discovered that some L-nucleosides have exhibited antiviral and anticancer activity^[10-16]. Compared to their D-configuration counterparts, some of the L-nucleosides have good selectivity with potent antiviral activity and low toxicity^[10-16]. Although only few L-nucleosides (e.g. 3TC) have so far gained Food and Drug Administration (USA FDA) approval for clinical use against HIV-1, other L-enantiomers of nucleoside analogues, which have shown antiviral or anticancer activity in cell cultures, are in clinical trials. Their resistance to enantioselective enzymes, such as thymidine phosphorylase, thymidylate synthase, (deoxy)-cytidine and dCMP deaminases, and their lower affinity for the mitochondrial thymidine kinase can ensure a higher selectivity and lower cytotoxicity with respect to those exerted by their corresponding natural D-enantiomers and might be exploited to solve problems arising during chemotherapy, such as metabolic inactivation, cytotoxicity and drug-resistance. Recent research has shown the L-BVOddU has potential anti-cancer activity by inhibiting thymidylate synthase, an enzyme essential in the synthesis of DNA, and reducing cancer cell proliferation.

Those characteristics of L-BVOddU described above make it necessary to fully understand its pharmacological and pharmacokinetic properties in order for development of antiviral or anticancer drug.

To investigate tissue distribution and the basic pharmacokinetic parameters of L-BVOddU, we developed an accurate, sensitive and reproducible HPLC method for the quantification of L-BVOddU in mouse plasma, brain, liver, heart, lung, spleen, kidney, skin and rat plasma. The method was used successfully to study the pharmacokinetics of L-BVOddU following administration of a 100 mg/kg i.v. or oral dose in rat model, and tissue distribution of L-BVOddU at steady state in mice.

EXPERIMENTAL

Materials

L-BVOddU was synthesized by Dr. Chu (College of Pharmacy, UGA). The chemical structure of L-BVOddU was identified by nuclear magnetic resonance and mass spectrometry. Acetonitrile and ethyl acetate (HPLC grade) were obtained from Fisher Scientific Inc. The internal standard, triamterene, was purchased from Sigma Aldrich. Other reagents were of analytical grade.

Preparation of stocks, calibration standards and quality control samples

Stock solutions of 3.0 mg/ml L-BVOddU and triamterene were individually prepared in acetonitrile. Standard solutions of L-BVOddU were prepared by mixing and diluting the appropriate amounts from the individual stock solutions. The final concentrations of the standard solutions were 1500, 800, 500, 100, 25, 10, and 1 µg/ml. A 100 µg/ml standard solution of triamterene was prepared with acetonitrile from 1 mg/ml stock. The quality control samples (QCs) were prepared in duplication from separate stock solutions. High-, mid- and low-level

quality control samples contained 1000, 250 and 20 $\mu\text{g/ml}$ of L-BVOddU and were prepared in a manner similar to that used for the preparation of the calibration standards. Stock solutions were kept refrigerated when not in use and replaced on a bi-weekly basis. Fresh standard solutions were prepared for each day of analysis or validation.

Calibration curves

Blank plasma (mice and rats), and liver, brain, kidney, heart, lung, spleen tissue were collected from untreated anesthetized mice. The tissues were homogenized with an equivalent volume of deionized water (w/v) using an Ultra-Turbax T8 tissue grinder (IKA Labortechnik, Germany). Plasma calibration points were prepared by spiking 100 μL of plasma with 10 μL of L-BVOddU and triamterene standard solutions. Tissue calibration points were prepared by spiking 200 μL of the biological matrices with 10 μL of L-BVOddU and triamterene standard solutions. The calibration curves of all matrices were in the range of 0.1–150 $\mu\text{g/ml}$, with an internal standard concentration in each sample of 10 $\mu\text{g/ml}$. After each matrix was spiked, it was subject to further sample preparation before analysis.

Sample Preparation

After spiked with 10 μl of triamterene (100 $\mu\text{g/ml}$), 100 μl plasma or 200 μl (equal to 200 μg) of tissue homogenate (prepared as above) was mixed with 300 μl acetonitrile and vortex for 15 s. Then, samples were extracted with 0.6 ml ethyl acetate. After centrifugation for 10 min at $2000\times g$, the upper organic layer was removed and evaporated to dryness under reduced pressure in a vacuum centrifuge. The residue obtained was reconstituted in 100 μl acetonitrile with ultrasonic treatment for 1 min. 20 μl injection volumes were used for HPLC analysis.

Chromatographic system

The HPLC measurements were carried out using an Agilent 1100 series HPLC coupled with a UV detector. Data acquisition was performed using chemstation chromatography software package. The chromatographic separation of L-BVOddU was achieved using a Phenomenex Gemini 5 μ C18 110Å column 250x4.6 mm coupled with a Phenomenex Security Guard C18 guard column (Torrance, CA, USA).

Chromatographic conditions

The mobile phase was isocratic: A: 20 mM KH₂PO₄ (pH= 9.0): ACN (10:1); B: MeOH; A: B = 63:37. The mobile phase flow rate was 1.0 ml/min and the UV detection wavelength was set at 254nm. Under the chromatographic conditions described, L-BVOddU and triamterene eluted at 8.7 min, 10.2 min, respectively.

Bioanalytical method validation

Linearity, precision and accuracy

The linearity of the HPLC method for the determination of L-BVOddU was evaluated by a calibration curve in the range of 0.1–150 μ g/ml or μ g/g. The calibration curve was obtained by plotting the ratio of peak area of each analyte to internal standard versus the L-BVOddU theoretical concentration. Least squares linear regression analysis was used to determine the slope, intercept and correlation coefficient. The calibration curve required a correlation coefficient (r^2) of 0.99 or better, which was considered appropriate for a validated method. To evaluate precision, at least five QCs at each of the three different concentrations were processed and injected on a single day (intra-day) and on different days (inter-day). The variability of L-BVOddU determination was expressed as coefficient of variation (%CV), which should be $\leq 15\%$ for all concentrations. Accuracy was expressed as % bias of theoretical versus calculated concentrations, and it should be within limits of $\pm 15\%$ for all concentrations of L-BVOddU.

Recovery

The absolute recoveries of L-BVOddU from plasma and tissues were determined at different standard concentrations by spiking the drug into the corresponding fresh blank plasma or tissues. The percentage of recovery was calculated by comparing the peak area of extracted samples with samples in which the same amount of compounds were diluted with acetonitrile and injected directly. The recoveries at three QC concentration levels of L-BVOddU in plasma and tissues were examined at least five times.

Determination of plasma protein binding using ultrafiltration method

Stock solutions of L-BVOddU in DMSO were added to rat plasma (1%, v/v) to provide plasma samples at a nominal concentration of 500, 50, 5 $\mu\text{g/mL}$. Those concentrations were selected in order to investigate plasma protein binding within the range of the expected plasma concentrations of L-BVOddU after i.v. or oral administration of 100 mg/kg dose in rats. Aliquots of plasma were immediately removed for determination of the initial drug concentration. The remaining plasma samples were placed in a rolling incubator at 37 °C for 30 min to ensure equilibrium was established. Following incubation, an aliquot of plasma was removed for determination of the drug concentration post incubation. Triplicate 500 μL aliquots of the plasma samples were added to the sample reservoir of the standard ultrafiltration (UF) unit (*Amicon Centrifree*, obtained from Millipore) having pre-weighed the filtrate collection tubes. All ultrafiltration units were centrifuged at $2,000 \times g$ for 10 min at ambient temperature. The sample reservoirs containing the plasma retentate were removed and retained whilst the filtrate collection tubes were re-weighed to determine the volume of ultrafiltrate produced (approximate 150-200 μL of the ultrafiltrates were collected). The volume of filtrate produced was calculated from the weights of the collection vials measured both pre-and post filtrate generation assuming

1 mg was equivalent to 1 μ L. The filtrate and retentate were removed, and analyzed as described above to determine both free and total drug. In addition, the analysis of both filtrate and retentate enables the calculation of the recovery of drug from the device. The percentage of bound drug was determined using the following formula: % bound = $100 \times [C_{TOT} - C_{UF}] / C_{TOT}$

Tissue distribution at steady-state of L-BVOddU in mice

Two groups (n=5/group) of female mice received high and low doses (150 mg/kg/day and 8 mg/kg/day) of L-BVOddU orally for 21 days. Plasma, liver, brain, heart, kidney, lung, spleen and skin were collected 1 hr after last dose. L-BVOddU concentration in plasma and tissues was determined as described above. Concentration ratios of tissue to plasma were calculated.

Pharmacokinetic study in rat

Male Sprague–Dawley (SD) rats (280 ± 20 g) were obtained from Harlan laboratories. Animal studies were approved by the University of Georgia Institutional Animal Care and Use Committee, and conducted in accordance with guidelines established by the Animal Welfare Act and the National Institutes of Health Guide for the Care and Use of Laboratory Animals. Animals were maintained (2 rats/ cage) on Purina Lab Rodent Chow 5001 and water *ad libitum* and maintained at light/dark cycle from 6:00 am to 18:00 pm at an AAALAC approved facility on campus. Animals were conditioned for a week before they were utilized in the experiments. The rats were cannulated so that serial blood samples could be taken to characterize the time-course of L-BVOddU, and given a 48 hr recovery period. Water was provided *ad libitum*, but food was withheld for 12 hr prior to dosing. Food was provided 3 h after dosing. L-BVOddU was given orally a 100 mg/kg dose with a solution at a concentration of 50 mg/ml using 50% ethanol as the vehicle. For 100 mg/kg i.v. dosing, L-BVOddU was given with a solution at a

concentration of 100 mg/ml using 70% ethanol as the vehicle. Blood samples from each rat (n=5) were taken at 2, 5, 10, 15, 30 min, and 1, 2, 3, 4, 6, 8, 12, 24, 48 hr post-dosing. Blood samples were analyzed for L-BVOddU using a method developed previously. For oral dosing, L-BVOddU was given at a concentration of 50 mg/ml using 50% ethanol as the vehicle. Blood samples from each rat (n=5) were taken at 2, 10, 15, 30, 45 min, and 1, 2, 3, 4, 6, 8, 12, 24, 48 hr post-dosing. Blood samples were analyzed for L-BVOddU using a method developed previously. The plasma concentration data was subjected to compartmental analysis using WinNonlin (version 5.2, Pharsight, Mountain View, CA, USA). A two-compartment intravenous bolus model with first-order elimination was used to fit the plasma concentration data after i.v. administration. Plasma data after oral administration were subjected to 1-compartmental analysis with first order absorption and elimination. A $1/y^2$ -weighting scheme was used throughout the analyses. The following parameters were calculated: absolute bioavailability (F), volume of distribution (V_d), half-life ($t_{1/2}$), peak concentration (C_{max}), area under the concentration-time curve (AUC), time to reach peak concentration (T_{max}) and total body clearance (CL).

RESULTS AND DISCUSSION

Chromatography method development

The developed HPLC method for quantitatively determining L-BVOddU in all biomatrices achieved good separation between peak of L-BVOddU and background. Figures 5.2 and 5.3 show the typical chromatogram of L-BVOddU in mouse plasma and liver, respectively. Calibration curves were linear over the range of 0.1-150 $\mu\text{g/ml}$ ($r^2 > 0.99$, Table 5.1). The inter- and intra-day assay precision and accuracy (shown in Table 5.2) were less than 15%. The lowest limit of quantification (LLOQ) was 0.1 $\mu\text{g/ml}$. Absolute recovery (shown in Table 5.3) was

larger than 82%. Results of freeze/thaw stability of L-BVOddU in plasma and tissues are shown in Table 5.4, % RSD were less than 6%.

Protein binding determination

The present assay has been successfully applied to quantify the concentration of L-BVOddU in rat plasma in a drug–protein binding study using ultrafiltration. The plasma protein binding at different concentration of L-BVOddU is shown in Table 5.5. The protein binding of L-BVOddU in rat plasma was not changed as the total analyte concentration increased. The plasma protein binding was in the range 95.0–98.1% over all concentrations studied.

Tissue distribution at steady state of L-BVOddU in mice

The concentration at steady state of L-BVOddU in plasma and tissues were shown in Table 5.6. L-BVOddU achieved higher concentration in kidney, liver and lung than those in other tissues at steady state with either high or low dose, whereas the concentration of L-BVOddU in brain was the lowest. The concentration ratios of tissue to plasma were shown in Table 5.6. The ratios of most the tissues were greater than 1, which indicated exclusive tissue distribution of L-BVOddU in mice body with either high or low dose. The highest ratio and lowest ratio belong to lung and brain respectively, which suggested very good distribution in lung, and relatively limited distribution of L-BVOddU in brain. For all the tissues, concentration ratios of tissue to plasma with high dose were lower than those with low dose (in t-test, there is statistically significant difference between conc. ratio of high dose and low dose groups for each tissue), which indicated the non-linear tissue distribution of L-BVOddU in mice. Although dosage was increased 18.75 times from low dose to high dose, the concentrations of L-BVOddU in some of tissues increased with the different pattern (shown in Figure 5.4), which also indicated the non-linear tissue distribution of L-BVOddU in mice. In plasma and spleen, the

concentration of L-BVOddU increased 40 and 34 times from low dose group to high dose group, respectively. This is possibly because the elimination process such as metabolism in liver or the active excretion by some transporter in kidney could be saturated. In brain, lung, liver and skin, the concentration of L-BVOddU increased less than 18 times that dose increased. Saturation of nucleoside transporters might be involved in L-BVOddU distribution process into those tissues after high dose administration, because nucleoside transporters mediate the uptake of physiologic nucleosides as well as both anticancer and antiviral drugs.

Pharmacokinetic analysis

The mean plasma concentration-time profiles of L-BVOddU following the i.v. bolus administration of 100 mg/kg, and fitted curve using a two-compartment model are shown in Figure 5.5. In Figure 5.6, the mean plasma concentration-time profiles of L-BVOddU following oral administration of 100mg/kg, and fitted curve using one-compartment models are shown. The pharmacokinetic parameters generated using two- and one-compartment model with WinNonlin for i.v. and oral administration, respectively, are given in Table 5.7.

After i.v. administration, the plasma L-BVOddU concentrations declined in biexponential fashion. Distribution and elimination half lives of L-BVOddU were 0.32 hr and 9.13 hr, respectively, which indicted that L-BVOddU was rapidly distributed into rat tissues after i.v. administration, and is consistent with the tissue data from the mouse study. The volume of distribution of L-BVOddU was 0.55 ± 0.025 L/kg, which was equal to the total body water (0.53 ± 0.03 L/kg)^[21] of rats, indicating that L-BVOddU was extensively distributed in both extracellular and intracellular fluid in rats. The systemic clearance was 0.044 ± 0.003 L/hr/kg, which suggests that this compound is slowly cleared from the body (value of blood flow of liver and kidney in rat are 3.64 L/hr/kg and 3.80 L/hr/kg, respectively^[22]).

The concentration-time profile of oral treatment displayed obvious absorption and elimination phases. The mean concentration profile demonstrates that L-BVOddU was rapidly absorbed into the systemic circulation after oral administration with a mean peak concentration of 43.0 ± 1.29 $\mu\text{g/ml}$ reached at 0.58 ± 0.09 hr. After that, plasma concentration of L-BVOddU declined in a mono-exponential fashion, which indicated the presence of first order elimination. The half life, V_d and CL of oral administration were consistent with those of i.v. administration, which indicate that the oral administration route did not alter the intrinsic pharmacokinetic behavior of L-BVOddU. Bioavailability of oral administration was 26.8%. Because the value of L-BVOddU clearance is low compared to value of blood flow of liver and kidney in rat, the low bioavailability might be caused by the incomplete absorption or instability of L-BVOddU in GI tract of rat.

CONCLUSION

An HPLC method was developed for the determination of L-BVOddU in mouse plasma, liver, brain, kidney, heart, lung, spleen, skin and rat plasma. This method was accurate, sensitive, and simple. It has been successfully applied to investigate the tissue distribution at steady state of L-BVOddU in mice and the pharmacokinetics of L-BVOddU in rats. The pharmacokinetic characteristics (e.g., extensively and rapidly tissue distribution, high plasma protein binding, rapid oral absorption, long elimination half life) were determined.

REFERENCE

1. Cheng YC, Dutschman GE, De Clercq E, Jones AS, Rahim SG, Verhelst G and Walker RT (1981a) Differential affinities of 5-(2-halogenovinyl)-29-deoxyuridines for deoxythymidine kinases of various origins. *Mol Pharmacol* 20:230–233.

2. Cheng YC, Dutschman GE, Fox JJ, Watanabe KA and Machida H (1981b) Differential activity of potential antiviral nucleoside analogs on herpes simplex virus induced and human cellular thymidine kinases. *Antimicrob Agents Chemother* 20:420–423.
3. Zou FC, Dutschman GE, De Clercq E and Cheng YC (1984) Differential binding affinities of sugar-modified derivatives of (E)-5-(2-bromovinyl)-2'-deoxyuridine for herpes simplex virus-induced and human cellular deoxythymidine kinases. *Biochem Pharmacol* 33:1797–1800.
4. Balzarini J, Bohman C and De Clercq E (1993) Differential mechanism of cytostatic effect of (E)-5-(2-bromovinyl)-2'-deoxyuridine, 9-(1,3-dihydroxy-2 propoxymethyl) guanine, and other antiherpetic drugs on tumor cells transfected by the thymidine kinase gene of herpes simplex virus type 1 or type 2. *J Biol Chem* 268:6332–6337.
5. Allaudeen HS, Kozarich JW, Bertino JR, De Clercq E (1981) On the mechanism of selective inhibition of herpesvirus replication by (E)-5-(2-bromovinyl)-2'-deoxyuridine. *Proc Natl Acad Sci USA*;78: 2698–702.
6. Bednarski K, Dixit D, Wang W, Evans CA, Jin H, Yuen L and Mansour TS (1994) Inhibitory activities of herpes simplex virus type 1 and 2 and human cytomegalovirus by stereoisomers of 2'-deoxy-3'-oxa-5(E)-(2-bromovinyl) uridines and their 4'-thio analogues. *Bioorg Med Chem Lett* 4:2667–2672.
7. Li L, Dutschman G E., Gullen E A., Tsujii E, Grill S P., Choi Y, Chu C K., and Cheng Y (2000) Metabolism and mode of inhibition of varicella-zoster virus by L-b-5-bromovinyl-(2-hydroxymethyl)-(1,3-dioxolanyl)uracil is dependent on viral thymidine kinase, *Mol Pharmacol* 58:1109–1114,

8. Choi Ys, Li L, Grill S, Gullen E, Lee CS, Gumina G (2000) Structure-activity relationships of (E)-5-(2-bromovinyl)uracil and related pyrimidine nucleosides as antiviral agents for herpes viruses. *J Med Chem*;43:2538–46.
9. Li L, Dutschman GE, Gullen EA, Tsujii E, Grill SP, Choi Y, Chu CK, Cheng YC. Metabolism and mode of inhibition of varicella-zoster virus by L-beta-5-bromovinyl-(2-hydroxymethyl)-(1,3-dioxolanyl)uracil is dependent on viral thymidine kinase. *Mol Pharmacol*. 2000 Nov;58(5):1109-14.
10. Chang CN, Doong SL, Zhou JH, Beach JW, Jeong LS, Chu CK, Tsai CH, Cheng YC, Liotta D and Schinazi R (1992) Deoxycytidine deaminase-resistant stereoisomer is the active form of (1/-)-29,39-dideoxy-39-thiacytidine in the inhibition of hepatitis B virus replication. *J Biol Chem* 267:13938–13942.
11. Chu CK, Ma T, Shanmuganathan K, Wang C, Xiang Y, Pai SB, Yao GQ, Sommadossi JP and Cheng YC (1995) Use of 29-fluoro-5-methyl-beta-L-arabinofuranosyluracil as a novel antiviral agent for hepatitis B virus and Epstein-Barr virus. *Antimicrob Agents Chemother* 39:979–981.
12. Grove KL, Guo X, Liu SH, Gao Z, Chu CK and Cheng YC (1995) Anticancer activity of beta-L-dioxolane-cytidine, a novel nucleoside analogue with the unnatural L configuration. *Cancer Res* 55:3008–3011.
13. Lin JS, Kira T, Gullen E, Choi Y, Qu F, Chu CK and Cheng YC (1999) Structureactivity relationships of L-dioxolane uracil nucleosides as anti-Epstein Barr virus agents. *J Med Chem* 42:2212–2217.
14. Lin TS, Luo MZ, Liu MC, Zhu YL, Gullen E, Dutschman GE and Cheng YC (1996) Design and synthesis of 29,39-dideoxy-29,39-didehydro-beta-L-cytidine (beta-L-d4C)

and 29,39-dideoxy 29,39-didehydro-beta-L-5-fluorocytidine (beta-L-Fd4C), two exceptionally potent inhibitors of human hepatitis B virus (HBV) and potent inhibitors of human immunodeficiency virus (HIV) in vitro. *J Med Chem* 39:1757–1759.

15. Ma T, Pai SB, Zhu YL, Lin JS, Shanmuganathan K, Du J, Wang C, Kim H, Newton MG, Cheng YC and Chu CK (1996) Structure–activity relationships of 1-(2-deoxy-2-fluoro-beta-L-arabinofuranosyl)pyrimidine nucleosides as anti-hepatitis B virus agents. *J Med Chem* 39:2835–2843.

16. Dutschman GE, Bridge EG, Liu SH, Gullen E, Guo X, Kukhanova M and Cheng CY (1998) Metabolism of 29,39-dideoxy-29,39-didehydro-beta-L(2)-5-fluorocytidine and its activity in combination with clinically approved anti-human immunodeficiency virus beta-D(1) nucleoside analogs in vitro. *Antimicrob Agents Chemother* 42: 1799–1804.

Table 5.1. Linear regression equations generated from validation data from mouse plasma, brain, liver, kidney, lung, heart, spleen, skin, and rat plasma. (n=3)

Matrix	Slope	Intercept	R ²
Mouse brain	17.3 ± 0.47	-0.015 ± 0.002	0.993 ± 0.002
Mouse heart	17.4 ± 0.04	-0.418 ± 0.11	0.998 ± 0.001
Mouse kidney	17.1 ± 0.4	-0.328 ± 0.04	0.996 ± 0.003
Mouse liver	17.2 ± 0.7	-0.135 ± 0.017	0.993 ± 0.004
Mouse lung	17.2 ± 0.04	-0.211 ± 0.05	0.997 ± 0.002
Mouse plasma	17.7 ± 0.17	-0.072 ± 0.02	0.997 ± 0.001
Mouse skin	17.0 ± 0.24	-0.306 ± 0.13	0.993 ± 0.002
Mouse spleen	17.1 ± 0.29	-0.517 ± 0.09	0.995 ± 0.001
Rat plasma	17.9 ± 0.04	-0.102 ± 0.06	0.998 ± 0.001

Table 5.2. Intra-day (n=5) and Inter-day (n=15) precision (%R.S.D) and accuracy (%Error) of the method in. T.C denotes theoretical concentration and E.C denotes experimental concentration.

Mouse Plasma:

T.C (ug/ml)	Day1 E.C (ug/ml)	%Error	%R.S.D	Day2 E.C (ug/ml)	%Error	%R.S.D	Day3 E.C (ug/ml)	%Error	%R.S.D	Inter- day E.C (ug/ml)	%Error	%R.S.D
100	102	2.3	3.0	102	3.2	4.7	98.4	4.5	3.4	101	4.0	5.8
25	25.1	4.4	5.6	25.80	4.1	3.5	24.72	3.7	5.8	25.16	5.5	4.9
2	2.17	9.7	7.7	2.23	8.5	7.8	2.04	7.3	8.5	2.01	4.1	11.7
0.1	0.01	7.2	8.7	0.098	8.3	6.8	0.095	8.1	8.4	0.099	4.8	7.1

Mouse Brain:

T.C (ug/g)	Day1 E.C (ug/g)	%Error	%R.S.D	Day2 E.C (ug/g)	%Error	%R.S.D	Day3 E.C (ug/g)	%Error	%R.S.D	Inter- day E.C (ug/g)	%Error	%R.S.D
100	102	6.3	6.3	101	0.77	2.4	99.4	8.7	3.8	101	3.7	4.7
25	25.7	3.8	5.8	24.9	5.20	4.0	24.9	7.3	3.4	25.4	3.2	2.1
2	2.10	9.2	8.6	1.89	12.34	9.8	1.97	5.5	9.1	1.98	2.3	3.5
0.1	0.106	2.7	4.9	0.096	0.80	5.9	0.099	10.8	7.7	0.101	6.8	8.4

Mouse Liver:

T.C (ug/g)	Day1 E.C (ug/g)	%Error	%R.S.D	Day2 E.C (ug/g)	%Error	%R.S.D	Day3 E.C (ug/g)	%Error	%R.S.D	Inter- day E.C (ug/g)	%Error	%R.S.D
100	101	3.0	6.0	98.2	1.8	5.6	99.1	2.7	6.3	100	8.2	6.1
25	25.3	2.3	2.9	24.9	4.2	2.8	24.8	3.0	7.7	25.1	8.6	5.1
2	2.01	11.0	6.0	2.12	3.8	6.7	1.97	4.5	9.0	2.06	6.0	8.5
0.1	0.095	9.6	4.8	0.099	6.9	4.8	0.109	7.0	9.7	0.103	1.2	1.8

Mouse Kidney:

T.C (ug/g)	Day1 E.C (ug/g)	%Error	%R.S.D	Day2 E.C (ug/g)	%Error	%R.S.D	Day3 E.C (ug/g)	%Error	%R.S.D	Inter- day E.C (ug/g)	%Error	%R.S.D
100	101	2.1	7.0	98.5	1.8	5.5	101	3.2	5.2	100	5.5	3.3
25	24.7	3.9	2.6	24.6	4.1	5.3	25.2	4.5	7.4	25.1	10.6	1.6
2	2.06	9.5	5.0	1.96	3.2	8.9	2.02	9.2	8.2	2.01	5.8	5.9
0.1	0.098	6.3	17.6	0.097	4.1	14.7	0.102	9.5	8.9	0.101	3.6	5.2

Mouse Heart:

T.C (ug/g)	Day1 E.C (ug/g)	%Error	%R.S.D	Day2 E.C (ug/g)	%Error	%R.S.D	Day3 E.C (ug/g)	%Error	%R.S.D	Inter- day E.C (ug/g)	%Error	%R.S.D
100	99.6	2.9	7.7	99.5	1.8	4.2	101.8	3.1	5.0	100	4.5	3.3
25	25.0	3.49	2.6	25.3	4.1	5.3	24.8	4.5	7.4	25.1	10.6	1.6
2	2.11	9.6	5.2	1.96	3.6	8.9	2.11	9.2	8.2	2.08	5.7	5.9
0.1	0.11	6.3	17.5	0.09	4.1	14.7	0.09	9.5	8.9	0.10	3.6	5.2

Mouse Lung:

T.C (ug/g)	Day1 E.C (ug/g)	%Error	%R.S.D	Day2 E.C (ug/g)	%Error	%R.S.D	Day3 E.C (ug/g)	%Error	%R.S.D	Inter- day E.C (ug/g)	%Error	%R.S.D
---------------	-----------------------	--------	--------	-----------------------	--------	--------	-----------------------	--------	--------	--------------------------------	--------	--------

100	101	2.19	7.07	99.6	1.9	5.1	99.9	3.7	5.4	101	3.7	3.4
25	24.8	3.9	2.6	25.2	4.1	5.7	24.8	4.5	7.9	24.7	10.1	1.6
2	2.09	9.5	5.0	1.96	3.6	8.9	2.11	9.2	8.9	2.07	5.8	5.9
0.1	0.101	6.3	14.4	0.11	4.4	14.1	0.10	9.5	8.9	0.11	3.6	5.2

Mouse Spleen:

T.C (ug/g)	Day1 E.C (ug/g)	%Error	%R.S.D	Day2 E.C (ug/g)	%Error	%R.S.D	Day3 E.C (ug/g)	%Error	%R.S.D	Inter- day E.C (ug/g)	%Error	%R.S.D
100	101	2.9	8.7	98.9	1.8	3.2	101	3.1	5.9	102	2.5	4.3
25	25.7	3.5	2.6	24.8	4.1	5.3	25.2	4.5	7.9	25.3	11.6	1.9
2	2.21	9.0	5.0	0.19	3.7	9.0	2.21	9.5	8.2	2.78	5.8	5.9
0.1	0.09	6.3	12.5	0.11	4.4	10.7	0.096	9.0	8.0	0.1	3.9	5.2

Mouse Skin:

T.C (ug/g)	Day1 E.C (ug/g)	%Error	%R.S.D	Day2 E.C (ug/g)	%Error	%R.S.D	Day3 E.C (ug/g)	%Error	%R.S.D	Inter- day E.C (ug/g)	%Error	%R.S.D
100	101	2.8	7.7	99.3	1.9	5.5	101	3.1	6.2	102	3.5	4.7
25	25.4	3.4	2.6	25.6	4.1	5.7	24.8	4.7	7.4	25.3	10.9	1.6
2	2.15	9.1	5.2	2.03	3.2	9.9	2.11	8.2	8.7	2.18	5.8	6.9
0.1	0.101	6.2	10.6	0.1	4.1	12.8	0.099	9.8	8.9	0.11	3.6	5.4

Rat Plasma:

T.C (ug/g)	Day1 E.C (ug/g)	%Error	%R.S.D	Day2 E.C (ug/g)	%Error	%R.S.D	Day3 E.C (ug/g)	%Error	%R.S.D	Inter- day E.C (ug/g)	%Error	%R.S.D
100	102	2.1	8.0	101	2.1	6.2	98.8	3.2	5.2	102	2.7	3.4
25	25.7	3.9	2.6	25.6	4.0	5.3	24.7	4.5	7.4	25.3	10.1	2.6
2	2.15	9.2	5.2	1.92	3.6	8.9	2.05	8.8	8.9	1.96	5.9	5.7
0.1	0.10	6.3	11.5	0.095	4.4	11.7	0.095	9.5	8.6	0.098	3.3	5.2

Table 5.3. Percent absolute recoveries of L-BVOddU from mouse plasma, brain, kidney, lung, heart, and spleen, skin, and rat plasma. (mean \pm s.d., n=20)

Conc. (ug/ml or ug/g)	Mouse Plasma	Mouse Brain	Mouse Liver	Mouse Kidney	Mouse Lung	Mouse Heart	Mouse Spleen	Mouse Skin	Rat Plasma
100	93.6 \pm 1.0	98.4 \pm 1.9	97.5 \pm 2.1	96.7 \pm 2.2	97.3 \pm 1.6	93.9 \pm 3.2	95.4 \pm 2.3	92.3 \pm 2.4	95.1 \pm 2.2
25	92.2 \pm 3.3	95.4 \pm 1.5	93.7 \pm 1.8	94.5 \pm 3.0	88.3 \pm 2.0	82.1 \pm 4.2	89.4 \pm 2.8	94.6 \pm 2.1	94.3 \pm 2.0
2	92.7 \pm 1.5	94.9 \pm 2.2	90.5 \pm 3.4	92.1 \pm 2.4	86.7 \pm 2.4	91.1 \pm 3.9	87.9 \pm 3.0	89.0 \pm 3.1	89.8 \pm 3.0
0.1	91.5 \pm 3.1	89.8 \pm 2.6	90.1 \pm 3.5	90.4 \pm 2.9	89.1 \pm 2.7	90.2 \pm 3.1	87.2 \pm 3.9	88.1 \pm 4.7	89.4 \pm 4.1

Table 5.4. Results of freeze/thaw stability of L-BVOddU in mouse plasma, brain, liver kidney, heart, lung, spleen, skin, and rat plasma, represented by area \pm s.d. (n=5) of each day and % R.S.D of the area between days.

	Mouse Plasma	Mouse Brain	Mouse Liver	Mouse Kidney	Mouse Heart	Mouse Lung	Mouse Spleen	Mouse Skin	Rat plasma
Day 1	357 \pm 15	359 \pm 14	345 \pm 13	344 \pm 15	359 \pm 15	349 \pm 16	349 \pm 13	347 \pm 13	357 \pm 16
Day 2	369 \pm 9.2	361 \pm 10	339 \pm 12	339 \pm 9.3	359 \pm 8.2	353 \pm 10	341 \pm 11	349 \pm 10	361 \pm 9.5
Day 3	358 \pm 14	349 \pm 14	335 \pm 9.1	338 \pm 15	347 \pm 13	349 \pm 14	339 \pm 9.1	339 \pm 15	345 \pm 10
Day 4	355 \pm 7.3	358 \pm 7.5	341 \pm 11	335 \pm 9.3	345 \pm 7.3	348 \pm 6.5	331 \pm 13	335 \pm 8.7	345 \pm 8.6
%R.S.D	4.02	5.1	5.52	4.46	4.07	5.1	5.12	4.73	3.82

Table 5.5. Protein binding of L-BVOddU in rat plasma

Concentration (ug/ml)	Plasma protein binding (% \pm SD)	Recovery (% \pm SD)
5	98.1 \pm 1.7	102.3 \pm 1.3
50	97.9 \pm 1.9	99.1 \pm 1.7
500	95.1 \pm 2.0	98.1 \pm 1.6

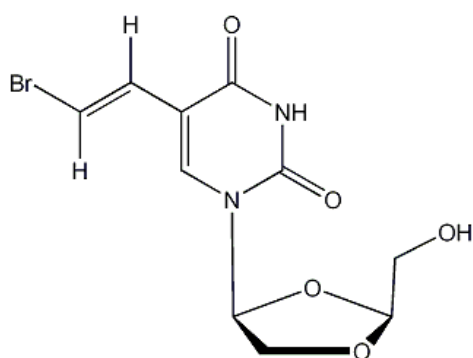
Table 5.6. Concentration of L-BVOddU in mouse plasma and tissues after oral administration of L-BVOddU (150 or 8 mg/kg/day) for 21 days in mice. (mean \pm s.d.)

Biomatrix	Concentration of (ug/ml or ug/g) after high dose (150 mg/kg/day)	Conc. Ratio of tissue to plasma	Concentration of (ug/ml or ug/g) after low dose (8 mg/kg/day)	Conc. Ratio of tissue to plasma
Brain	1.11 \pm 0.34	0.08 \pm 0.03	0.12 \pm 0.02	0.31 \pm 0.11
Heart	13.7 \pm 2.81	1.01 \pm 0.16	0.67 \pm 0.12	1.95 \pm 0.46
Kidney	27.4 \pm 3.53	2.05 \pm 0.35	1.30 \pm 0.24	3.80 \pm 0.34
Liver	19.8 \pm 4.08	1.47 \pm 0.3	1.38 \pm 0.54	4.08 \pm 1.14
Lung	30.4 \pm 2.77	2.29 \pm 0.45	3.0 \pm 0.77	8.75 \pm 2.6
Plasma	13.9 \pm 3.93	-	0.343 \pm 0.1	-
Skin (hu)	11.3 \pm 1.12	0.88 \pm 0.29	0.72 \pm 0.08	2.10 \pm 0.51
Skin (mu)	11.8 \pm 0.96	0.89 \pm 0.2	0.69 \pm 0.08	2.00 \pm 0.54
Spleen	18.8 \pm 6.20	1.36 \pm 0.10	0.55 \pm 0.16	1.72 \pm 0.13

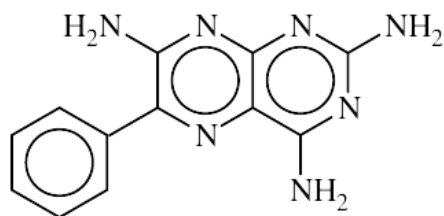
Table 5.7. Pharmacokinetic parameters (mean \pm SD) generated from WinNonlin analysis of plasma data collected after i.v. and oral administration of L-BVOddU.

	i.v. (2-compartmental analysis)	Oral (1-compartmental analysis)
C_{\max} (ug/ml)	385 ± 26.3	42.99 ± 1.29
T_{\max} (hr)	-	0.58 ± 0.09
$AUC_{0 \rightarrow \infty}$ (hr ug/ml)	2300 ± 138	617 ± 34.3
Distribution Half Life (hr)	0.32 ± 0.03	-
Elimination Half life (hr)	9.13 ± 0.16	9.57 ± 0.34
Clearance (L/hr/kg)	0.044 ± 0.003	0.043 ± 0.001
K_a (hr ⁻¹)	-	9.01 ± 1.07
V_d (L/kg)	0.55 ± 0.03	0.6 ± 0.05
Bioavailability (%)	-	26.8 ± 0.01

In the case of i.v. administration, C_{\max} was represented by the extrapolated C_0 .



L-BVOddU



TRIAMTERENE

Figure 5.1. Chemical structure of L-BVOddU (top) and trimterene (bottom)

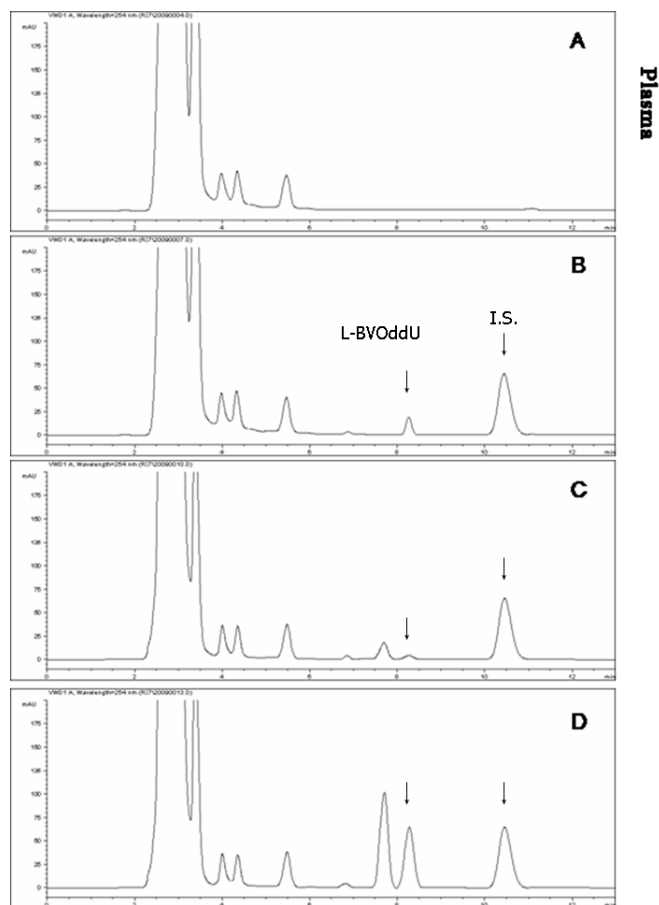


Figure 5.2. Representative HPLC chromatograms: (A) blank Plasma sample, (B) a 2 µg/ml L-BVOddU quality control Plasma sample, (C) a mouse Plasma sample after 8 mg/kg/day dose of L-BVOddU for 21 days, (D) a mouse Plasma sample after 150 mg/kg/day dose of L-BVOddU for 21 days.

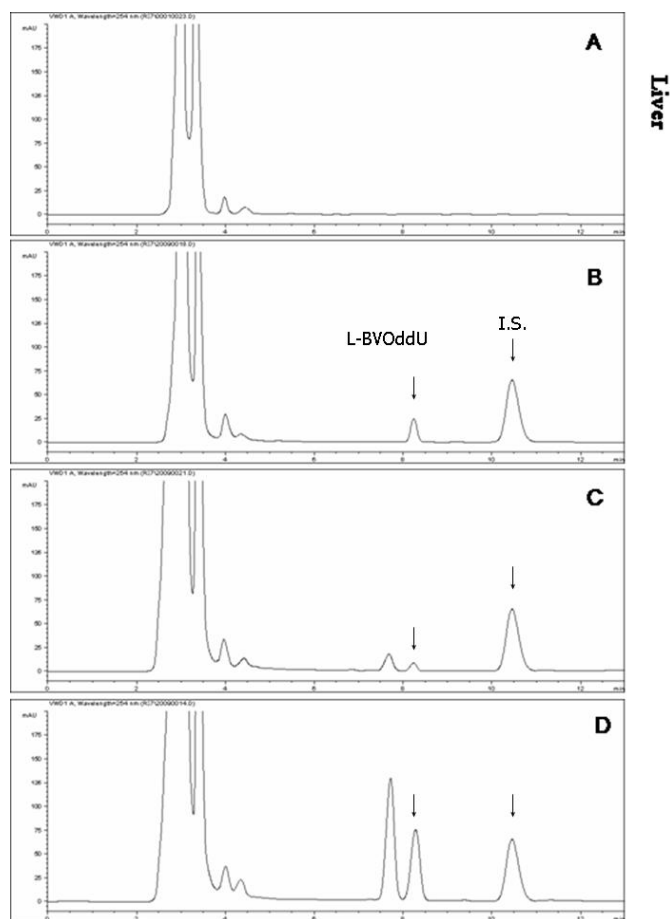


Figure 5.3. Representative HPLC chromatograms: (A) blank Liver sample, (B) a 2 µg/ml L-BVOddU quality control liver sample, (C) a mouse liver sample after 8 mg/kg/day dose of L-BVOddU for 21 days, (D) a mouse liver sample after 150 mg/kg/day dose of L-BVOddU for 21 days.

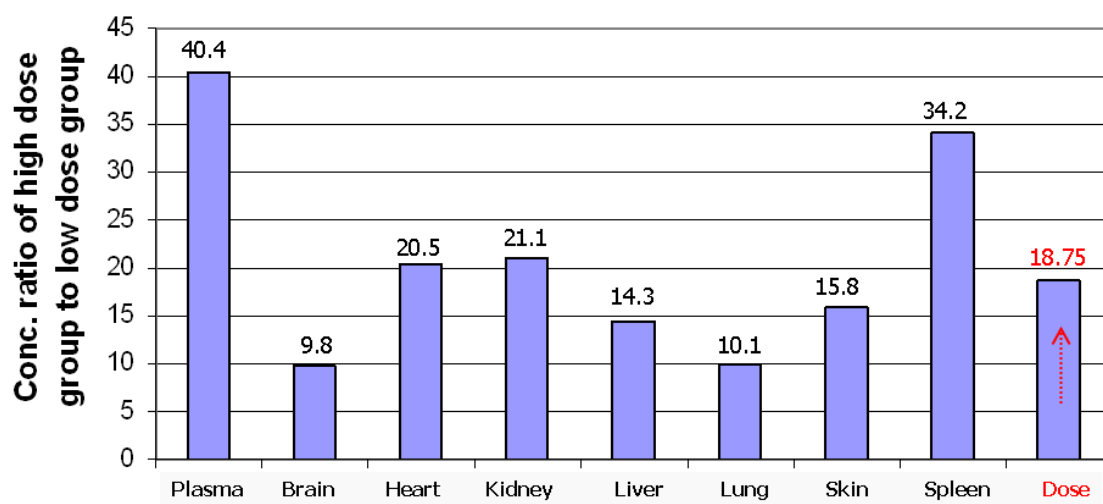
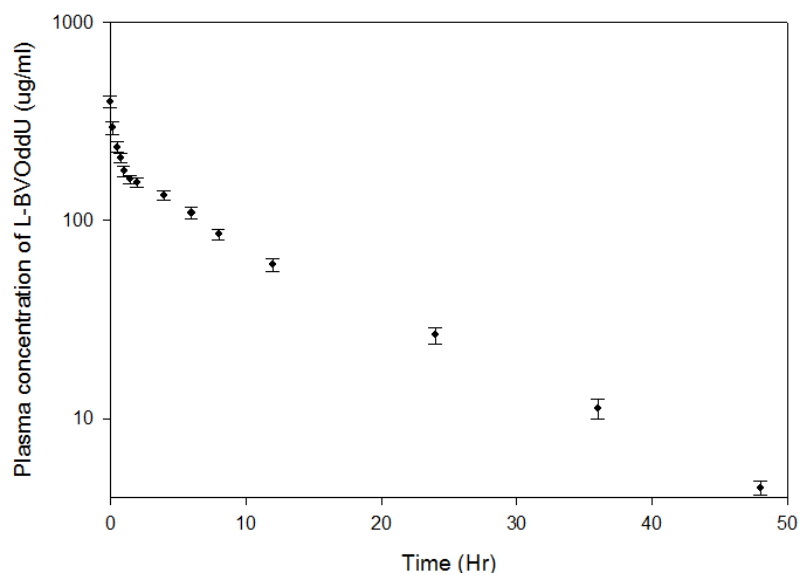


Figure 5.4. L-BVOddU's mean concentration ratio of high dose to low dose group for each tissue

A



B

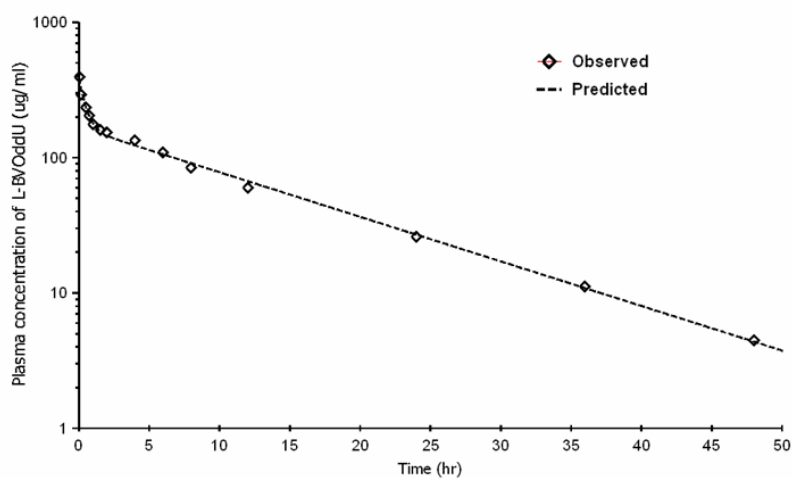
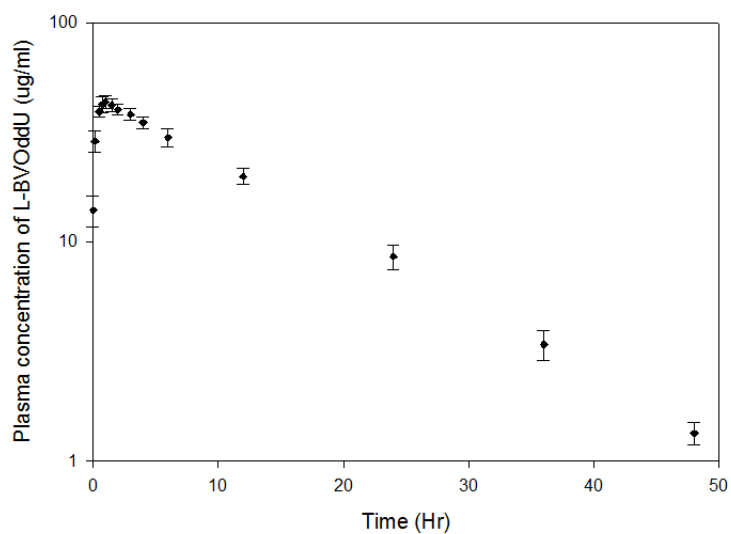


Figure 5.5. A: plasma concentration v.s. time profile of L-BVOddU in rats after i.v. 100 mg/kg dose. **B:** the mean plasma concentration-time profile after i.v. administration of L-BVOddU was fitted to a two-compartment model.

A:



B:

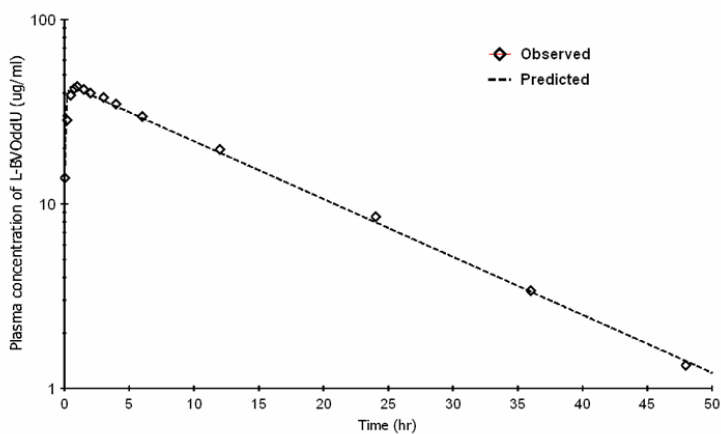


Figure 5.6. A: plasma concentration v.s. time profile of L-BVOddU in rats after i.v. 100 mg/kg dose. B: the mean plasma concentration-time profile after oral administration of L-BVOddU was fitted to a one-compartment model.

CHAPTER 6

ESTIMATING THE LIPOPHILITY OF NATURAL PRODUCTS USING A POLYMERIC REVERSED PHASE HPLC METHOD¹

¹Bo Zheng and Lyndon M. West. To be submitted to *Journal of Liquid Chromatography & Related Technologies*

ABSTRACT

The integration of physicochemical profiling screens such as Log P into natural products drug discovery programs is emerging as an approach to front-load drug-like properties of natural product libraries for high-throughput screening. In this study, a fast-gradient HPLC method using a polystyrene-divinylbenzene PRP-1 column was developed to estimate the lipophilicity of marine natural products. An excellent correlation was found between the results of the experimentally determined and the literature log P values for a diverse set of commercially available drugs using the PRP-1 column. The log P of a series of 24 marine natural products were evaluated using the new method and a good correlation was observed between the experimentally determined and software calculated log P values. Some discrepancies were observed between the measured value of log P and the software calculations of the natural products containing halogen atoms. The method is rapid, insensitive to impurities, and requires very little compound and is amenable for integration into a natural products drug discovery research program.

Keywords: Lipophilicity, Natural Products, Drug discovery, Polystyrene-divinylbenzene, Reversed-phase HPLC.

INTRODUCTION

Lipophilicity, expressed as the logarithmic value of the octanol/water partition coefficient ($\log P_{\text{oct}}$), is a fundamental parameter that models the biological partition behavior of drug molecules.^[1] For example, drug absorption and $\log P_{\text{oct}}$ are directly related because of passive diffusion across the cell membrane. We can estimate absorption, even permeability and distribution of drug candidates in body by $\log P_{\text{oct}}$. If the $\log P$ value is below 0 or above 5, drug candidates usually have intestinal and central nervous system (CNS) permeability problems or low solubility and poor oral bioavailability. Actually, the $\log P_{\text{oct}}$ corresponding to the 90th percentile of drug candidates that reached phase II clinical trials is between 0 and 5.^[2] Therefore, consideration of $\log P_{\text{oct}}$ in the process of drug development can prioritize leads from high-throughput screening and reduce the failure rate of drug candidates during development.^[3, 4]

Reversed-phase liquid chromatography (RP-HPLC) has been widely used to estimate $\log P_{\text{oct}}$.^[4, 5, 6] All of these methods achieve satisfactory correlations with $\log P_{\text{oct}}$, even for very hydrophobic compounds ($\log P_{\text{oct}} > 6$). Valkó *et al.* proposed a rapid method for measurement of $\log P$ via reversed-phase HPLC and established a general solvation equation for $\log P$ values and Chromatographic Hydrophobicity Indices with acetonitrile (CHI_{ACN}).^[7, 8, 9] The main advantage of an HPLC-based lipophilicity measurement is that the partition coefficients can be obtained from time measurements instead of concentration determinations. The result of this is that retention time (t_R) is independent of the compound concentration/amount injected into the chromatographic system. Consequently, impurities do not affect the measurements, and the low solubility of some compounds does not affect the measurements. Another important feature of this method is that very little compound is required and the $\log P$ of a mixture of several

compounds can be obtained from a single injection. These characteristics make HPLC a practical method to determine drug lipophilicity in the early stages of drug discovery. HPLC-based methods suffer some disadvantages such as short linear range of $\text{Log } P_{\text{oct}}$ and retention time, and the lipophilicity assessment of charged compounds such as basic drugs are unreliable. The discrepancies of $\log P$ measurements of charged compounds have been attributed to silanophilic interactions with free silanol groups on silica based C_{18} columns, which results in increases in retention times.^[10]

The integration of physicochemical profiling screens such as $\text{Log } P$ into natural products drug discovery programs is emerging as an approach to front-load lead-like properties of natural product libraries for high-throughput screening.^[11] We have been utilizing polystyrene-divinylbenzene (PS-DVB) chromatographic stationary phases (Diaion HP-20 and PRP-1) for the initial fractionation of crude extracts and the isolation and purification of marine natural products.^[12] Unlike silica based stationary phases such as C_8 or C_{18} , the polymer-based chromatographic resins have no stationary phase coating, is a rigid, macroporous, cross-linked polymer that lacks any polar sites and so does not suffer from irreversible binding of polar solutes. In addition polymeric resins are also chemically inert in most organic solvents, can be used at a wide range of pH values (pH 1-13), and has been found to afford improved separation of basic compounds.^[13] These characteristics make PS-DVB based separation media a versatile stationary phase for the separation of a broad range of compound classes in a wide range of applications.^[14] Although polymeric stationary phases such as octadecyl-poly(vinyl alcohol) (ODP), and PS-DVB based stationary phases (ACT-1, PRP-1, and PLRP-S) have been used to estimate lipophilicity ($\text{Log } P$) using isocratic HPLC methods with varied success, there is no

rapid gradient method available to estimate lipophilicity ($\text{Log } P_{\text{oct}}$) of compounds using a PRP-1 column.^[10, 15, 16]

In this study we have developed a fast-gradient HPLC method using a polystyrene-divinylbenzene PRP-1 column to estimate the lipophilicity of natural products. We believe that the evaluation of $\log P$ in natural products chemistry will be useful to optimize the generation of drug-like natural product screening libraries, to prioritize leads and improve the success rate of natural products at the later stages of the drug discovery process.

METHOD

Materials

All solvents were HPLC grade and were supplied by Sigma-Aldrich. Water used throughout the study was purified with a Milli-Q water purification system from Millipore (Millipore, Bedford, MA, USA). All reference compounds were obtained from Sigma (St. Louis, MO, USA) and Aldrich (Milwaukee, WI, USA) with high purity (>98%). The marine natural products were isolated from marine organisms collected from the coast of Florida and the Bahamas.

Instrumentation

A Shimadzu (Kyoto, Japan) quaternary low pressure gradient system was used for the HPLC measurements. The solvents were degassed using a DGU-20AT degassing unit and mixed in an FCV-20AL mixer. An LC-20AT pump equipped with a Shimadzu SCL-20AT System controller, permitting automated operation, was used to deliver the mobile phase to the analytical column. Sample injection was performed using a Rheodyne 7725i injection valve (Rheodyne, Cotati California, U.S.A) equipped with a 20 μL sample loop. Detection was

achieved using an UV-SPD-M20A diode array detector and a Shimadzu ELSD-LTII detector. Data acquisition was performed using EZStart chromatography software package version 7.4.

Chromatographic Conditions

Samples were prepared by dissolving 0.1 mg/mL of the solute in 50% (v/v) acetonitrile and 50 % (v/v) 50 mM ammonium acetate buffer. An aliquot of the solution (20 μ L) was injected onto the HPLC system. The stationary phase consisted of a Hamilton PRP-1 column (5 μ m, 150 mm \times 4.6 mm). The flow rate was 1 mL/min. The mobile phase was filtered through a 0.5 μ m Fluoropore membrane filter (Millipore, USA) membrane before use. Retention times t_r were measured at least from three separate injections, dead time t_0 was the retention time of sodium nitrate. For the isocratic mode, the mobile phase consisted of different mixtures of acetonitrile and 25 mM AcONH₄ adjusted at pH 4.5, 7.2, 9.8 in the range 0 – 100%. For the fast gradient mode, the following gradient program was applied: 0-1.5 min, 0% acetonitrile; 1.5 – 16.5 min, 0 – 100% acetonitrile; 16.5 – 18.5 min, 100% acetonitrile; 18.5 – 23.0 min, 100 – 0% acetonitrile; 23.0 – 25.0 min, 0% acetonitrile. The dead time (t_0) was measured by injecting sodium nitrate together with the sample.

Measurement of the hydrophobicity index (Φ_0) of the reference compounds in isocratic mode.

Theophylline, 5-phenyl-1*H*-tetrazole, benzimidazole, colchicine, 8-phenyltheophylline, indole, acetophenone, propiophenone, butyrophenone, and valerophenone were used as reference compounds that covers the log P_{oct} range from -0.02 – 3.26. These compounds are not ionized at pH 7.4, so their distribution coefficient is equivalent to their log P_{oct} values. The standard solutions were injected onto the system and their retention times were recorded. The standard mixture contains reference compounds at a concentration of approximately 0.1 mg/mL in

acetonitrile:buffer, (50:50) (v/v). The retention times of some of the components varied with pH. This is because some of the components are charged at low or high pH. The retention time of the acetophenone, propiophenone, butyrophenone and the valerophenone should be constant, respectively at all pH values. We used longest t_R under mobile phase at pH 4.5, 7.2, 9.8 to measure hydrophobicity index (φ_0).

For each reference compound, the average retention time (t_R) of three consecutive injections of 20 μ L of sample was used to calculate the $\log k'$ values ($\log k' = \log[(t_R - t_0)/t_0]$).

At least 5 mobile phases with different organic-phase concentrations were applied for each reference compounds. Then the $\log k'$ values were plotted against the applied acetonitrile concentration. The slope (S) and the intercept ($\log k'_w$) value were calculated based on $\log k'$ values obtained by a minimum of five organic-phase concentrations. The correlation coefficients of the linear fit were always higher than 0.99. The isocratic chromatographic hydrophobicity index (φ_0) was calculated as $\log k'_w/S$.

Setup CHI- t_R standard curve in gradient mode with reference compounds.

Reference compounds were dissolved in an acetonitrile/buffer mixture described above. With gradient chromatography, the retention times (t_R) were measured with mobile phases with three different pH values described above. We used the longest retention times (t_R) of each compound to calculate CHI. A standard curve was created by plotting the highest t_R of each reference compound against its isocratic hydrophobicity index, φ_0 , obtained above. An equation relating t_R to φ_0 is also generated from the standard curve. The slope and the intercept of the standard curve were used to convert the gradient retention times of each reference compound to CHI values, φ_0 (predicted value).

Log P_{oct} calculation

According to the equation:^[9]

$$\text{Log } P_{\text{oct}} = 0.047 \text{ CHI}_{\text{ACN}} + 0.36 \text{ HBC} - 1.10 \quad (1)$$

Where HBC is hydrogen bond count. The log P was calculated.

Validation of the Method

The fast-gradient HPLC method using the PRP-1 column was validated using a set of 21 commercially available drugs with diverse structures. Using the gradient chromatographic run described above, we used the standard curve to convert t_R measured to CHI value, then we used equation 4 to calculate log P_{oct} . We also obtain the literature log P_{oct} value of the 21 compounds from Drug Bank (<http://www.drugbank.ca/>). The comparison and correlation analysis between calculated and literature Log P_{oct} were performed.

Estimating the lipophilicity of Marine Natural Products.

The log P of 24 marine natural products were assessed by the fast-gradient HPLC method using the PRP-1 column. Evaporative Light scattering detection (ELSD) was used to detect compounds that did not contain a strong UV chromophore. We also used software ChemBioDraw Ultra (CambridgeSoft Corporation) to calculate Log P_{oct} .

RESULTS AND DISCUSSION

According to the HPLC theory, the phase preference of a single solute can be expressed by the capacity factor k ($k = (t_r - t_0)/t_0$). The sample k values are also related to the volume fraction, φ , of the organic solvent in the mobile phase as:

$$\log k = \log k_w - S\varphi \quad (2)$$

The intercept log k_w corresponds to the retention in pure water as a mobile phase and represents the commonly employed chromatographic hydrophobicity parameter. S is a solute

dependent solvent strength parameter specific to the organic modifier on the stationary phase under consideration. Another retention-related parameter has been introduced recently, the chromatographic hydrophobicity index (CHI), φ_0 .^[8, 17] The φ_0 value represents the volume fraction of the organic solvent in the mobile phase for which the amount of solute in the mobile phase is equal to that in the stationary phase, i.e. the capacity factor is 1 ($\log k = 0$):

$$\varphi_0 = \log k_w / S \quad (3)$$

where φ_0 is equal to the ratio of the intercept and slope of equation 2. In addition to determining the $\log P$ -values experimentally, they can also be predicted by using a number of $\log P_{\text{oct}}$ calculation methods.

The isocratic retention times were measured by using various volume percents of acetonitrile in the mobile phase, preferably bracketing the retention when $\log k' = 0$ (that is the retention time was close to the double of the dead time). The isocratic hydrophobicity index, φ_0 , was calculated from the slope (S) and the intercept ($\log k'_w$) values of the straight lines obtained by plotting $\log k'$ vs φ ($\varphi_0 = \text{intercept/slope}$), based on minimum three points and $r > 0.99$. (Shown in Table 6.1)

The gradient retention time (t_R) (Shown in Table 6.1) was measured under the gradient profile, which included a 15 min linear acetonitrile gradient from 0 to 100%. The chromatographic hydrophobicity index (CHI) method used fast-gradient reversed phase HPLC to model octanol/water partitioning of a compound by correlating the retention time with the percentage of acetonitrile required to achieve an equal distribution of the compound between the mobile and stationary phases. By plotting φ_0 (obtained in isocratic mode) against t_R (obtained in

gradient mode), a standard curve (Figure 6.1) and equation (Equation 4) were generated. Based on this equation, CHI of each reference compound was calculated (Shown in Table 6.1).

$$\text{CHI} = \varphi_0 (\text{predicted value}) = 8.8207 t_R - 40.49 \quad (4)$$

$$R^2 = 0.9972$$

We used 21 commercially available drugs (Table 6.2) to validate the method. The set represents a wide range of chemical structures and lipophilicities. The plot of the calculated and literature Log P_{oct} values can be seen in Figure 6.2. The correlation coefficient is 0.9664.

Paired t test results: the two-tailed P value equals 0.7732, $t = 0.2922$, $df = 20$, standard error of difference = 0.053, $t < t_{0.05}$.

The difference between the calculated and literature Log P_{oct} values was considered to be not statistically significant. It can be seen that an excellent correlation was found and it provided experimental confirmation of the hypothesis that a linear gradient retention time can be used as a measure of compounds' lipophilicity using a polymeric PRP-1 column.

For application of this method for the assessment of the log P of natural products, we used 24 biologically active marine natural products isolated in our laboratory (Shown in Table 6.3). Since the number of hydrogen bonds of a compound, i.e. the number of protons available for hydrogen bonding, can influence calculated Log P_{oct} , we also have the potential to use this method to estimate the lipophilicity range of natural products, even though we may not know its structure.

P value and statistical significance: The two-tailed P value equals 0.8137. By conventional criteria, this difference is considered to be not statistically significant. The mean of group one minus group two equals 0.0975. 95% confidence interval of this difference: from -

0.7304 to 0.9254. Intermediate values used in calculations: $t = 0.2370$, $df = 46$, standard error of difference = 0.411.

Although natural products are considered to be an enormous resource of drug candidates and can provide countless opportunities to discover new drugs, interest in the development of natural products by the pharmaceutical industry has declined.^[18, 19, 20] A major factor for the decrease in natural products is that modern drug discovery research requires rapid screening, hit identification and hit to lead development. If natural products are to be considered again as an invaluable resource of lead compounds by industry natural products programs need to comply with the current timelines of the current drug discovery paradigm established with the high-throughput screening of synthetic chemical libraries.

Recently, Quinn et al prepared a screening library of 814 natural products in which 85% of the compounds had no Lipinski violations and demonstrated the possibility of generating natural libraries that conform to the physicochemical properties required in today's drug discovery environment.^[11, 21] According to Lipinski's "Rule of Five", drug candidates should possess suitable hydrophobicity (partition coefficient $\log P$ less than 5).^[2] Thus, integration of drug-like properties screening into the early stages of drug development could potentially speed up the drug development process. The shake-flask procedure is the standard method for determining $\log P_{\text{oct}}$'s in the range of -2 – 4.^[22] However, it is time and labor consuming and requires relatively large amounts of pure compounds. So, the traditional shake-flask method is not suitable for natural product research in which sample is limited. The RP-HPLC method is an indirect way to estimate $\log P_{\text{oct}}$ values in the range of 0 – 6 and has become a standard procedure. The advantages of this approach such as, speed, insensitivity to impurities, reduced

sample handling and sample sizes makes it amenable for natural products drug discovery research.

Valkó introduced a chromatographic hydrophobicity index based on a fast-gradient RP-HPLC method, and also established equation of Log P calculation.^[9] Based on his work, we applied this methodology using a polymeric PRP-1 column to estimate lipophilicity. The result of this study validated the use of the PRP-1 polymeric reversed phase fast gradient HPLC method for determining lipophilicity and showed that we can estimate the lipophilicity of natural products with good accuracy.

The estimated log P 's of the 24 marine natural products isolated in our laboratory matched the requirement of drug-like criteria ($0 < \text{Log } P_{\text{oct}} < 5$). We did see some large differences in the experimentally determined log P values and the calculated values. The most significant differences were for the natural products containing bromine and chlorine. The large variation in natural products containing bromine has been previously reported.^[11] In the future, we believe integration of a HPLC method to estimate lipophilicity into our natural product isolation process will allow us to optimize the generation of natural product libraries for HTS and develop an efficient polarity-optimized approach for the discovery of potential bioactive natural products.

CONCLUSION

In this study a fast-gradient HPLC method using a polystyrene-divinylbenzene PRP-1 column has been demonstrated to be useful for the estimation of lipophilicity. An excellent correlation was found between the results of the experimental determinations and the literature values of log P for a diverse set of commercially available drugs. We also found a good correlation between the experimentally determined and software calculated log P 's for a diverse

set of marine natural products. Some discrepancies were observed between the measured value of $\log P$ and the software calculations of the natural products containing halogens atoms. The method is rapid, insensitive to impurities, and requires very little compound and is amenable for integrated into a natural products drug discovery research program.

ACKNOWLEDGMENTS

We thank Prasoon Gupta, Upasana Sharma, and Maia Mukherjee for the isolation of the marine natural products.

REFERENCES

- [1]. Alex Avdeef. Physicochemical profiling (solubility, permeability and charge state). *Current Topics in Medicinal Chemistry* 2001, *1*, 277–351.
- [2]. Lipinski, C.A.; Lombardo, F.; Dominy B.W.; Feeney, P.J Experimental and computational approaches to estimate solubility and permeability in drug discovery and development settings. *Advanced Drug Delivery Reviews* 1997, *23*, 3-25.
- [3]. Lipinski, C.A. Lead- and drug-like compounds: the rule-of-five revolution, *Drug Discovery Today: Technologies*. 2004, *1*, 337-341.
- [4]. Hartmann, T.; Schmitt, J. Lipophilicity – beyond octanol/water: a short comparison of modern technologies, *Drug Discovery Today: Technologies*. 2004, *1*, 431-439.
- [5]. Zhao, Y.; Jona, J.; Chow, D. T.; Rong, H.; Semin, D.; Xia, X.; Zanon, R.; Spancake, C.; Maliski, E. High-throughput $\log P$ measurement using parallel liquid chromatography/ultraviolet/mass spectrometry and sample-pooling. *Rapid Communications in Mass Spectrometry*, 2002, *16*, 1548-1555.

- [6]. Chen, Z.; Weber, S. G. High-Throughput method for lipophilicity measurement, *Anal. Chem.* 2007, *79*, 1043-1049.
- [7]. Kaliszan, R.; Haber, P.; Czek, T. B.; Siluk, D.; Valkó, K. Lipophilicity and pK_a estimates from gradient high-performance liquid chromatography. *Journal of Chromatography A*, 2002, *965*, 117-127.
- [8]. Valkó, K.; Bevan, C.; Reynolds, D. P. Chromatographic Hydrophobicity Index by Fast-Gradient RP-HPLC: A High-Throughput Alternative to $\log P/\log D$. *Anal. Chem.* 1997, *69*, 2022-2029.
- [9]. Valkó, K.; Du, D.M.; Bevan, C.; Reynolds, D. P.; Abraham, M. H. Rapid Method for the Estimation of Octanol/Water Partition Coefficient ($\log P_{oct}$) from Gradient RP-HPLC Retention and a Hydrogen Bond Acidity Term (Sa_2H). *Current Medicinal Chemistry*. 2001, *8*, 1137-1146.
- [10]. Giaginis, C.; Tsantili-Kakoulidou, A. Current state of the art in HPLC methodology for lipophilicity assessment of basic drugs. *Journal of Liquid Chromatography & Related Technologies*. 2008, *31*, 79-96.
- [11]. Quinn, R.J.; Carroll, A. R.; Pham, N.B.; Baron, P.; Palframan, M. E.; Suraweera, L.; Pierens, G.K.; Muresan, S. Developing a drug-like natural product library. *Journal of Natural Products*. 2008, *71*, 464 – 468.
- [12]. Houssen, W.E.; Jaspars, M. *Isolation of Marine Natural Products*, in *Natural Products Isolation*. Sarker, S.D.; Latif, Z.; Gray, A. I.; Eds.; Humana Press Inc; Totowa, NJ, 2006, *20*, 353-391.
- [13]. van Liedekerke, B.M.; Nelis, H.J.; Lambert, W.E.; de Leenheer, A.P. High performance liquid chromatography of quaternary ammonium compounds on a polystyrene-divinylbenzene column." *Anal. Chem.* 1989, *61*, 728-732.

- [14]. Huck, C.W.; Bonn, G.K. Poly(Styrene-Divinylbenzene) based media for liquid chromatography. *Chem Eng. Technol.* 2005, 28, 1457-1472.
- [15]. Haky, J.E.; Vemulapalli, S. Comparison of octadecyl-bonded alumina and other stationary phases for lipophilicity estimation by high performance liquid chromatography. *Journal of Liquid Chromatography.* 1990, 13, 3111-3131.
- [16]. Abraham, M.H.; Chadha, H.S.; Leitao, R.A.E.; Mitchell, R.C.; Lambert, W.J.; Kalisan, R.; Nasal, A.; Haber, P. Determination of solute lipophilicity, as log P(octanol) and log P(alkane) using poly(styrene-divinylbenzene) and immobilized artificial membrane stationary phases in reversed-phase high-performance liquid chromatography. *Journal of Chromatography A.* 1997, 766, 35-47.
- [17]. Valkó, K.; Slégel P. New chromatographic hydrophobicity index (ϕ_0) based on the slope and the intercept of the log k' versus organic phase concentration plot. *Journal of Chromatography.* 1993, 631, 49-61.
- [18]. Cragg G.M.; Newman D.J. Discovery and development of antineoplastic agents from natural sources. *Cancer-Invest.* 1999, 17, 153–163.
- [19]. Itokawa H.; Morris-Natschke S.L.; Akiyama T.; Lee, K.H. Plant-derived natural product research aimed at new drug discovery. *Nat Med (Tokyo)*, 2008, 62, 263-280.
- [20]. Koehn F.E.; Carter G.T.; The evolving role of natural products in drug discovery. *Nat Rev Drug Discov.* 2005, 4, 206-220.
- [21]. Koehn F.E. High impact technologies for natural products screening. *Progress in Drug Research.* 2008, 65, 177-210.
- [22]. *OECD Guidelines for the Testing of Chemicals, Test No. 107*; Organization for Economic Co-operation and Development (OECD): Paris, 1995.

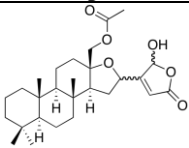
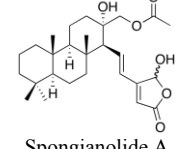
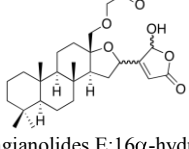
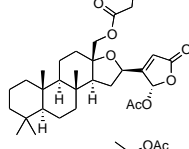
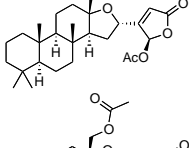
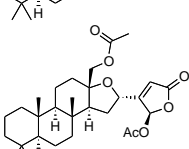
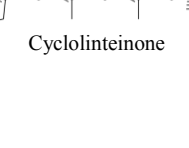
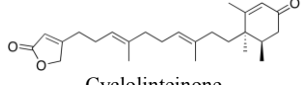
Table 6.1. The CHI and Log P values of 10 reference compounds for the gradient HPLC calibration for CHI measurement using an acetonitrile gradient.

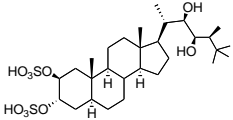
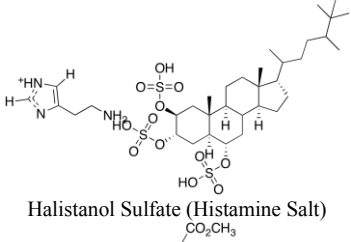
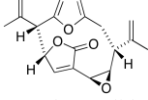
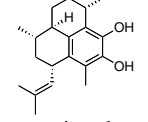
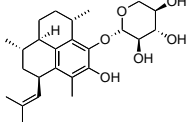
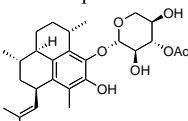
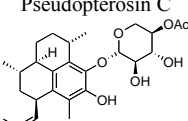
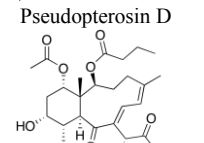
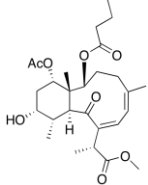
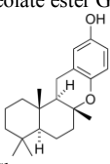
Reference Compound	φ_0	t_r (gradient)	CHI	HBC	Log P_{oct} (calc.)	Log P_{oct} (literature)
Theophylline	12.57	5.89	11.46	1	-0.2	-0.05
5-Phenyl-1H-Tetrazole	14.29	6.04	12.79	1	-0.14	1.42
Benzimidazole	24.26	7.32	24.03	1	0.39	1.38
Colchicine	32.86	8.61	35.46	1	0.93	0.92
8-Phenyltheophylline	43.88	9.82	46.13	2	1.79	2.05
Acetophenone	64.67	12.03	65.62	0	1.98	1.66
Indole	77.94	13.16	75.59	1	2.81	2.14
Propiophenone	81.45	13.79	81.15	0	2.71	2.19
Butyrophenone	93.18	14.95	91.38	0	3.19	2.73
Valerophenone	98.76	15.95	100.2	0	3.61	3.28

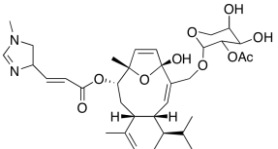
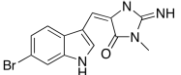
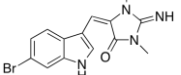
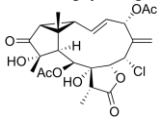
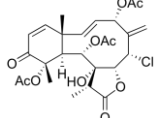
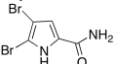
Table 6.2. Log P_{oct} values of 21 drug compounds calculated from Gradient retention times (t_R), CHI values and hydrogen bond count (HBC) using gradient elution on a PRP-1 column and literature log P_{oct} values.

Drug	tr (min)	CHI	HBC	Log P_{oct}	Log P_{oct} (literature)
Adenine	5.21	5.12	2	-0.14	-0.45
Caffeine	5.66	9.43	2	0.06	-0.07
Cimetidine	6.87	19.80	3	0.91	0.46
Acetaminophen	7.06	21.76	2	0.64	0.9
Sumatriptan	7.31	23.83	3	1.09	1.1
Hydrocortisone	9.12	39.78	3	1.85	1.69
Bendroflumethiazide	10.12	48.76	3	2.27	2.09
Lidocaine	11.31	59.03	2	2.40	2.48
Diazepam	12.07	65.16	2	2.71	2.8
Dibucaine	16.38	104.15	1	4.15	4.29
Tinidazole	7.95	29.41	0	0.28	0.12
Trimethoprim	8.46	33.93	2	1.21	1.36
Triamterene	8.11	30.83	3	1.43	1.24
Terbutaline	6.52	16.73	4	1.13	1.57
Tripelennamine	14.5	87.48	0	3.01	2.65
Tolazoline	10.21	49.45	1	1.59	1.21
Benzthiazide	11.20	58.22	3	2.72	2.92
Oxybutynin	16.36	103.97	2	4.51	4.68
Atropine	9.9	46.70	2	1.81	1.83
Hetacillin	7.59	17.35	4	1.52	1.86
Scopolamine	8.73	36.33	3	1.69	1.66

Table 6.3. Log P_{oct} values determined from Gradient retention times (t_R), CHI values and hydrogen bond count (HBC) using gradient elution on a PRP-1 column and software calculated log P_{oct} for a series of marine natural products.

Compound	t_R (min)	CHI	HBC	Log P_{oct}	Log P_{oct} (Calc.)
 Spongianolides C:16 α -hydrogen D:16 β -hydrogen	15.89	99.80	1	3.95	4.36
 Spongianolide A	13.3	76.84	2	3.23	4.5
 Spongianolides E:16 α -hydrogen F:16 β -hydrogen	14.74	89.61	2	3.78	3.52
 (Spongianolide with AcO group)	16.33	103.70	0	3.77	3.98
 (Spongianolide with AcO group)	17.94	117.98	0	4.44	3.98
 (Spongianolide with AcO group)	16	100.78	0	3.64	4.59
 (Spongianolide with AcO group)	15.85	99.45	0	3.57	5
 Cyclolinteinone	13.91	81.91	0	2.75	5

 <p>Sch 572423</p>	7.44	24.89	2	0.77	0.5
 <p>Halistanol Sulfate (Histamine Salt)</p>	9.16	40.12	2	1.51	3.52
 <p>Pseudopterolide</p>	13.9	82.16	0	2.76	1.51
 <p>Pseudoptosin aglycone G-P</p>	18.19	120.19	2	5.27	5.47
 <p>Pseudoptosin A</p>	14.22	84.00	3	3.97	4.17
 <p>Pseudoptosin C</p>	15.83	99.27	3	4.59	4.4
 <p>Pseudoptosin D</p>	16.05	101.22	3	4.68	4.4
 <p>Briareolate ester G E $\Delta^{7,8}$</p>	13.63	79.77	1	3.01	2.65
 <p>Briareolate ester G Z $\Delta^{7,8}$</p>	14.48	87.30	3	4.08	2.65
 <p>Chromazonorol</p>	17.7	115.85	1	4.70	5.52

 Eleutherobin	10.73	54.06	4	3.08	2.11
 6-bromo-2'-de- <i>N</i> -methylaplysinopsin	10.48	51.84	2	2.16	1.52
 6-bromoaplysinopsin	12.31	68.06	2	2.06	1.75
 Erythrolide A	9.75	45.37	3	2.11	0.32
 Erythrolide B	10.32	50.42	2	1.74	0.74
 4,5-dibromopyrrole-2-carbamide	9.85	46.26	2	3.90	1.02

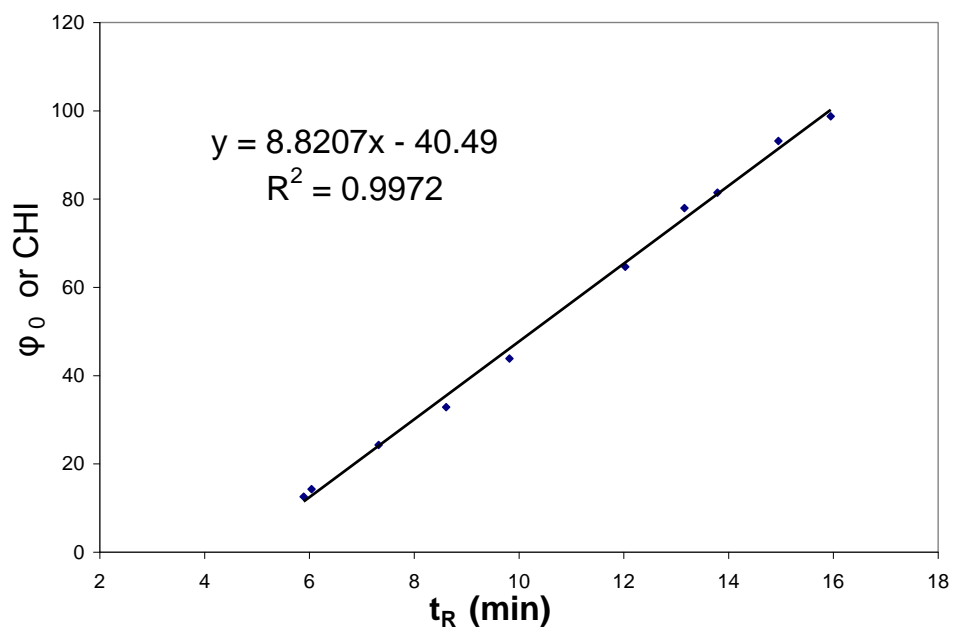


Figure 6.1. Calibration plot for the measurements of the Chromatographic Hydrophobicity Index (CHI) of 10 reference compounds.

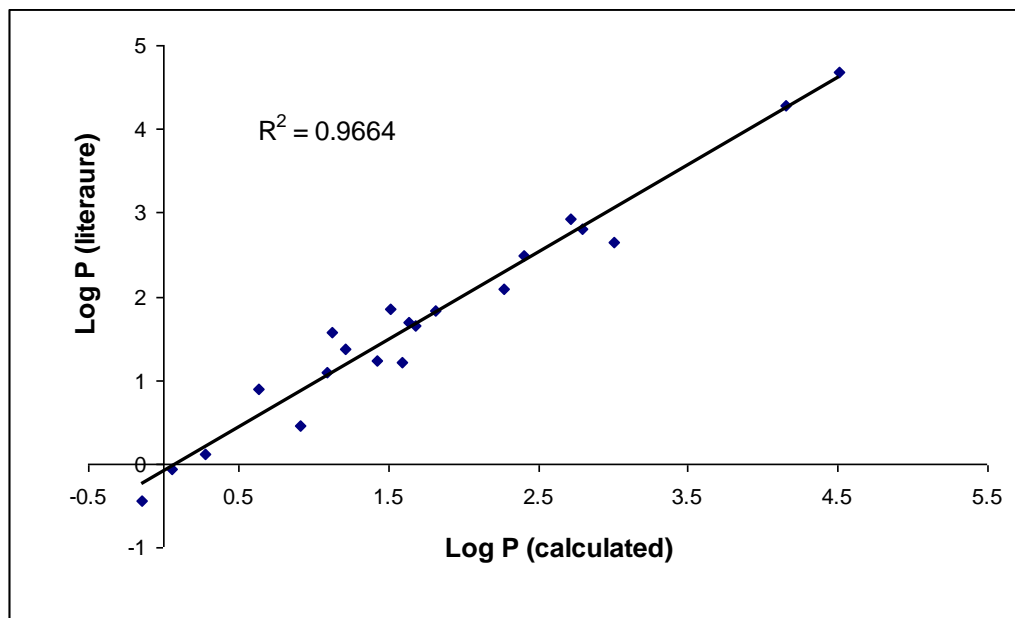


Figure 6.2. Correlation between calculated and literature Log P_{oct} for 21 drugs.

CHAPTER 7

CONCLUSION

The goal of pharmacokinetic evaluation or ADME characterization is to provide, with reasonable accuracy, a preliminary prediction of the behavior of a compound to assess its potential to become a drug. A variety of experimental assays have been developed to characterize pharmacokinetic profiles or determine pharmacokinetic parameters of compounds in the drug discovery and development process. Knowledge about pharmacokinetic parameters is important in terms of providing prior estimates for designing clinical trials, predicting concentration–time profiles in future studies and clinical practice. *In vivo* animal models as pharmacokinetic assays are often used to evaluate pharmacokinetic parameters of an investigational agent.

The pharmacokinetic study of Pseudopecterin A (PsA) following administration of a 50 mg/kg i.v. dose in mice was performed in chapter 3. A simple, rapid and sensitive method for determination of PsA in mouse plasma, liver, brain, and kidney using pre-column derivatization and HPLC-ultraviolet detection was developed and successfully used to evaluate the pharmacokinetics study of PsA in mice. The pharmacokinetic characteristics were determined. The pharmacokinetic profile of PsA indicated that PsA had rapid tissue uptake and extensively tissue distribution. Pharmacokinetic characteristics in brain also documented PsA can cross the blood-brain barrier easily and achieve high concentrations, which could be attributed to its high lipophilicity.

Bioadhesive gel formulations which utilize unique polymers, can improve adherence time, transmucosal absorption and bioavailability of drugs to the nasal mucosa when administered intranasally. To improve therapeutic effectiveness of midazolam, we developed a biohasive gel formulation of midazolam for intranasal administration in the dog. We compared the pharmacokinetics of a novel midazolam gel formulation given intranasally to pharmacokinetics of parenteral midazolam given intrnasally, intravenously and rectally in dogs. Data from this study demonstrated the rapid absorption of midazolam from the intranasal gel formulation from the nasal cavity and into the systemic circulation. The increased bioavailability of midazolam of the gel formulation indicated that the administered midazoalm intranasal gel formulation could potentially reduce time to cessation of seizues because of desirable pharmacokinetic profiles such as rapid absorption and high bioavailability.

In order to understand the pharmacokinetic profile of L- β -5-Bromovinyl-(2-hydroxymethyl)-1,3-(dioxolanyl)uracil (L-BVOddU), an HPLC method for the quantification of L-BVOddU in mouse plasma, brain, liver, heart, lung, spleen, kidney, skin and rat plasma was developed and successfully applied in studies of the pharmacokinetic and tissue distribution at steady state of L-BVOddU in rats and mice, respectively. Pharmacokinetic parameters (e.g. elimination half life, bioavailability, plasma protein binding, volume of distribution and clearance) were determined.

Lipophilicity, expressed as the logarithmic value of the octanol/water partition coefficient ($\log P_{\text{oct}}$), is a fundamental parameter that models the biological partition behavior of drug molecules. Consideration of $\log P_{\text{oct}}$ in the process of drug development can prioritize leads from high-throughput screening and reduce the failure rate of drug candidates during development. An indirect method to estimate lipophility using fast-gradient HPLC method was

developed and used to estimate the lipophilicity of marine natural products. We believe integration of a HPLC method to estimate lipophilicity into our natural product isolation process will allow us to optimize the generation of natural product libraries for HTS and develop an efficient polarity-optimized approach for the discovery of potential bioactive natural products.

APPENDIX 1

QUANTITATIVE DETERMINATION OF (-)-FLURO-CARBODINE IN MOUSE PLASMA, LIVER, BRAIN AND KIDNEY TISSUES BY ION-PAIRING LIQUID CHROMATOGRAPHY*

*Bo Zheng, David C.K. Chu, Catherine A. White. Poster in AAPS annual meeting, Atlanta, 2008

ABSTRACT

Objective: To develop and validate an Ion-pair HPLC method for the quantitative determination of antiviral drug (-)-Fluro-Carbodine (FC) in a mouse model which includes plasma, liver, brain and kidney homogenates.

Methods: Blood and tissues homogenate spiked with FC were extracted using liquid-liquid extraction method. An ion-pairing HPLC method with UV detector was used for analysis of FC in mouse plasma, brain, liver and kidney.

Results: Methods were validated, precision and accuracy data was acceptable. Relative recovery and stability was satisfactory.

INTRODUCTION

(-)-Fluro-Carbodine (FC) has activity both *in vitro* and *in vivo* against DNA and RNA viruses such as Venezuelan equine encephalitis virus, and anti-cancer activity as well. The main mode of antiviral action by carbodine is through the inhibition of cytidine triphosphate (CTP) synthetase that converts uridine-5'-triphosphate (UTP) to cytidine triphosphate (CTP) that results in a depletion of cytidine triphosphate (CTP) pools. The purpose of this study was to develop an HPLC method for the quantification of (-)-Fluro-Carbodine (FC) in mouse plasma, brain, liver and kidney.

EXPERIMENT AND METHOD

Chemical and Reagents

FC (Code No: RJR3-57-25, MF: $C_{10}H_{14}FN_3O_4$, MW: 259.23), Sulfadiazine (Internal standard), HPLC-grade acetonitrile (ACN), methanol (MeOH), SDS, TFA.

Preparation of stock and standard solutions

A stock solution of 1.0 mg/ml FC was prepared in deionized water. Standard solutions of FC were prepared by serial dilution with deionized water. The final concentrations of the standard solutions were 250, 25, 10, 5, 2.5, 1 and 0.25 ug/ml. Quality control standards with concentrations of 12.5, 0.75, 0.1, 0.025 ug/ml were also made with the same method. Stock solutions were kept refrigerated when not in use and replaced on a bi-weekly basis. Fresh standard solutions were prepared for each day of analysis or validation.

Chromatographic system

The chromatographic analyses were performed using an HPLC system consisting of Waters 515 HPLC pumps, Waters 717 plus autosampler, and Waters 2487 UV detector. Chromatographic separations were achieved using a sphereclone column (4.6mm×250mm) with a Phenomenex Security Guard C₁₈ guard column (Torrance, CA, USA).

Chromatographic conditions

---For analysis of plasma and brain tissues

The mobile phase used was 15% acetonitrile (ACN), 5% methanol (MeOH), 0.5 mM SDS, 10 mM NaAcO, 0.1% Trifluoroacetic Acid (TFA), adjusted to pH=3.16. Mobile phase flow rate was 1.0ml/min and the detection wavelength was optimized and set at 285nm. Under the chromatographic conditions described, FC and internal standard eluted at 9.2 min and 10.3 min, respectively.

---For analysis of liver and kidney tissues

The mobile phase used was 22% ACN, 0.4% Acetic acid, 0.5 mM SDS (adjusted to pH 3.0). The mobile phase flow rate was 1.0 ml/min and the detection wavelength was optimized and set at 285 nm. Under the chromatographic conditions described, FC and internal standard eluted at 14.5 min and 10.3 min, respectively.

Calibration curves

Plasma calibration points were prepared by spiking 100 ul of blank mouse plasma, homogenate of mouse brain, liver and kidney tissue with 10 ul of each FC and Sulfadiazine (internal standard) standard solution.

Sample preparation

Plasma or tissue samples were prepared with liquid-liquid extraction. After spiking, samples were vortexed gently and 200 ul of $(\text{NH}_4)_2\text{SO}_4$ and 1ml ice-cold ACN were added. Samples were vortexed and centrifuged for 10 min at 13,000 rpm. The pellet and ion solution were discarded and the ACN-phase was evaporated until reaching dryness. The residue was reconstituted in 100ul of mobile phase. An injection volume of 20 ul was used for all samples.

Method validation

Calibration curves were acquired by plotting peak area against the analyte concentration. Precision and accuracy were determined for the 3 QC points (12.5, 0.75, 0.2 ug/ml) and the LOQ (0.025 ug/ml). Five replicates of each QC point and LOQ were analyzed every day to determine the intra-day accuracy and precision. This process was repeated three times over 3 days in order to determine the inter-day accuracy and precision.

Absolute recovery was determined by dividing the response of the analyte in plasma and tissues by the response of the standard solution in deionized water.

Freeze and thaw stability was determined over 3 cycles. Autosampler stability was determined by preparing samples and injecting them at different time intervals over 24 hours.

RESULTS AND DISCUSSION

The chemical structure of FC is shown in Figure A.1. Separation of FC was explored using different kind of columns and mobile phases. Different mobile phase pH and different UV

wavelengths were tried and optimized. Several extraction and protein precipitation methods were investigated. Meanwhile, the recoveries were also considered.

Figure A.2 shows chromatograms of separation results. The calibration curves for each day of validation and analysis showed very good linear response (Blood Plasma: $r^2=0.996-0.999$; Brain: $r^2=0.990-0.994$; Liver: $r^2=0.990-0.999$; kidney: $r^2=0.998-0.999$) through a range of 0.025-25 ug/ml. Linear regression equations were generated with JMP statistical software using a $1/x^2$ -weighting scheme for each day of validation (Table A.1).

The extraction efficiencies for FC from plasma are expressed in terms of absolute recovery. The absolute recoveries were determined by comparing the peak areas of spiked plasma to the corresponding peak areas of the untreated standard solutions (n=20) (Table A.2). FC recoveries ranged from 70-81%.

Precision and accuracy measurements were acquired for 3 QC points and the LOQ for each compound. Precision was reported as percent relative standard deviation (RSD) and accuracy was reported as percent error. Values for the intra-day (n=5) precision and accuracy ranged from 2.16-8.48% and 2.36-9.76%, respectively (Table A.3). Inter-day (n=15) precision and accuracy ranged from 3.19-9.56% and 2.61-9.84%, respectively (Table A.3).

Spiked samples were found stable over 3 freeze/thaw cycles (Table A.4). Prepared samples were stable in the autosampler for up to 24 hours. Spiked samples were stable at room temperature for 24 hours as well. For all stability studies, there was no significant decline in the peak areas for the analytes.

CONCLUSION

The calibration curves for each day of validation and analysis showed good linear response through a range of 0.025-25 ug/ml with $r^2>0.99$. The extraction recovery ranged from

70-81%. Values for the intra-day (n=5) precision and accuracy ranged from 2.16-9.48% and 2.36-9.76%, respectively. Inter-day (n=15) precision and accuracy ranged from 2.56-9.67% and 2.66-9.65%, respectively. For all stability studies, there was no significant decline in the peak areas for the analytes.

A validated method which was sensitive, specific, accurate, and reliable was developed. The method will be utilized to study the pharmacokinetics of FC in mice.

Table A.1. Linear regression equations generated from validation data from mouse plasma, brain, liver and kidney. (n=3)

Matrix	Slope	Intercept	R ²
Plasma	4.38 ± 0.17	-0.07 ± 0.01	0.997 ± 0.001
Brain	4.77 ± 0.47	0.01 ± 0.002	0.993 ± 0.002
Liver	1.34 ± 0.07	-0.03 ± 0.37	0.995 ± 0.004
Kidney	1.31 ± 0.004	0.41 ± 0.0004	0.998 ± 0.0005

Table A.2. Percent absolute recoveries of FC from mouse plasma, brain, liver and kidney.
(n=20)

Concentration (ug/ml or ug/g)	Plasma	Brain	Liver	Kidney
2.5	80.6±1.0	79.4±1.9	77.5±2.1	76.7±2.2
0.75	72.2±3.3	75.4±1.5	73.7±1.8	74.5±3.0
0.2	72.7±1.5	74.9±2.2	70.5±3.4	72.1±2.4
0.025	71.5±3.1	70.8±2.6	70.1±3.5	70.4±2.9

Table A.3. Intra-day (n=5) and Inter-day (n=15) precision (%R.S.D) and accuracy (%Error) of the method in. T.C denotes theoretical concentration and E.C denotes experimental concentration.

Plasma:

T.C (ug/ml)	Day1 E.C (ug/ml)	%Error	%R.S.D	Day2 E.C (ug/ml)	%Error	%R.S.D	Day3 E.C (ug/ml)	%Error	%R.S.D	Inter- day E.C (ug/ml)	%Error	%R.S.D
2.5	2.41	2.37	3.08	2.31	3.12	4.27	2.44	4.65	3.34	2.39	2.04	2.859
0.75	0.715	4.49	5.69	0.658	4.71	3.75	0.721	3.47	5.68	0.698	3.06	4.982
0.2	0.176	9.76	7.97	0.223	8.65	7.89	0.204	7.31	8.65	0.201	4.01	11.76
0.025	0.025	7.23	8.67	0.0285	8.43	6.89	0.0254	8.19	8.43	0.026	4.81	7.15

Brain:

T.C (ug/g)	Day1 E.C (ug/g)	%Error	%R.S.D	Day2 E.C (ug/g)	%Error	%R.S.D	Day3 E.C (ug/g)	%Error	%R.S.D	Inter- day E.C (ug/g)	%Error	%R.S.D
2.5	2.66	6.53	6.13	2.48	0.77	2.04	2.72	8.67	3.48	2.62	3.73	4.77
0.75	0.72	3.98	5.48	0.71	5.20	4.00	0.69	7.38	3.45	0.707	3.24	2.16
0.2	0.18	9.27	8.66	0.175	12.34	9.80	0.188	5.95	9.19	0.183	2.31	3.53
0.025	0.0256	2.27	4.19	0.0248	0.80	5.59	0.029	17.78	7.07	0.265	6.8	8.43

Liver:

T.C (ug/g)	Day1 E.C (ug/g)	%Error	%R.S.D	Day2 E.C (ug/g)	%Error	%R.S.D	Day3 E.C (ug/g)	%Error	%R.S.D	Inter- day E.C (ug/g)	%Error	%R.S.D
2.5	2.46	3.06	6.06	2.485	1.81	5.61	2.55	2.75	6.34	2.501	1.28	1.1715
0.75	0.75	2.52	2.79	0.755	4.21	2.84	0.738	3.20	7.17	0.747	8.67	1.169
0.2	0.231	11.6	6.00	0.227	3.82	6.78	0.197	4.58	9.09	0.218	6.00	8.511
0.025	0.0249	9.67	4.58	0.0254	6.49	4.87	0.0245	7.09	9.07	0.0249	1.2	1.809

Kidney:

T.C (ug/g)	Day1 E.C (ug/g)	%Error	%R.S.D	Day2 E.C (ug/g)	%Error	%R.S.D	Day3 E.C (ug/g)	%Error	%R.S.D	Inter- day E.C (ug/g)	%Error	%R.S.D
2.5	2.65	2.19	7.07	2.52	1.80	5.25	2.48	3.21	5.29	2.55	2.56	3.399
0.75	0.752	3.49	2.66	0.766	4.01	5.73	0.742	4.57	7.49	0.753	10.67	1.6
0.2	0.206	9.56	5.20	0.1963	3.62	8.99	0.221	9.82	8.92	0.207	5.82	5.99
0.025	0.0231	6.23	17.65	0.0249	4.41	14.87	0.0256	9.58	8.90	0.0245	3.69	5.257

Table A.4. Results of freeze/thaw stability of FC in mouse plasma, brain, liver and kidney, represented by area \pm S.D. (n=5) of each day and % R.S.D of the area between days.

	Plasma	Brain	Liver	Kidney
Day 1	357 \pm 15.8	359 \pm 14.5	345 \pm 13.7	347 \pm 13.4
Day 2	369 \pm 9.2	363 \pm 10.1	321 \pm 12.1	329 \pm 9.3
Day 3	348 \pm 14.1	349 \pm 14.3	320 \pm 9.1	318 \pm 15.4
Day 4	335 \pm 7.3	338 \pm 7.5	311 \pm 11.4	315 \pm 8.3
%R.S.D	4.02	3.1	4.52	4.46

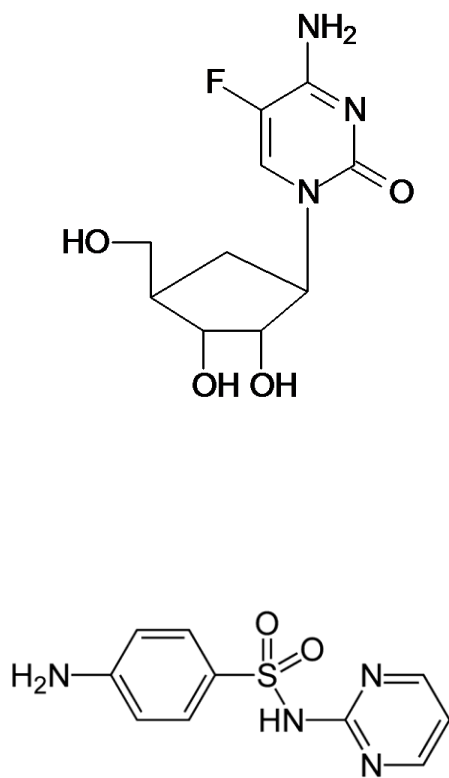


Figure A.1. Chemical structure of FC (top) and Sulfadiazine (bottom).

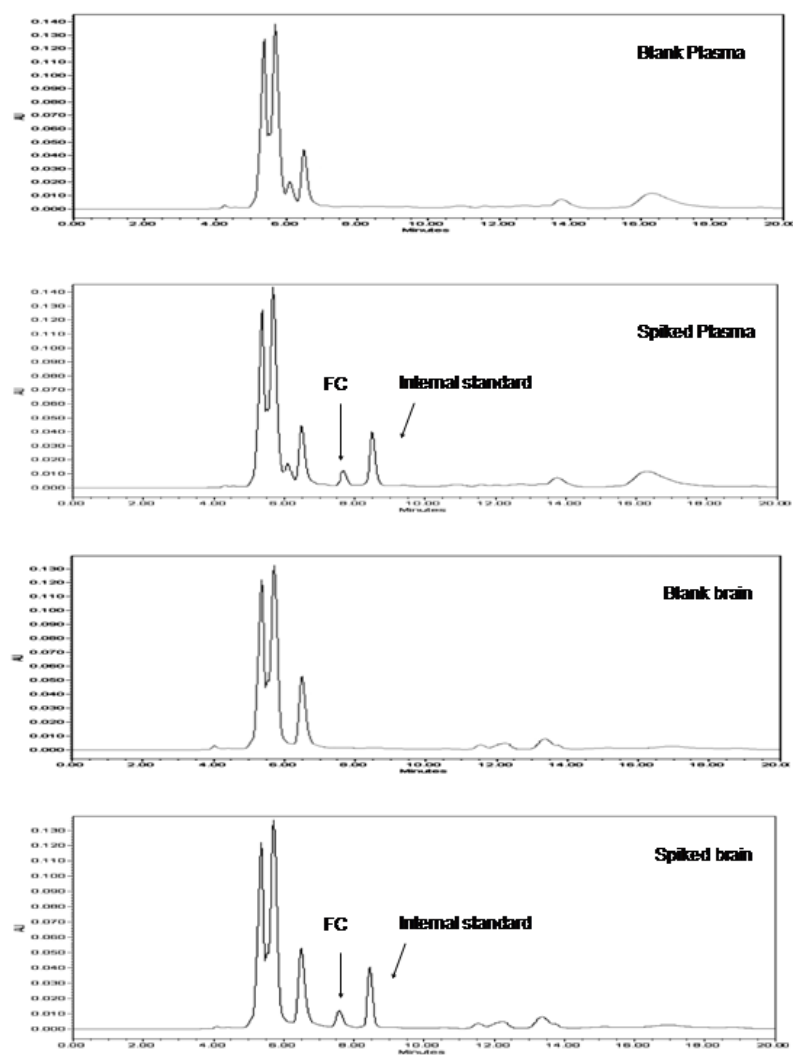


Figure A.2. Chromatograms from blank blood and brain, blood and brain spiked with 0.2 ug/ml or ug/g of FC, respectively.

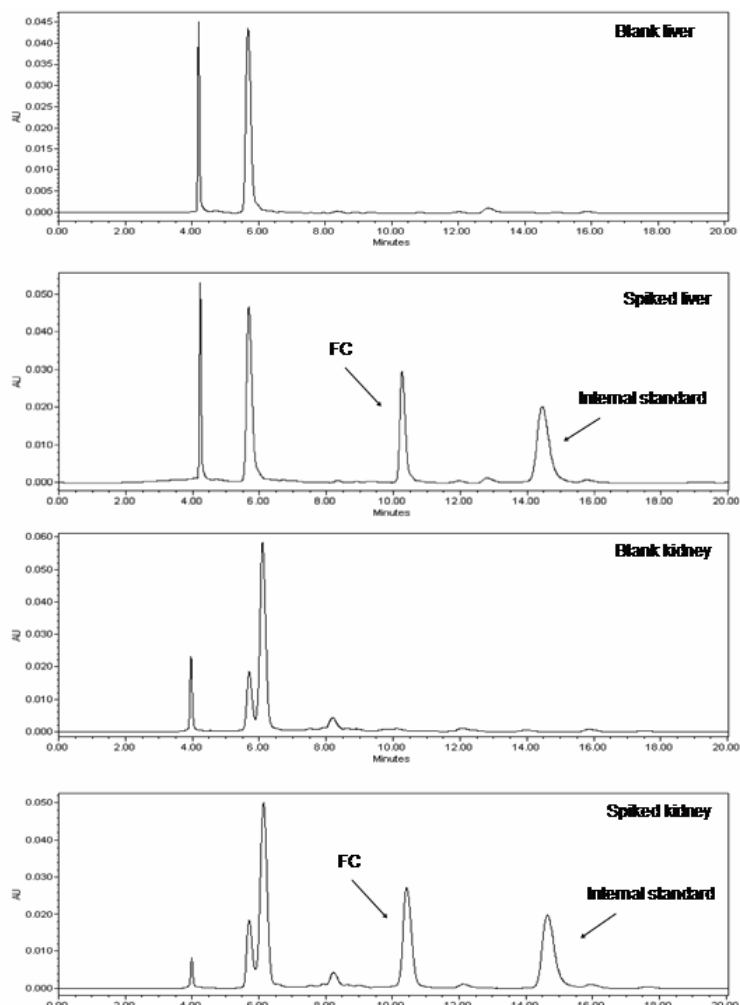


Figure A.3. Chromatograms from blank liver and kidney, liver and kidney spiked with 0.75 ug/g of FC, respectively.